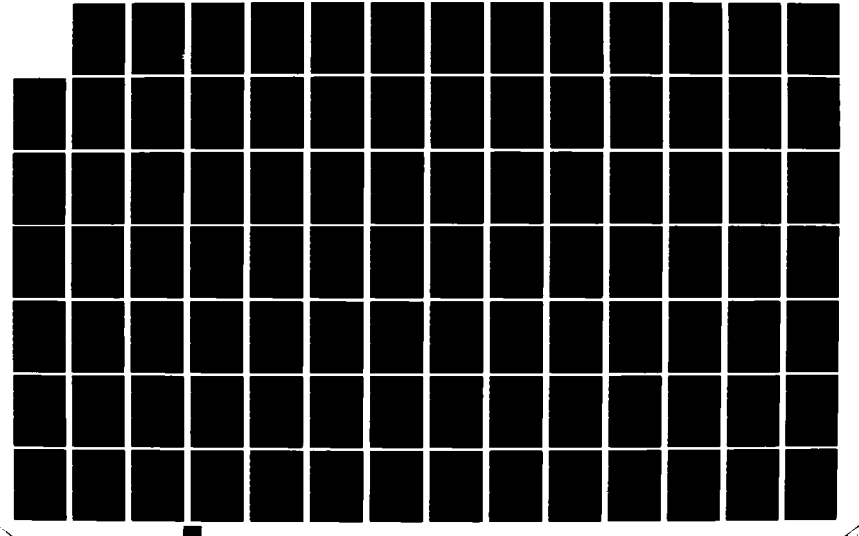

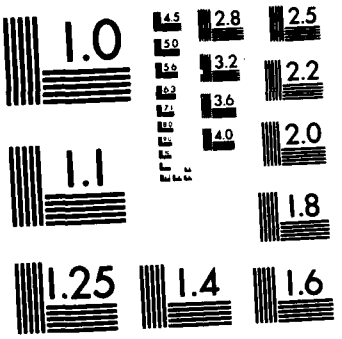

EFFECT OF DIVIDER PLATE TRAILING EDGE SHAPE ON THE MIXING OF PARALLEL FLOWS

THESIS

AFIT/GAE/AA/82D-29 WILLIAM D. VAHLE
CAPTAIN USAF

DEPARTMENT OF THE AIR FORCE
AIR UNIVERSITY (ATC)
AIR FORCE INSTITUTE OF TECHNOLOGY

Wright-Patterson Air Force Base, Ohio

AFIT/GAE/AA/82D-29

EFFECT OF DIVIDER PLATE TRAILING EDGE SHAPE ON THE MIXING OF PARALLEL FLOWS

THESIS

Presented to the Faculty of the School of Engineering
of the Air Force Institute of Technology
Air University
in Partial Fulfillment of the
Requirements for the Degree of
Master of Science

by
William D. Vahle, B.S.
Captain USAF
Graduate Aeronautical Engineering
December 1982

Preface

This thesis presents the results of my investigation of the effects of divider plate trailing edge shape on the mixing of parallel flows.

I wish to express my appreciation to Dr. William C. Elrod for his assistance and inspiration during this research effort. Major John Vonada, Mr. William W. Baker and Mr. Harold L. Cannon also deserve my thanks. Finally, I wish to express thanks to my wife, Cheryl, and sons, Jeremy and Anthony, for their patience and devotion during this endeavor.

William D. Vahle

Contents

List of Figures

List of Figures

List of Figures

List of Tables

List of Symbols

Symbol		Units
dy/dx	Wake growth rate	---
m	Slope of calibration curve	---
P_1	Stilling chamber pressure	in H_2O
P_a	Ambient pressure	in Hg
R	Jet width in y-direction	in
Re	Reynold's number based upon x	---
t	Plate thickness	in
T_1	Stilling chamber temperature	R
TU	Turbulence parameter	---
u	X-component of velocity	ft/sec
$\overline{U}$	Local mean velocity	ft/sec
Ur	Velocity ratio	---
v	Y-component of velocity	ft/sec
$\overline{V}$	Y-component of mean velocity	ft/sec
V	DC voltage	volts
V_{rms}	RMS voltage	volts
W	Trailing edge shape parameter	---
α	Angle	deg
β	Angle	deg
δ	Boundary layer thickness	in
1	Subscript relating to Sensor 1	---
2	Subscript relating to Sensor 2	---

List of Symbols

Symbol		Units
A	Subscript relating to traverse location A . .	---
x	Subscript x-component	---
y	Subscript y-component	---
′	Fluctuating value	---

Abstract

The objective of this thesis is to investigate the mixing process as characterized by velocity and turbulence data and to experimentally determine the effect of divider plate trailing edge shape upon the mixing of parallel, co-flowing air streams. An apparatus was built which provided uniform, two-dimensional velocity profiles which, at the divider plate trailing edge, are similar in appearance to fully developed turbulent velocity profiles. Testing was accomplished at stream velocity ratios of nominally 1.0, 0.6 and 0.3 with the high speed flow velocity being 300 ft/sec. A two element hot film probe was used to determine flow velocities and turbulence intensity at various points in the flow streams. The primary indicator of mixing was found to be the wake growth rate. Wake width, used in determination of wake growth rate, was determined from two flow parameters; first, the mean velocity profiles and secondly, the turbulence profiles. The following trailing edge configurations were considered: a flat plate with a square trailing edge, a flat plate with slots in the trailing edge, a flat plate with a tapered trailing edge, a plate with top and bottom of the trailing edge alternately rounded at 0.2 in increments, and a trailing edge consisting of tabs alternately bent upward and downward.

The tab plate was found to be the best mixer based upon wake growth rate. Wake growth increased progressively with decreasing velocity ratio; and maximum turbulence level in the wake was found not to be a reliable indicator of mixing.

I. Introduction

This research involves the experimental determination of the effects of divider plate trailing edge shape upon the mixing of parallel flows in a constant area duct. Also, various parameters are evaluated for their suitability as indicators of mixing.

Wake width, wake growth rate, and magnitude of the turbulence were selected as potential indicators of the degree of mixing. Rajagopalon and Antonio (Ref 8: 1052-1058) state that the growth rate of a wake may depend upon the flow field outside the shear layer, the freestream turbulence, and/or tripping of the flow at the trailing edge. Also, El-Assar and Page (Ref 6: 1389) state that the velocity profile of the boundary layer and the turbulence intensity distribution in the transitional region play an important role in development of the wake.

Knowledge in this area is of significance when mixing in a short distance is desired. The mixing could involve flows of different density, temperature and/or velocity. Examples include the effect of compressor rotor blade wakes upon the flow through the stator. Rotor-stator spacing is generally less than one chord length, however, as stated by Kerrebrock (Ref 10: 551) "I would just point out that the rotor-stator spacing in the big new fan engines is many

chords. Those fans are pushing an awful lot of us across the country and 1% on fan efficiency is 1% on fuel consumption and there are thousands of dollars lost because of the inefficiency in the fan". Therefore, a reduction of the wake effects as a result of improved mixing will reduce the distortion in the flow to the stator and result in increased efficiency. Another example is the mixing of high temperature core flow with the relatively low temperature by-pass flow of a turbofan engine, thus reducing the detectability of the exhaust plume.

This research involves testing of modifications to the trailing edge of a flat plate and their effects on the mixing of two turbulent air streams. Kline (Ref 10: 543) states that more complex geometries than airfoils -- like shapes that strain the flow field differently and alter the turbulence production and/or decay -- should be tested. The flat plate was chosen as an appropriate first step in the evaluation of such shapes. Various velocity ratios were evaluated to simulate the differing velocities on the pressure and suction sides of a compressor blade or between the core and by-pass flows.

Purpose and Scope

The purpose of this work is to investigate the mixing process as characterized by velocity and turbulence data. In addition, the effects of modifications to the trailing edge of a dividing plate on the mixing process are evaluated.

The desired result is to determine a configuration which will shorten the distance required for mixing of the two co-flowing air streams.

The research involves turbulent flow with velocities less than 300 ft/sec which allows use of incompressible flow relationships. Testing was accomplished at velocity ratios of 1.0, 0.6 and 0.3. The flow is assumed to be two-dimensional which, based upon research by de Brederode (Ref 5: 95), is valid for $\delta/h \leq 1/4$ where δ is the boundary layer thickness on one side of the plate, and h is the width of the duct along the plate trailing edge.

Five divider plate trailing edge modifications are examined. Four of the modifications were selected with the restriction that the modification be confined within the thickness of the plate. The fifth plate was not so restricted.

II. Divider Plate Design

As discussed by El-Assar and Page (Ref 6: 1388), the wake which forms behind a body in a flow field is generally discussed and analyzed in two parts. First, the region directly behind the body, which is referred to as the near wake region or transition region, where development of the wake is influenced by the boundary layer velocity profile and the turbulence intensity distribution. This research will exploit these characteristics of the near wake by introducing trailing edge configurations to alter the velocity profile and turbulence distribution. The second part of the wake, the similarity region, occurs downstream of the transition region. Initial disturbances decay in the transition region and plots of the non-dimensional velocity at various locations in the similarity region will collapse to a single universal curve as discussed by Abramovich (Ref 1: 8-10).

Five divider plate trailing edge configurations were tested. Figure 1 in Appendix A shows the divider plates, their dimensions, and the symbol used for each in the plotted data. The square plate was selected as a typical trailing edge configuration which will generate turbulence as a result of a small recirculation region immediately behind the trailing edge followed by the shear interaction of the two flow streams.

The knife-edge plate was selected as a configuration which would provide a small influence due to the trailing edge and the resulting wake would be due to the plate boundary layers and shear between the parallel flows.

The remaining plate configurations involve modifications for which the shape of the trailing edge is different at different locations along the edge. Each of these is expected to increase the mixing by the introduction of vertical velocity components which produce vorticity as a result of shear. Throughout this paper, the positive x-direction is defined to be the direction of flow and the positive y-direction is upward.

The slotted plate allows the flow in the slot to accelerate while the flow on the tab is being restrained by shear forces in the boundary layer. This results in a gradient in x-velocity between the tab and slot flows which produces a vertical shear layer and its associated turbulence.

The Coanda plate exploits the Coanda effect which is the tendency of a fluid to remain attached to a surface along which it is flowing as the surface curves away from the fluid. The curved surfaces were placed alternately along the trailing edge to provide positive and negative y-velocity components in the near wake region and to increase the mixing by producing shear which should result in the formation of a vortex behind each pair of curved edges.

The final configuration consists of tabs on the trailing edge which are alternately bent up and down. This plate will

introduce large y-velocity components by deflecting the flow. This trailing edge modification is unique among the five tested because its modification extends beyond the original plate thickness. Higher levels of vorticity and improved mixing are therefore expected.

Each of these plates was evaluated to determine its performance in promoting mixing and the best mixer determined.

III. Apparatus and Procedures

This chapter provides a description of the apparatus and test equipment and the procedures for their use. In addition, the data which was taken and the data reduction methods are described.

Apparatus Design

The test apparatus was designed to provide two parallel streams of air each of which exhibit low turbulence intensity and a uniform velocity profile similar in appearance to a fully developed turbulent velocity profile. It was also designed with the capability to limit flow through one of the two streams so that various velocity ratios could be tested.

The apparatus is shown in Figure 2. The assembly is divided into an upper and lower flow path by a divider plate. The butterfly valve in the upper path of the manifold was used to control the flow in the upper stream, allowing repeatable velocity ratio selection. The diffuser reduces the flow velocity prior to entry into the stilling chambers which are identical except for support columns in the upper chamber. The columns were required to prevent bending of the divider plate caused by the pressure differential during low velocity ratio testing. Temperature and pressure taps were installed in the side wall of each chamber to aid in estab-

lishing and monitoring the flow conditions. From continuity and assuming a velocity of 300 ft/sec in the test section, the maximum velocity in the stilling chamber was 19 ft/sec, thus the pressure and temperature measured were total values. To enhance the calming capability of the chambers, two open-cell foam baffles supported by screens were installed in each chamber. The baffles were very effective in eliminating the wakes produced by the support columns.

The convergent nozzle accelerates the flow to the desired test section velocity. The nozzle is of square cross section, has elliptical walls, and is divided into two channels by the central dividing plate. Its dimensions are based upon the ASME Standard long radius nozzle. This design was selected to provide smooth transition of the flow from the 4 by 8 in chambers into the 1 by 2 in ducts. Note that an asymmetry is introduced at the divider plate since the flow in each stream is accelerated on only three sides. To ensure transition to turbulent flow and to attenuate the asymmetry in the velocity profiles, two screens in a cross-hatch arrangement were placed at the exit of the nozzle and a duct was included upstream of the test section. The length of the duct was determined experimentally to provide uniform velocity profiles and to minimize boundary layer thickness on the duct walls and test plate. Figure 3 shows typical velocity profiles which were provided by the apparatus.

The test section incorporates optical glass side walls which allowed positioning of the anemometer probe. The test

plates were installed in grooves in the duct side walls and sealed to the divider plate to prevent leakage. The test plate was retained by the duct flange to which the test section was attached. The trailing edge of the test plate protruded one inch into the test section.

A traverse mechanism and probe support were attached to the test section to allow three-dimensional, repeatable positioning of the anemometer probe.

Data Acquisition

A two channel TSI Inc. Model 1050 constant temperature anemometer with a two element hot film sensor Model 1241-20 was the primary instrumentation. A Digitec Model 268 digital DC millivoltmeter and a Hewlett Packard HP 3400A True RMS voltmeter permitted accurate determination of the sensor voltages. The RMS voltmeter was calibrated prior to the test effort and the DC millivoltmeter was calibrated before each days testing by use of its built-it calibration capability.

A constant-temperature anemometer is a device which regulates the current passing through a very small diameter sensor, either wire or film, to keep the sensor at a constant temperature. This research used film sensors which are quartz substrates 0.002 in in diameter coated with a thin layer of gold. As the film is cooled by the moving air its resistance drops, the anemometer senses this drop in resistance and increases the current flow. The voltage drop

across the sensor is then proportional to the flow velocity by a fourth order relation as discussed in the TSI Operators Manual (Ref 7: 4-3). To use the anemometer for flow velocity determination, a calibration curve was generated for each sensor and equations of the curves determined by use of a fourth order Least Squares curve fit computer program. Appendix B provides a discussion of the calibration procedure. The resulting equations provided velocities within 0.5 percent at each point of the calibration data. Two probes were used during the testing. The first, K705, was calibrated three times and the second, K691, was calibrated twice. Calibration curves for each channel are shown in Figure 4 and will be discussed in the Results section.

The procedure for testing was as follows:

1. The instrumentation was turned on and allowed to warm up for at least one hour prior to testing.

2. Ambient pressure and temperature were recorded and the butterfly valve set to the desired velocity ratio setting.

3. The air flow was turned on and adjusted to provide approximately 300 ft/sec in the lower stream of the test section. The chamber pressure was recorded and monitored during the test to insure stable flow conditions throughout each test. Fluctuations of $\pm$ 0.5 in of H_2O were accepted.

4. Upper and lower chamber temperatures were recorded before and checked after each test. Variation of these temperatures was generally less than 3C which according to Bradshaw (Ref 4: 171) should not adversely affect the data.

5. With the anemometers in STANDBY, the probe was inserted into the probe holder and aligned so that the sensors were positioned in a plane perpendicular to the trailing edge as discussed in Appendix C.

This orientation allows determination of the x- and y-velocity components.

6. Both channels of the anemometer were then switched to RUN and the probe positioned in the flow by use of the traverse. DC and RMS voltage readings were then recorded for each channel of the anemometer at traverse increments of 0.1 in. When fluctuating voltage readings were encountered, as in the wake region near the plate trailing edge, as estimated average was recorded.

Initial tests were conducted to check out the test equipment and to determine the flow quality of the apparatus at several locations downstream of the divider plate trailing edge. Each test plate configuration was then tested.

Three traverse locations were used during the testing. Location A was 0.15 in downstream of the test plate trailing edge. Location B was 3.25 in downstream of A and location C was 6.5 in downstream of A. With a plate thickness t of 0.062 in, the locations are downstream from the trailing edge by a distance $\frac{x}{t}$ of 2.4, 54.8, and 107.3 respectively.

Testing was done at velocity ratios Ur of nominally 1.0, 0.6, and 0.3 where the velocity ratio is defined as the ratio of the low speed flow to the high speed flow at location A. The valve settings to provide these ratios were established by experimentation and marked on the valve body for repeatability.

Data Reduction

The calibration curve equations and their first derivatives were used in a computer program to determine the desired parameters from the DC and RMS voltage data. The

parameters which were calculated and are presented in graphical form are the local mean velocity $\bar{U}$, which, except in the near wake region is approximately equal to the x-component of the mean velocity, the y-component $\bar{V}$ of the mean velocity and the turbulence parameters TU_x and TU_y.

Appendix C gives a brief discussion of the derivation of the equations used to compute the velocity components from x-probe data. The resulting equations are presented here for convenience.

$$u = 0.707\ (u_1 + u_2)$$

$$v = 0.707\ (u_1 - u_2)$$

$$\bar{U} = (u^2 + v^2)^{1/2}$$

where u and v are the x- and y-velocity components and u_1 and u_2 are the velocity components which are perpendicular to sensors 1 and 2. These equations assume the sensors are perpendicular to each other and at 45 degrees to the x-direction. The velocity data were non-dimensionalized by dividing by the maximum mean velocity at the location A centerline traverse. These data were then used in determination of wake edge location.

The turbulence parameters were also selected as an aid in locating the edge of the wake and are defined by the following equations:

$$TU_x \equiv \frac{u'}{\bar{U}}$$

$$TU_y \equiv \frac{v'}{\bar{U}}$$

where u′ is the x-component and v′ is the y-component of the fluctuating velocity, and are determined from the DC and RMS voltage data as follows:

$$u_1' = m_1 (V_{rms})_1$$

$$u_2' = m_2 (V_{rms})_2$$

$$u' = 0.707 (u_1' + u_2')$$

$$v' = 0.707 (u_1' - u_2')$$

where m is the slope of the calibration curve for each sensor evaluated at the test point and V_{rms} is the RMS voltage across the sensor. This method assumes a linear calibration curve over the range of the fluctuation and is valid for turbulence levels less than 5 percent. Freestream turbulence was less than 2 percent so the turbulence parameter is acceptable for use in locating the wake edge. Within the wake, the turbulence parameter was used as an indicator of relative turbulence generated by the various trailing edge configurations and is later evaluated as an indicator of the mixing generated by the test plates.

All data is presented in non-dimensionalized form to reduce the effects of temperature and humidity changes which occurred during the research effort. Bradshaw (Ref 3: 117) states that errors of 2 percent can result from a temperature change of one degree Celcius. The temperature range for this test effort was 23 to 31 C and all tests were accomplished within 4 C of the applicable calibration temperature.

IV. Results and Discussion

This section presents a discussion of the data from each test configuration. Wake width and wake growth rate as determined from the velocity and turbulence data for each configuration as well as maximum turbulence levels are evaluated as indicators of mixing. The effectiveness of the modifications is also discussed.

Apparatus Flow Quality

Initial testing was conducted with the square test plate to determine boundary layer thickness on the plate and the test section walls. The upper and lower wall boundary layers were found to merge with the wake at a distance 7.88 in downstream from the plate trailing edge. The C traverse location was therefore located a distance of 6.5 in downstream of the trailing edge so that a wake edge would be clearly discernable. The traverse locations are shown in Figure 5. As will be discussed later, the wake edge location is not obvious at the low velocity ratio, Ur = 0.3. This trend is consistent throughout the data in that there is a high degree of variation among the test plates for 0.3 velocity ratio data at the C traverse location.

Figure 3 shows the velocity profiles of the lateral

and vertical traverses for the upper and lower streams. The boundary layers on the plate and upper and lower walls are approximately 0.25 in thick which correlates with the theoretical turbulent boundary layer thickness of 0.20 in from Schlichting (Ref 9: 638).

$$\delta = 0.37 x Re^{-1/5}$$

The Reynolds number of the flow was calculated based upon the distance x from the screens at the convergent nozzle exit. A value of 14.5×10^5 was determined for the high speed flow and 4.5×10^5 for the low speed flow (Ur = 0.3). The low speed flow Reynolds number is in the transition region and its plate boundary layer is shown to be approximately 0.1 in thick as compared to a calculated turbulent thickness of 0.24. Using the laminar boundary layer equation from Schlichting (Ref 9: 140)

$$\delta = 5 x Re^{-1/2}$$

the theoretical boundary layer thickness is 0.065 in which indicates the boundary layer of the low speed flow may be laminar or in transition. The velocity profiles and lateral traverses show uniform profiles similar in appearance to fully developed turbulent flow with no discontinuities in the profile.

With the apparatus in a configuration capable of providing the desired velocity profiles, no further changes to the apparatus were made and detailed testing was accomplished for each trailing edge configuration.

Detailed Testing

Several traverses were made and data taken at each location at increments of 0.1 in. The traverses are shown in Figure 5 for each of locations A, B, and C and will be referred to as centerline, slot, and lateral traverses. The "slot" traverse as used in this research is defined as a vertical traverse which is located 0.2 in from the channel centerline and does not imply the existence of a slot in the test plate trailing edge. For example, slot traverses were accomplished for the square plate to verify their similarity to the square plate centerline traverses. These data are plotted on the slot traverse profiles for comparison with data from the other configurations. Slot traverse data for the knife-edge plate was not taken due to this similarity but were taken for the other configurations since each exhibits a unique shape at the slot location which is different than the shape at its centerline location. Data at location B typically indicates that the flow is approaching uniformity in the lateral direction, i.e. disturbances have dissipated, so that only the centerline traverse was tested at location C. Figures 6-8 show that the flow is approaching similarity for each plate since the non-dimensional data collapse onto a single curve. This characteristic shows that the results are not dependent upon the test apparatus and verifies suitability of the apparatus for flow testing. Table I summarizes the wake width, wake growth rate dy/dx, and the maximum

TABLE I

Data Summary

Wake Width

Parameter	Location	Square			Slotted			Knife-edge			Coanda			Tab		
		1.0	0.6	0.3	1.0	0.6	0.3	1.0	0.6	0.3	1.0	0.6	0.3	1.0	0.6	0.3
$\bar{U}/\bar{U}MAX_A$	A	.43	.40	.30	.45	.45	.25	.45	.45	.23	.43	.40	.23	.53	.40	.35
	B	.45	.50	.50	.45	.50	.50	.45	.50	.50	.50	.55	.50	.60	.45	.75
	C	.52	.55	.80	.55	.60	.77	.50	.60	.75	.53	.67	.80	.75	.65	.95
	dy/dx	.014	.023	.077	.015	.023	.080	.008	.023	.080	.015	.042	.088	.034	.038	.092
TU_x	A	.6	.57	.33	.57	.55	.35	.57	.57	.3	.57	.60	.33	.70	.65	.50
	B	.65	.65	1.03	.60	.65	1.1	.60	.55	.97	.60	.60	.95	.80	.80	1.05
	C	.75	.75		.70	.73		.65	.67		.65	.70		.90	.90	
	dy/dx	.023	.028	.215	.020	.028	.231	.012	.015	.206	.012	.015	.191	.031	.038	.169
TU_y	A	.43	.40	.57	.45	.45	.75	.50	.40	.67	.45	.45	.35	.50	.45	.45
	B	.53	.40	.95	.50	.50	1.07	.53	.45	.75	.55	.47	.87	.70	.70	1.0
	C	.63	.60		.53	.63		.55	.60		.57	.60		.80	.83	
	dy/dx	.031	.031	.117	.012	.028	.098	.008	.031	.025	.018	.023	.160	.046	.058	.169

Maximum Wake Turbulence, Centerline Traverse

TU_x	A	.299	.242	.226	.345	.349	.430	.121	.148	.207	.315	.094	.331	.151	.115	.247
	B	.076	.105	.252	.066	.103	.304	.065	.097	.263	.071	.098	.231	.072	.112	.221
	C	.060	.100	.318	.055	.097	.337	.054	.088	.326	.054	.09	.268	.051	.09	.252
TU_y	A	.019	.020	.023	.031	.086	.129	.021	.043	.070	.076	.028	.117	.030	.025	.086
	B	.021	.031	.071	.018	.033	.074	.018	.029	.068	.018	.028	.057	.013	.025	.052
	C	.015	.028	.081	.016	.030	.105	.015	.026	.087	.013	.025	.064	.011	.025	.055

turbulence parameter data which were obtained from the plotted parameters. The wake growth rate is defined to be the wake width at location C minus the wake width at location A divided by the distance between A and C.

Mean Velocity: The mean velocity profiles for the centerline traverses, Figures 9-11, and the slot traverses, Figures 12-14, show an increase in wake width and in wake velocity, and a slight decrease in the high speed maximum velocity from location A to C. The edge of the wake was defined to be the point in the flow at which the wake velocity was equal to 90 percent of the freestream velocity on the corresponding side of the wake. As can be seen in Table I, the wake width of the four plates whose modifications were restricted to the plate thickness are nearly identical for a velocity ratio of 1.0. Consequently their wake growth rates are nearly identical. The tab plate, however, has a wake at location A which is 22 percent wider than the other plates due to its bent tabs protruding into the boundary layer. At location C, the tab plate wake is 41 percent wider than the wakes of the other plates which indicates the tab plate is a better mixer at a velocity of 1.0. This is also indicated by the tab plate wake growth rate which is more than twice that of the square, slotted and Coanda plates and four times that of the knife-edge plate. The relative results for the 0.6 velocity ratio are the same with the exception that the Coanda plate and tab

plate have nearly equal wake growth rates which are 70 percent greater than the other plates. Note that the wake growth rate for all plates is larger at the 0.6 velocity ratio than at the 1.0 ratio. The wake width at location A remained essentially constant for all plates except the tab when compared to the Ur = 1.0 data. The tab plate wake widths at each location were less for the Ur = 0.6 data.

The Ur = 0.3 data show a further decrease in wake width at location A and a notable increase in wake growth rate for all plates. This increase is in agreement with experiments by Yakovlevskiy and Zhestkov as cited by Abramovich (Ref 1: 153) which show that the angle of thickening of the mixing zone ceases to depend on the velocity ratio for ratios greater than 0.4. The Coanda and tab plates exhibit wake growth rates greater than the other plates with the tab plate wake growth rate being slightly greater than that of the Coanda. Note in Figure 11c that the wake and wall boundary layer have nearly merged which makes wake edge identification difficult.

In summary, the mean velocity data shows no difference between the square, slotted, and knife-edge plates ability to mix parallel flows at the three velocity ratios tested. An exception to this is the smaller wake growth rate for the knife-edge plate at Ur = 1.0. The tab plate is the best mixer of the configurations tested for Ur = 1.0 and 0.3 based upon the mean velocity data. The Coanda is a slightly better

mixer at the 0.6 velocity ratio.

These results show that the Coanda and tab plates are introducing disturbances into the flow, as discussed in section II, which result in improved mixing of the parallel flows.

The plots of the y-component of the mean velocity, Figures 15-20, were not useful in determining wake width but do show the negative and positive y-velocity components which, according to Prandtl as cited by Abramovich (Ref 1: 11), control the growth rate of a jet. As discussed by Abramovich (Ref 1: 173), the mixing at the edge of the wake results in a pressure gradient but, since the pressure must be constant across the flow, the streamlines are bent resulting in the y-velocity components. Note that the tab plate introduces significantly larger y-velocity components than the other test plate configurations. This was expected due to the tabs protruding into the boundary layer, deflecting the flow. Figure 15a shows that a positive component in the wake equal to 15 percent of the freestream velocity is introduced by the upward bent tab and Figure 18a shows a negative component of 15 percent of freestream is introduced by the downward bent tab. These traverses are separated by a distance of 0.2 in so a gradient in the lateral direction exists in the y-velocity which is equivalent to 30 percent of the freestream velocity. This gradient, which exists between each pair of tabs, introduces rotation in the flow downstream

of each pair of tabs. This rotation results in increased mixing in the near wake region and is evident in the lateral traverses which are discussed later. The location B traverses show that the effects of the tab plate are visible downstream as compared to those of the other configurations which are not. Velocity disturbances in the y-direction are negligible at location C for all configurations tested. Note at the A location, the square plate results in larger y-components than those of the Coanda plate. This result was not expected but may be due to the recirculation region created by the sudden disappearance of the square plate which could be disrupted somewhat by the Coanda flow for that plate. This is reinforced by the knife-edge data which exhibits the smallest y-velocity component and would, if one exists, have a very small recirculation region. Note that the y-components are typically less than 5 percent which is in agreement with Bradshaw (Ref 4: 57).

Data for the 0.3 velocity ratio exhibits irregularities on the low speed side which are unexplained. During the test effort a shift in the y-velocity "zero" was experienced. In reduction of the data, the y-velocity data was adjusted to zero by subtracting or adding a constant. This constant was determined by knowing that the y-component near the test section wall and at location C should be nearly zero. This is verified by the adjusted y-velocity profile at location C, Figure 15c, which shows a uniform profile of zero velocity.

Some of the irregularities in the Ur = 0.3 y-velocity data may be due to inadequacies in this correction. Possible causes of the zero shift are discussed later.

Turbulence Parameter: The turbulence data shown in Figures 21-32 were also used to identify the edge of the wake. The wake edge was defined to be the location in the wake where the magnitude of the turbulence is 3 percent or where it is 1 percent greater than the freestream turbulence. The wake width at location C for Ur = 0.3 was not determined due to the high degree of variation in the profiles on the low speed side of the flow as shown in Figure 23c. These variations are thought to be due to interaction of the wake with the upper wall boundary layer. Wake growth in Table I is based upon locations A and B for Ur = 0.3.

Table I summarizes the wake width and wake growth rate data for the x- and y-direction turbulence. In general, based upon y-turbulence data, the wake width for Ur = 1.0 and 0.6 nearly corresponds with that from the mean velocity data while the x-turbulence data consistently yields larger wake widths. Both x- and y-turbulence data show that as the velocity ratio decreases, the wake width at location A decreases but the wake growth rate increases. The wake growth rates based upon y-turbulence data are lower than those from x-turbulence data. The tab plate turbulence data shows higher wake growth rates than the other plates at all velocity ratios except for TU_x at Ur = 0.3.

Based upon the x-turbulence data, the square and slotted plates exhibit wake growth rates at all velocity ratios which are greater than those of the knife-edge and Coanda plates. The wake growth rates determined from the y-turbulence data do not indicate that one of the square, slotted, knife-edge or Coanda plates is a better mixer than the other three.

The turbulence data for Ur = 0.3 show wake growth rates at the B location which are larger than those from the velocity data at the C location. This supports the opinion that the wake and wall boundary layers for low velocity ratios are merging prior to location C and resulting in the profile variations at that location.

In summary, the tab plate provides the best mixing based upon its larger wake growth rate determined from the turbulence data. Also, the square plate provides slightly larger wake growth rates than the slotted, knife-edge, and Coanda plates. This is possibly due to a more organized recirculation region at the trailing edge which is disrupted by the flow patterns of the other configurations.

Relative magnitude of the turbulence data was also compared in the wake region. The turbulence values given in Table I are the values of maximum turbulence in the wake region. A surprising result is that no correlation between the maximum turbulence and the mixing ability of the plate is evident. Turbulence levels generated by the tab plate, which has been identified as the best mixer, are equal to or lower

than those of the other plates. The slotted plate generally had the highest turbulence levels at location A and yet was not identified by the other factors as a good mixer. This lack of correlation may be due to the traverse location not being located at the point of maximum turbulence for each configuration.

Note that the turbulence values at location C are less than those at location A in all cases except Ur = 0.3 for the square and knife-edge plates. According to Alber (Ref 2: 276) the turbulence intensity will decrease in a wake and increase in a jet with increasing downstream distance $\frac{x}{R}$ until $\frac{x}{R} \approx 30$. Schlichting (Ref 9: 751) shows a plot of a two-dimensional wall jet velocity profile which becomes similar at a downstream distance $x/R \geq 20$ where R is the width of the jet in the y-direction. Figure 33 is a plot of the velocity profiles of the square and knife-edge plates at location C and the curve from Schlichting. Note that x/R = 6.5 at location C so that similarity is not entirely obtained, however, the shape of the curves is generally the same as that of the similarity curve. It appears that the wake region behind the dividing plate of parallel flows transitions from a wake to a jet boundary at low velocity ratios. This would explain the increasing turbulence parameters at the low velocity ratio. Note that this reversal in turbulence level did not occur for the plate configurations whose shape varied along the trailing edge as discussed in section II. This

could indicate that Ur = 0.3 is nearly the maximum velocity ratio at which this transition occurs. Also note that for Ur = 0.3 the turbulence levels at location A for the square and knife-edge plates are lower than those of the other plate configurations. The higher level of turbulence in the near wake region for the other plates may have prevented the transition. As stated by El-Assar and Page (Ref 6: 1388) the turbulence intensity distribution in the transition region plays an important role in the development of the wake.

Lateral Traverse Data: Data was also taken parallel to the trailing edge of the plates at locations A and B. Data from these lateral traverses, Figures 34-45, show the effects of the trailing edge modifications upon the velocity and turbulence in the near wake region. Lateral traverse data for the square plate, which is constant along the trailing edge since the trailing edge shape is constant, were omitted from the lateral data plots for clarity.

A trailing edge shape parameter W was defined as the distance along the plate trailing edge from its centerline divided by 0.2 in, the width of a tab. In terms of this shape parameter the centerline traverse was located at W = 0 and the slot traverse at W = 1.0. The half values of the shape parameter, as marked on the vertical axis of the figures, are the location of the edges of the modifications, e.g. the edge of the tabs. Data were taken at 0.1 in increments so that the flow parameters were determined on the

edges and centerline of each modification.

In examining data from the lateral traverses, repeatability was generally found. In other words, a parameter measured on the centerline of a tab had nearly the same value as that measured on a similar tab centerline. Exceptions to this generality are noted and could be due to several factors. First, the flow in the wake at location A is very turbulent. The turbulence resulted in fluctuations in the DC voltage of the anemometer. When this occurred, an estimated average was taken which would introduce scatter into the data. Another source could be slight differences in the size or shape of the modifications. Also, the tabs on the tab plate may not have all been bent to the same angle.

The mean velocity profiles in Figures 34-36 show tab plate mean velocities $\overline{U}/\overline{U}MAX_A$ of 0.8 on the centerline of the tabs which deflect upward (toward low speed flow). This value is nearly constant for all velocity ratios. The mean velocities on the centerline of the tabs which deflect downward decrease with decreasing velocity ratio as do the velocities on the edges of the tabs. The difference in mean velocities between the upward and downward bent tabs was about 40 percent as compared to 20 percent for the slotted plate and 5 percent for the Coanda plate. This difference increases with decreasing velocity ratio. The slotted plate mean velocity behind the slots is higher than behind the tabs because the downstream distance $\frac{x}{t}$, where t is the plate

thickness, is three times that behind the tab. The greater distance allows more time for momentum transfer to accelerate the flow in the slot. The location B traverse shows the effects of the modifications are carried downstream but are much smaller than at A.

The y-velocity data in Figures 37-39 show the same trends. The vertical velocity gradient between adjacent tabs is seen to be about 35 percent of the freestream for the tab plate and about 8 percent for the slotted and Coanda plates and decreases with decreasing velocity ratio. As mentioned earlier this velocity gradient results in shear in the vertical plane between each pair of tabs. This shear generates a vortex in the wake behind each pair of tabs as shown in Figure 46. Note that counter rotating vortices exist. It is expected that the vortex flow system illustrated in Figure 46 would exhibit a relatively steady, low level of y-turbulence. The turbulence measurements shown in Figures 43a and 44a are consistent with this. These vortices act to entrain the freestream fluid and enhance mixing as is evident in the higher wake growth rates for the tab plate. The Coanda plate exhibits similar rotation but to a smaller degree. The lower effectiveness of the Coanda is possibly due to the thickness of the divider plate boundary layers.

Error Analysis

Potential sources of error will be discussed in this section as well as their effect upon the data.

Bradshaw stated that temperature variation of the test fluid can result in significant errors. He also indicates that these effects can be reduced by running the probe element at a high temperature. Overheat ratios of 1.5 were used to maintain a high probe temperature. Test fluid temperatures ranged from 23 to 31 C over the entire test effort with most testing accomplished in the 26 to 30 C range and within 4 degrees of the calibration temperatures. Changes in the ambient humidity also affect the data. To minimize the effects of these variables, all data are presented in normalized form. Since most testing was over a small range of temperature variation, this error is considered to be small.

Errors can also result from contamination of the probe elements by collection of dust. To minimize these effects one probe was calibrated three times and the other twice. As shown in Figure 4, a shift in the calibration curves occurred. Note that the curve for channel 1 shifted more than for channel 2. The existence of this shift was first noticed when the y-velocity zero shift occurred. As indicated by the calibration curves an error of about 3 percent could be present in data taken just prior to each recalibration. This shift in calibration was primarily due to a change in resistance of the probe elements with use. TSI Inc. is currently investigating the cause of this resistance change. This error is considered to be the primary source of error in this research.

As mentioned in the lateral traverse discussion, error occurs in high turbulence regions due to the DC voltage fluctuations which result. This is not considered to be significant since fluctuations did not occur at the wake edge which was used in determining the wake width and wake growth as indicators of mixing. Generally the fluctuations in the RMS voltage were small and turbulence data is therefore considered to be accurate throughout the flow. Repeatability of the data was verified by retest of selected points throughout the flow which are plotted with "blacked in" symbols. As shown, the data is repeatable.

A final source of error is the relative angle of the probe sensors to each other and the flow. The sensors should be perpendicular to each other and at 45 degrees to the flow direction. These assumptions were made in the derivation discussed in Appendix C. Both of the probes used were checked and found to be within 1 to 2 degrees of being perpendicular. Alignment of the probe with the stream was checked and corrected when necessary. Error due to sensor angles and misalignment are considered to be negligible.

V. Conclusions and Recommendations

The following conclusions are made with regard to the effect of divider plate trailing edge shape upon the mixing of parallel flows. Incompressible flow data for velocity ratios from 0.3 to 1.0 were evaluated.

1. Trailing edge modifications which do not extend beyond the plate thickness produce no significant improvement in the mixing. The plate with tabs which are bent to extend beyond the plate thickness into the boundary layer is the best mixer of the five configurations tested.
2. The wake growth rate parameter was a more reliable indicator of the mixing generated by a divider plate than the wake width or the maximum turbulence. The growth rate was determined from normalized velocity and turbulence profiles.
3. The normalized mean velocity profiles are more suitable for wake growth rate determination than the turbulence profiles. Both velocity and turbulence profiles show a progressive increase in wake growth rate with decreasing velocity ratio.
4. No correlation could be determined between mixing and the maximum turbulence in the wake.

5. The wake which forms between parallel, co-flowing streams behind a divider plate exhibits the characteristics of a jet boundary at low velocity ratios.

Recommendations

To increase the level of understanding of the effects of these and similar trailing edge modifications the following research could be accomplished.

1. Other trailing edge modifications could be made such as the use of vortex generators. The losses due to the protrusion of the bent tabs or vortex generators into the flow could be studied with the aid of a computerized data system to allow determination of momentum deficit. Investigation of vortex shedding from the various configurations and the effect of the vortices upon mixing could also be studied by taking data at smaller traverse increments.
2. The effect of plate thickness could also be investigated. In other words, the increased mixing may have been due to an effective increase in plate thickness for the tab plate.
3. Optical methods could be attempted with the use of seeding with a low molecular weight gas to increase the density gradient. The separate stilling chambers of the apparatus would be well suited to the seeding of one of the streams.

Bibliography

1. Abramovich, G. N. The Theory of Turbulent Jets. Cambridge, Massachusetts: The MIT Press, 1963.

2. Alber, I. E. "Turbulent Wake of a Thin, Flat Plate," AIAA Journal, 18: 1044-1051 (September 1980).

3. Bradshaw, P. An Introduction to Turbulence and its Measurement, Pergamon Press, 1971.

4. Bradshaw, P. "Turbulence," Topics in Applied Physics, 12; Springer-Verlag: Berlin, Aeidelberg, N.Y., 1976.

5. de Brederode, V. "Influence of the Side Walls on the Turbulent Center-Plane Boundary-Layer in a Square Duct," Journal of Fluids Engineering, 100: 91-95 (March 1978).

6. El-Assar, R. J. and R. H. Page. "Incompressible Turbulent Wake of a Flat Plate," AIAA Journal, 7: 1388-1389 (July 1969).

7. Operating and Service Manual for 1050 Series Constant Temperature Anemometers and Related Accessories. Product Manual. Cleveland, Minnesota: Thermo-Systems, Incorporated (updated).

8. Rajagopalon, S. and Antonio, R. A. "Characteristics of a Mixing Layer of a Two-Dimensional Turbulent Jet," AIAA Journal, 18: 1052-1058 (September 1980).

9. Schlichting, H. Boundary Layer Theory (Seventh edition). New York, New York: McGraw-Hill Book Company, 1979.

10. Turbulence in Internal Flows, A Project SQUID Workshop, PU-R1-77. Purdue University, West Lafayette, Indiana (May 1977).

APPENDIX A

Figures

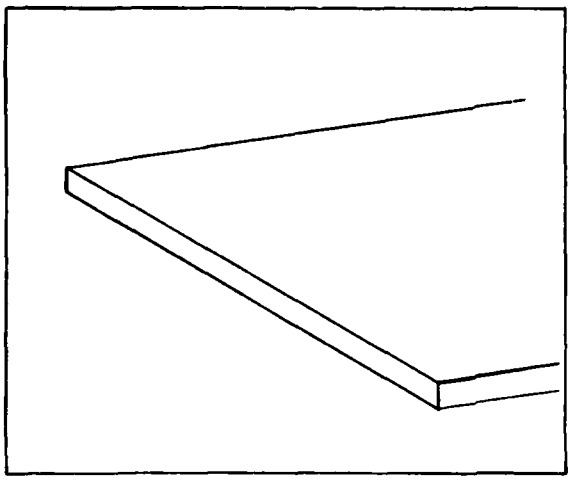

Plate: Square
Symbol: ⊡
Thickness: t = 0.062 in.
Cross Section:

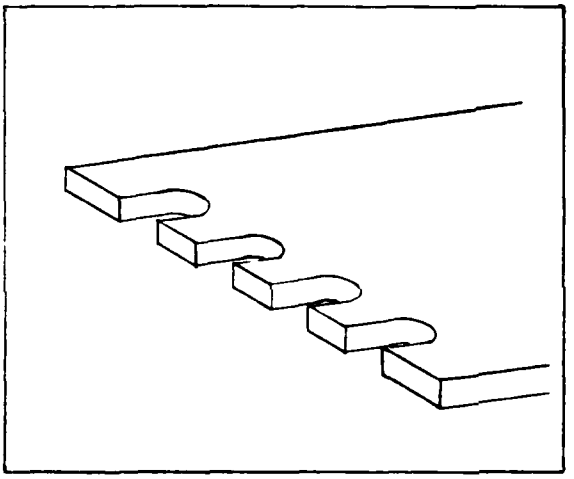

Plate: Slotted
Symbol: ◇
Thickness: t = 0.062 in.
Dimensions: .2 .2 0.2
Cross Section:
Centerline
Slot*

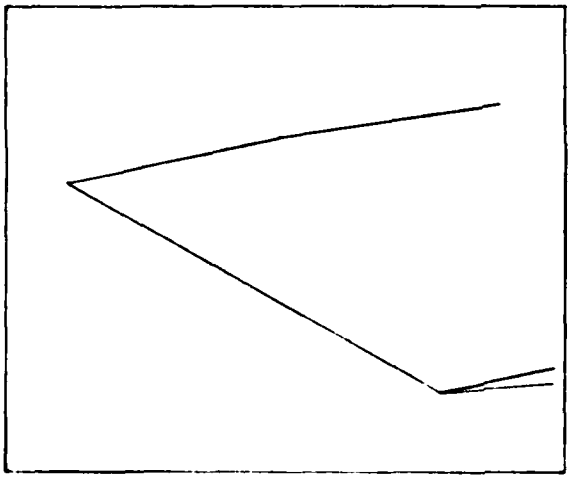

Plate: Knife-edge
Symbol: △
Thickness: t = 0.062 in.
Cross Section: 2.0

Figure 1. Trailing Edge Configurations

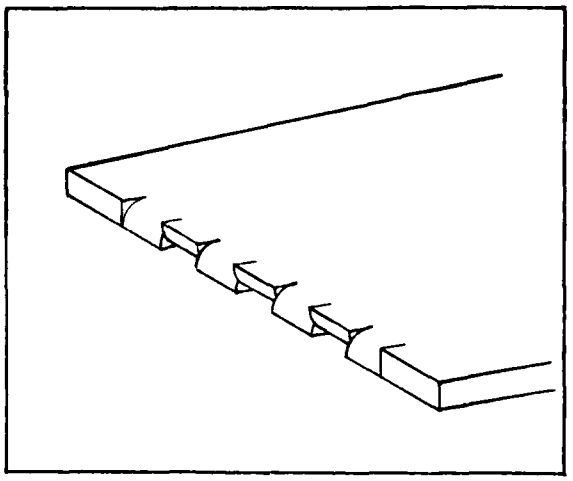

Plate: Coanda

Symbol: ⊙

Thickness: t = 0.062 in.

Dimensions: .2 .2

.062 R

Cross Section:

Centerline

Slot*

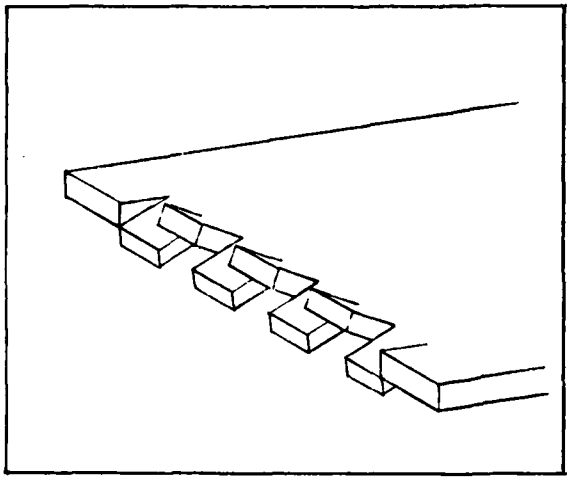

Plate: Tab

Symbol: +

Thickness: t = 0.062 in.

Dimensions: .2 .2

0.2

Cross Section:

Centerline

Slot*

* See Fig. 5 for traverse location

Figure 1 (cont)

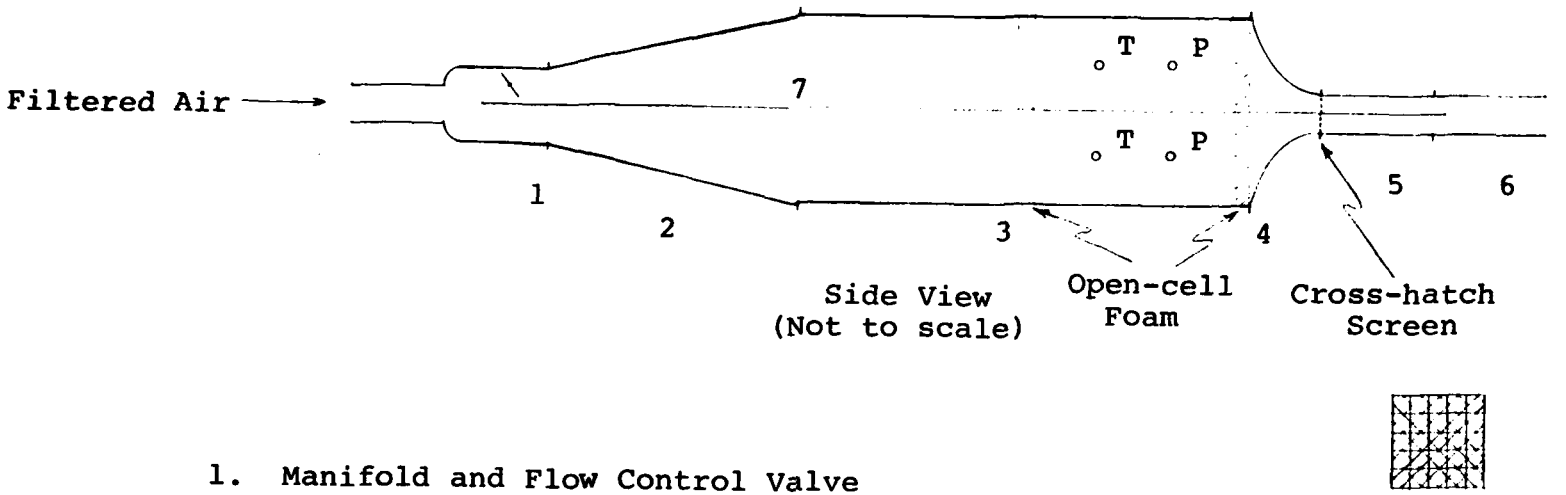

1. Manifold and Flow Control Valve
2. Diffuser
3. Stilling Chamber
4. Convergent Nozzle
5. Duct, 8 in in Length
6. Test Section
7. Divider Plate

T. Thermometer

P. Pressure Tap

Figure 2. Test Apparatus

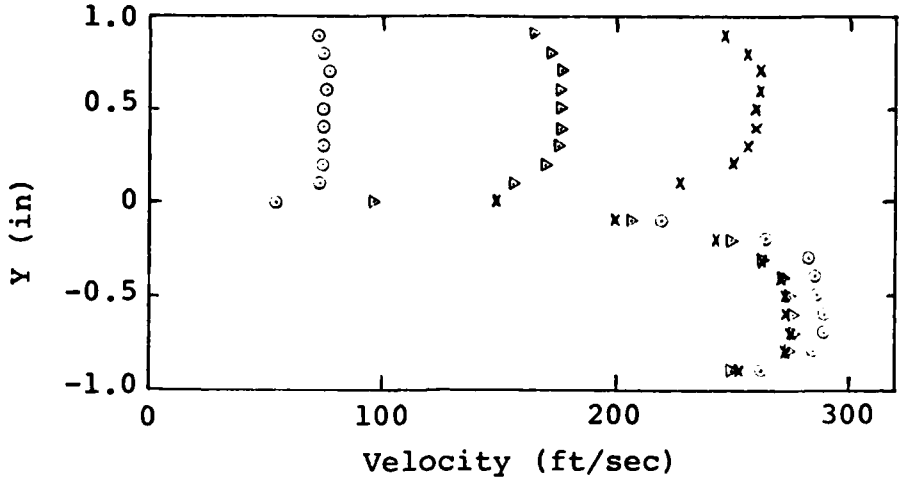

a. Vertical Traverses, Ur = 0.3, 0.6 and 1.0

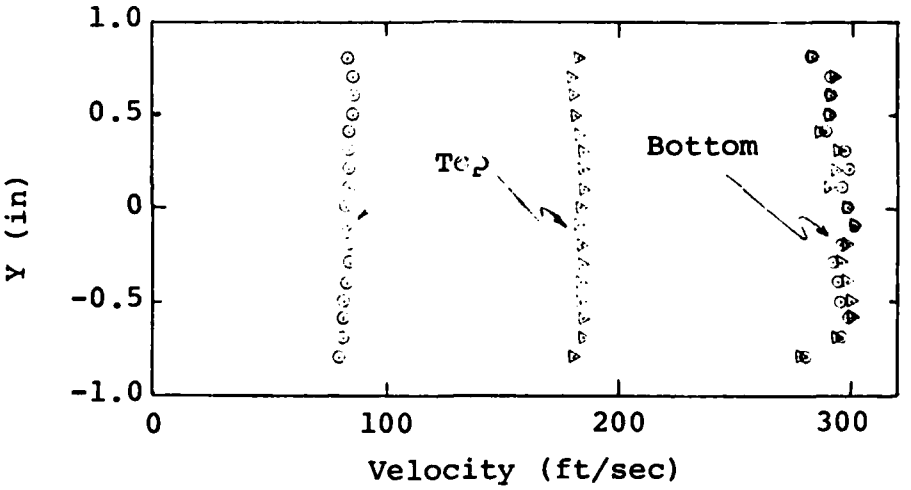

b. Top and Bottom Lateral Traverses, Ur = 0.3 and 0.6

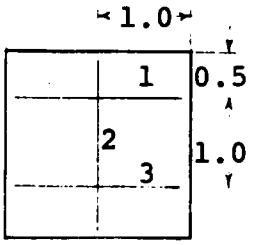

1. Top Lateral Traverse
2. Vertical Traverse
3. Bottom Lateral Traverse

c. Traverse Locations

Figure 3. Velocity Profiles of Apparatus, Location A

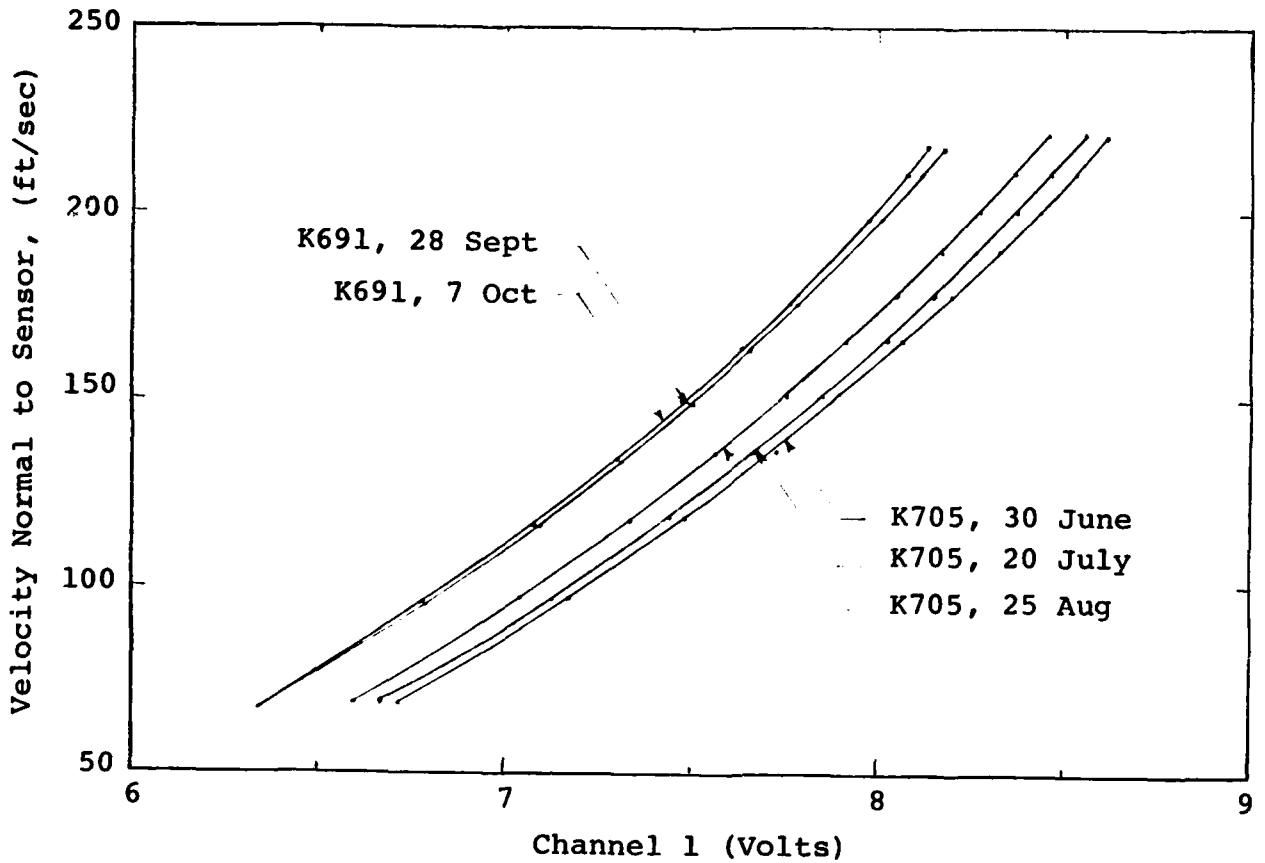

Figure 4. Calibration Curves

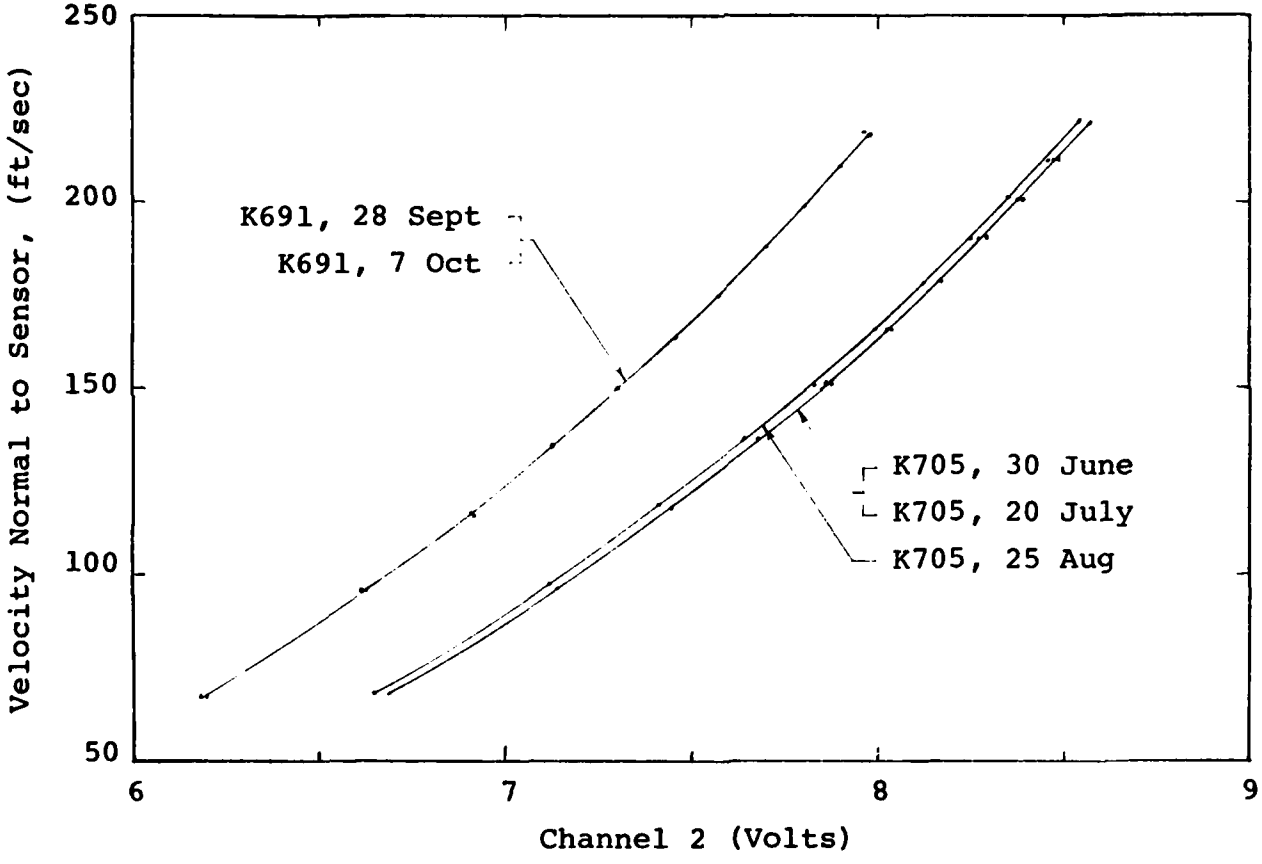

Figure 4 (cont)

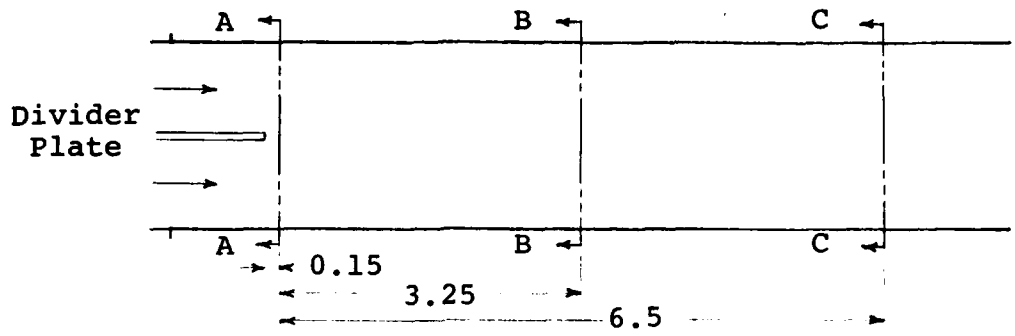

Test Section

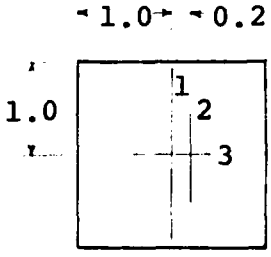

1. Centerline Traverse
2. Slot Traverse
3. Lateral Traverse

A-A

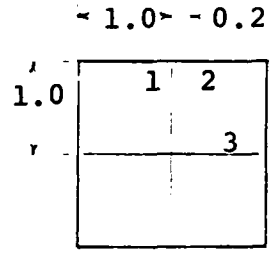

1. Centerline Traverse
2. Slot Traverse
3. Lateral Traverse

B-B

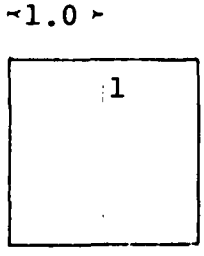

1. Centerline Traverse

C-C

Figure 5. Traverse Locations

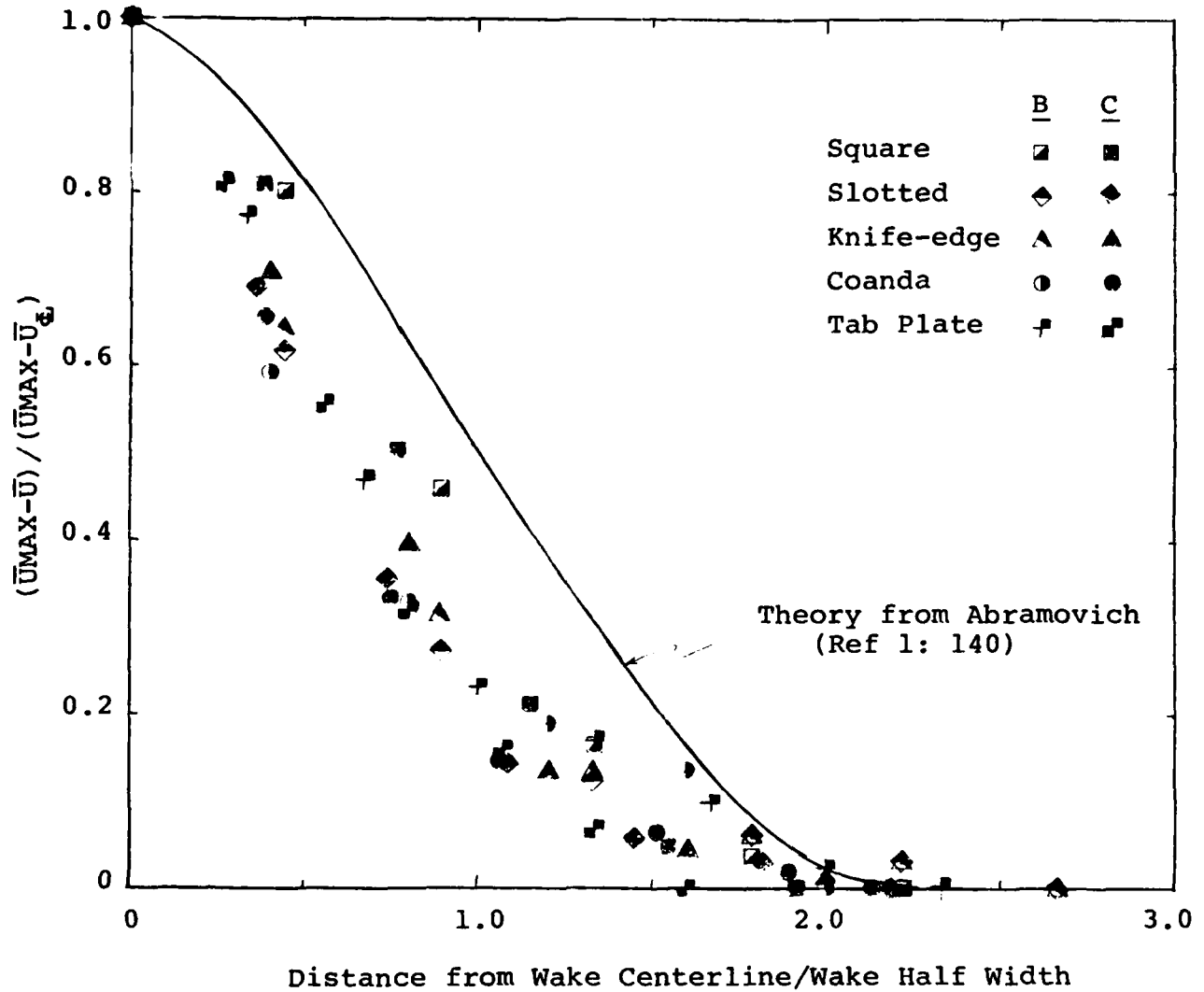

Figure 6. Similarity Plot, Ur = 1.0

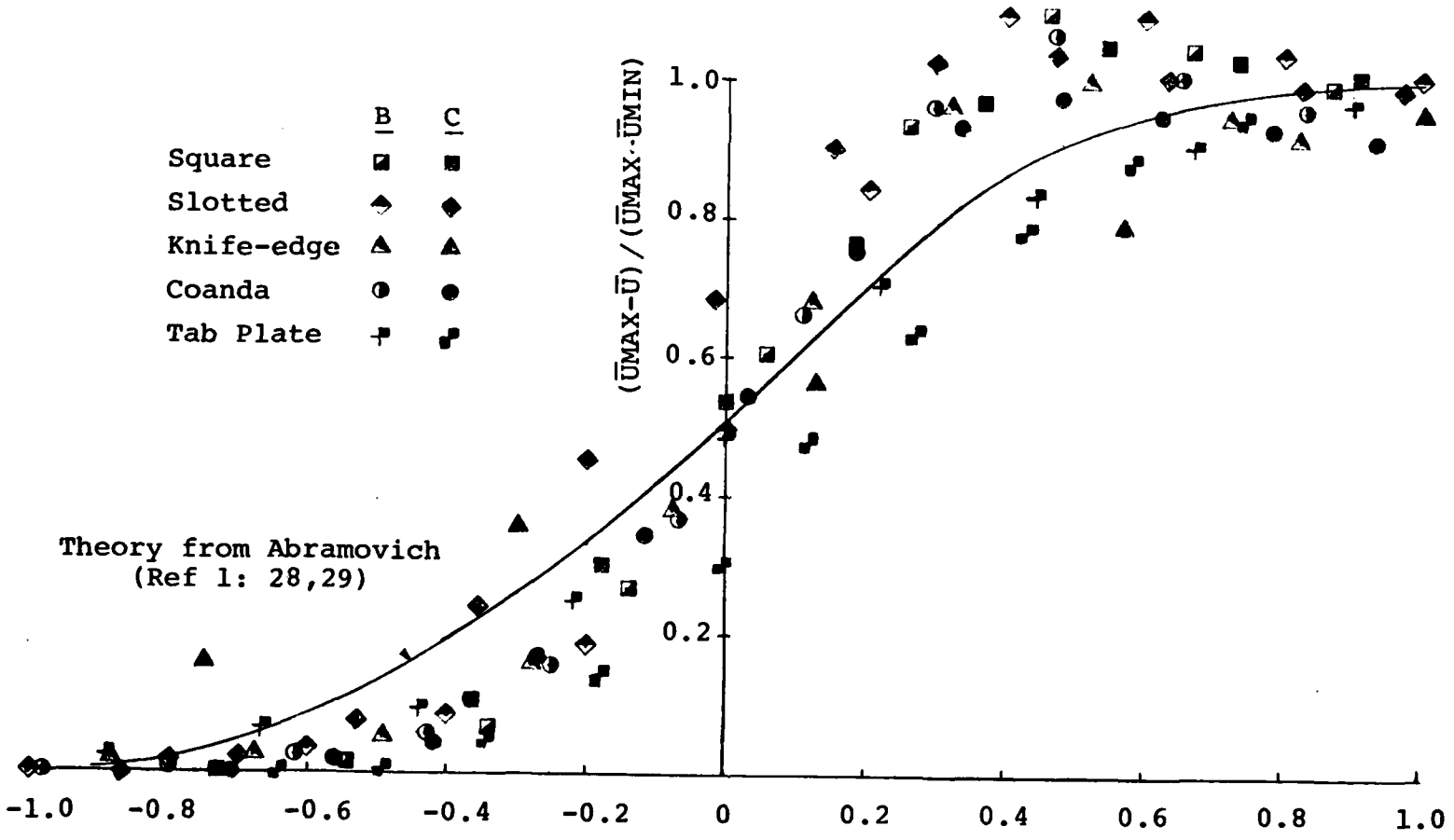

Figure 7. Similarity Plot, Ur = 0.6

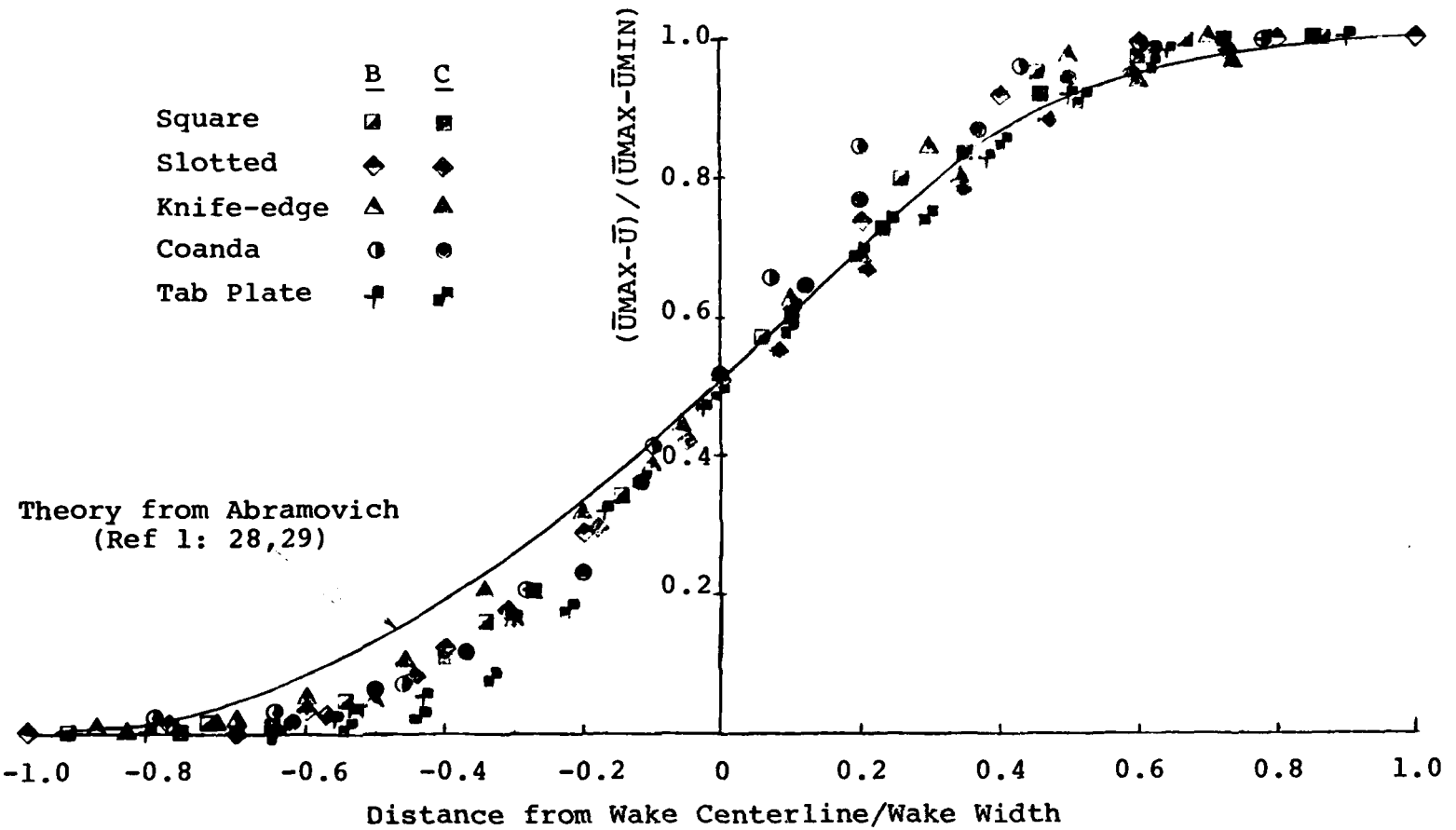

Figure 8. Similarity Plot, Ur = 0.3

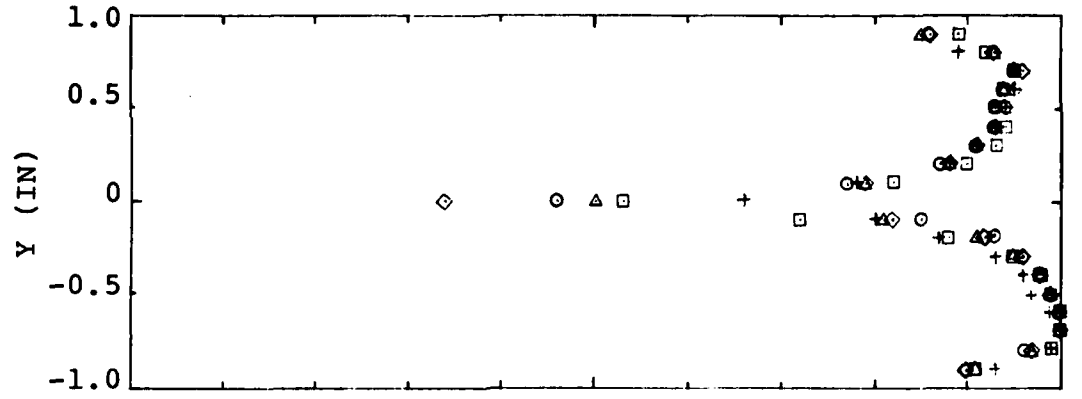

a. Location A

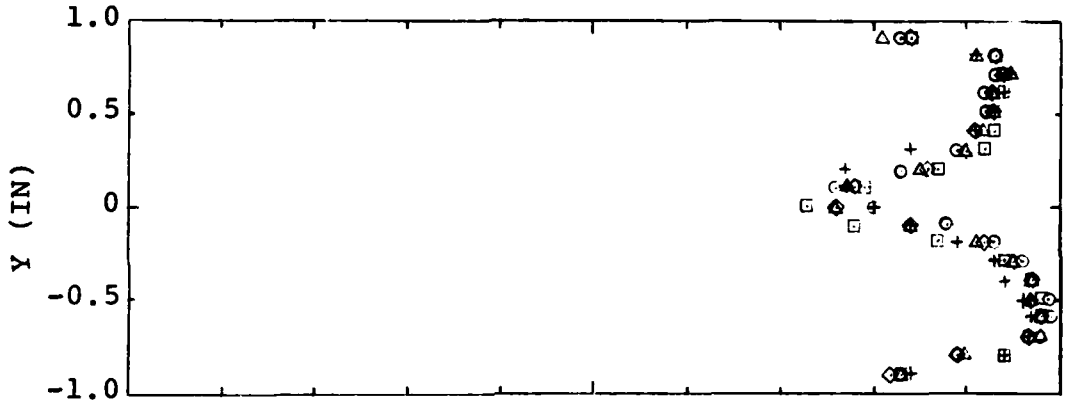

b. Location B

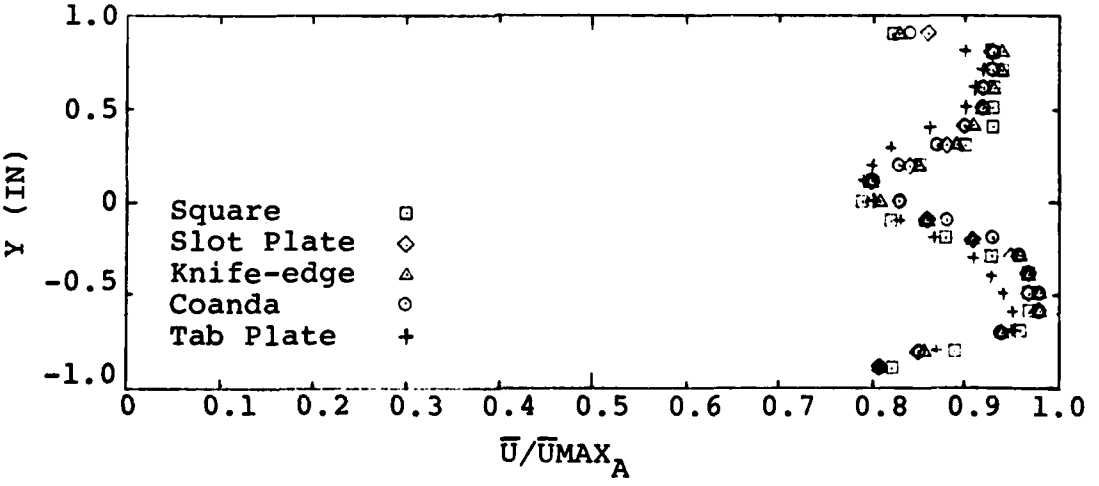

c. Location C

Figure 9. Centerline Mean Velocity Profile, Ur=1.0

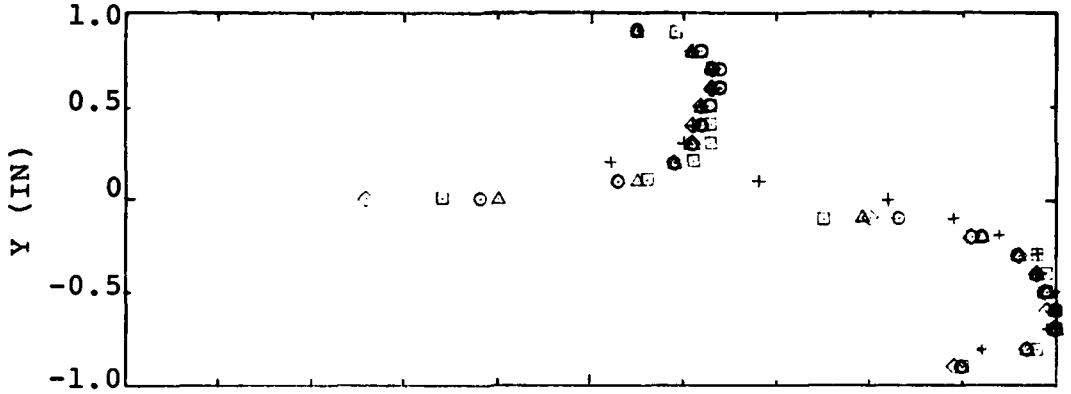

a. Location A

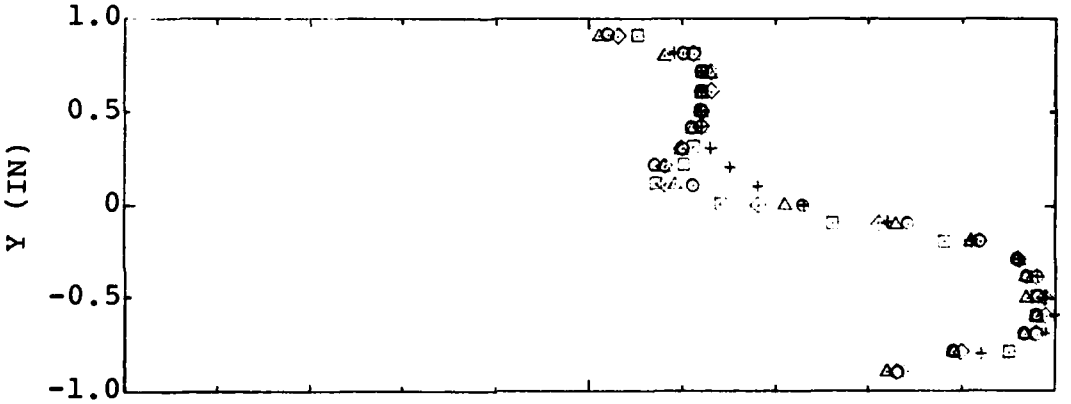

b. Location B

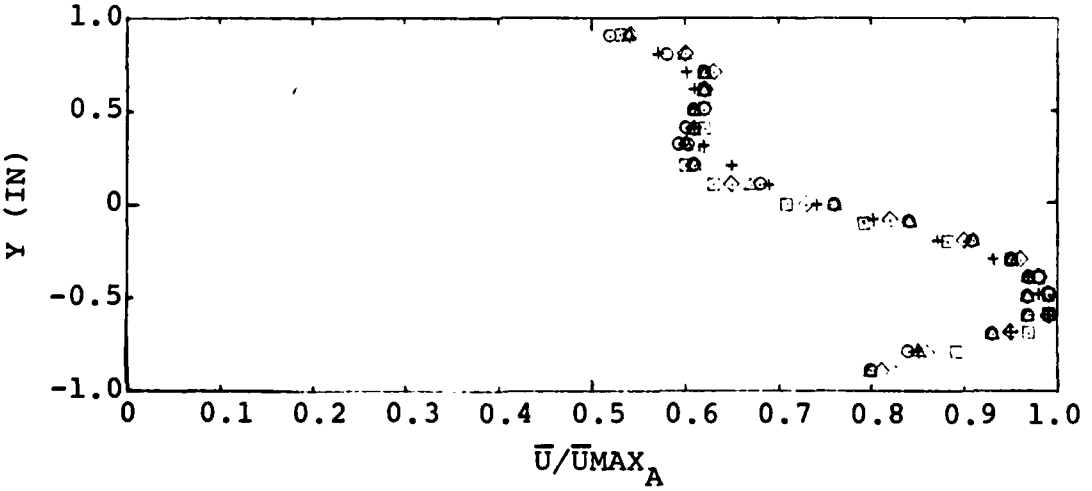

c. Location C

Figure 10. Centerline Mean Velocity Profile, Ur=0.6

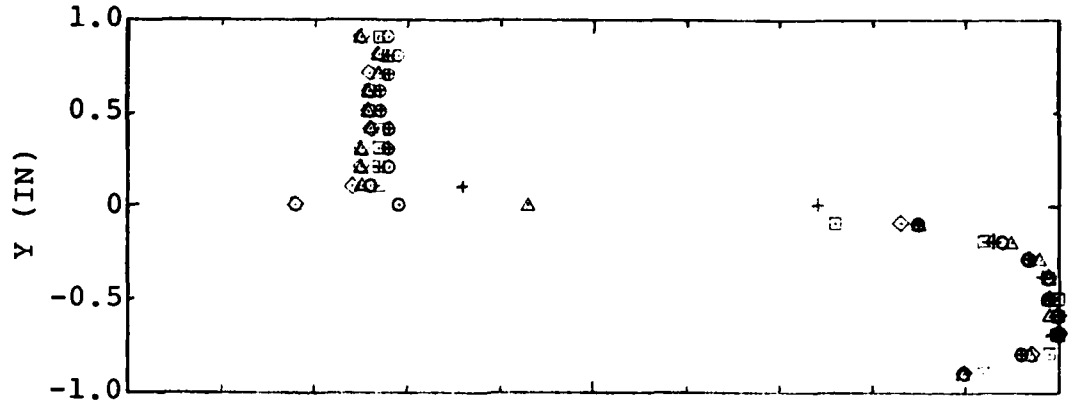

a. Location A

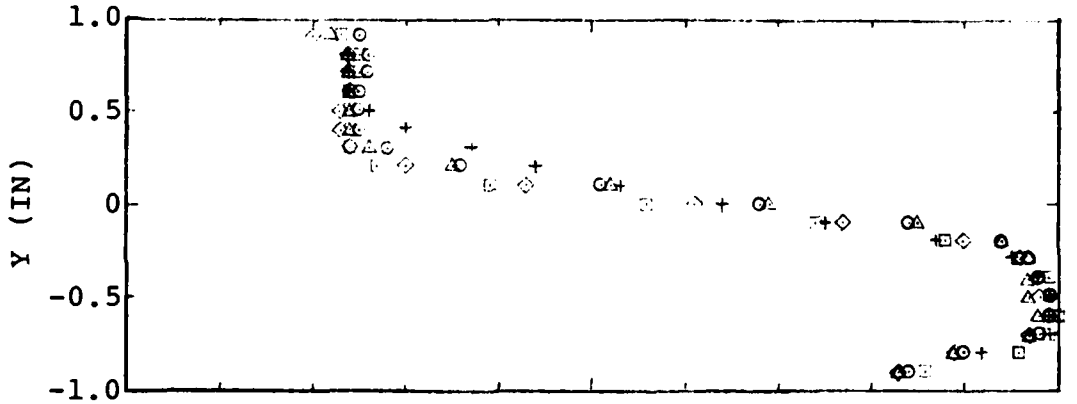

b. Location B

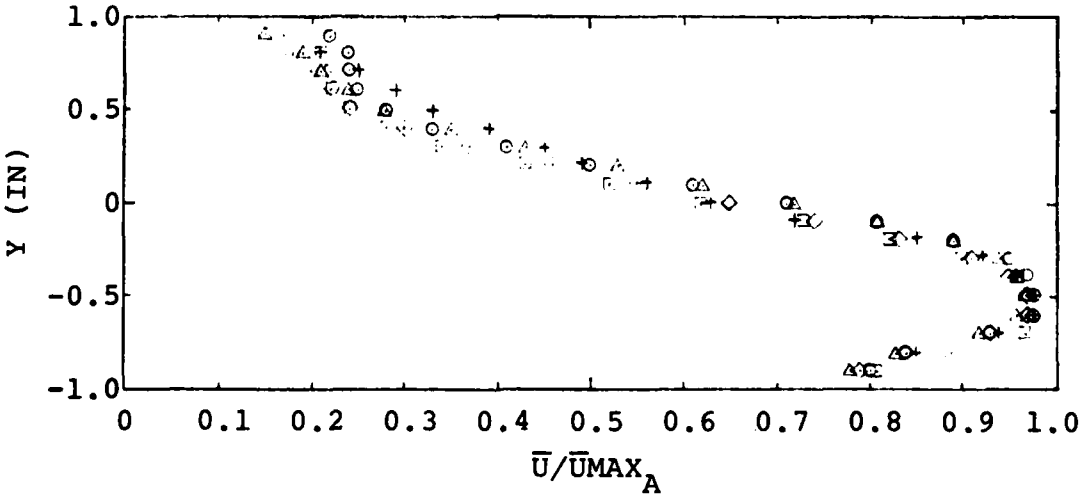

c. Location C

Figure 11. Centerline Mean Velocity Profile, Ur=0.3

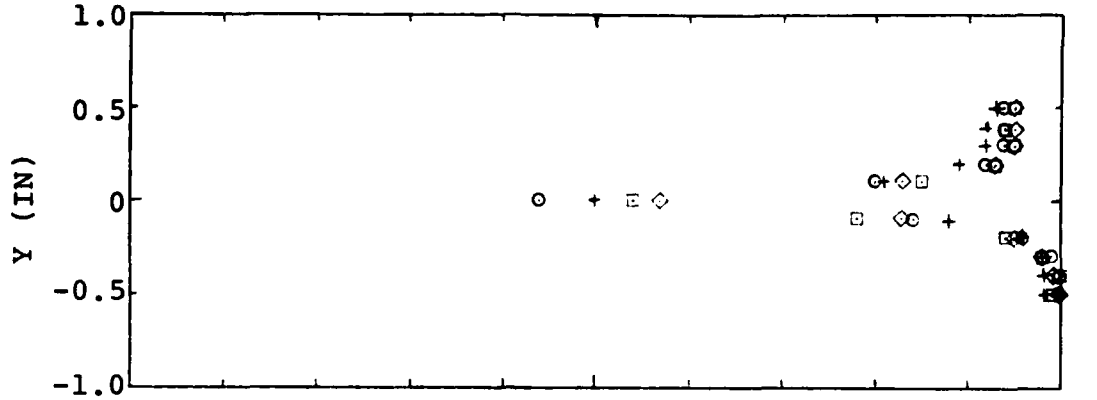

a. Location A

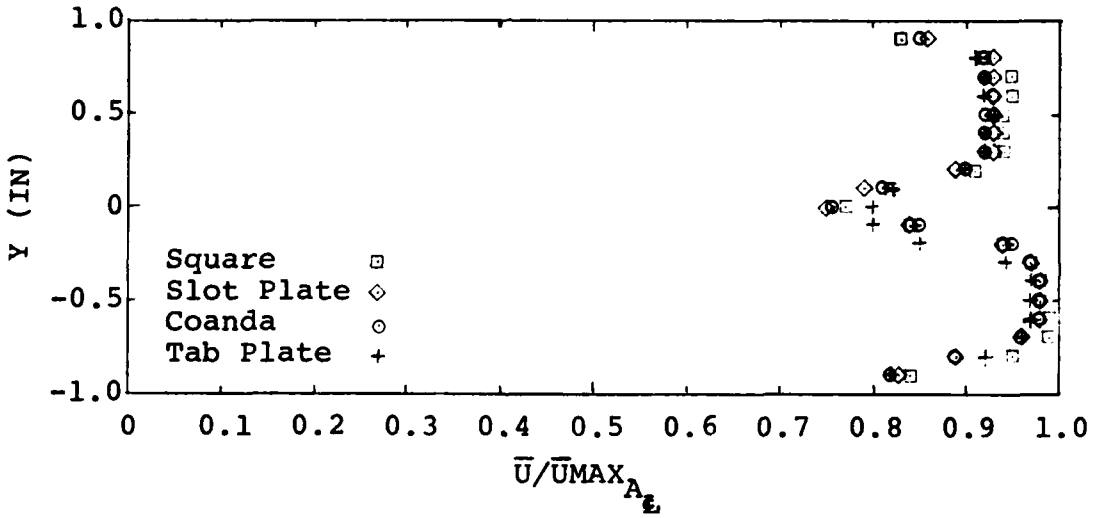

b. Location B

Figure 12. Slot Mean Velocity Profile, Ur=1.0

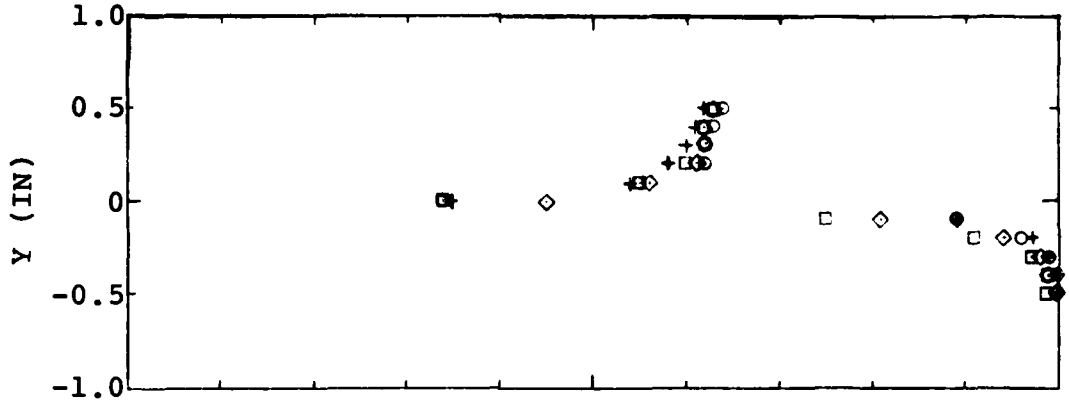

a. Location A

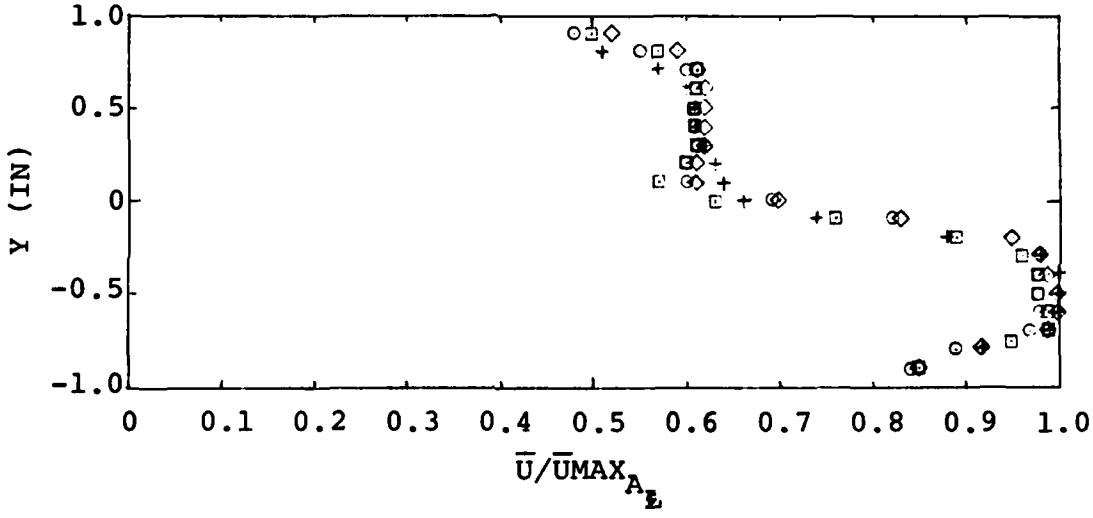

b. Location B

Figure 13. Slot Mean Velocity Profile, Ur=0.6

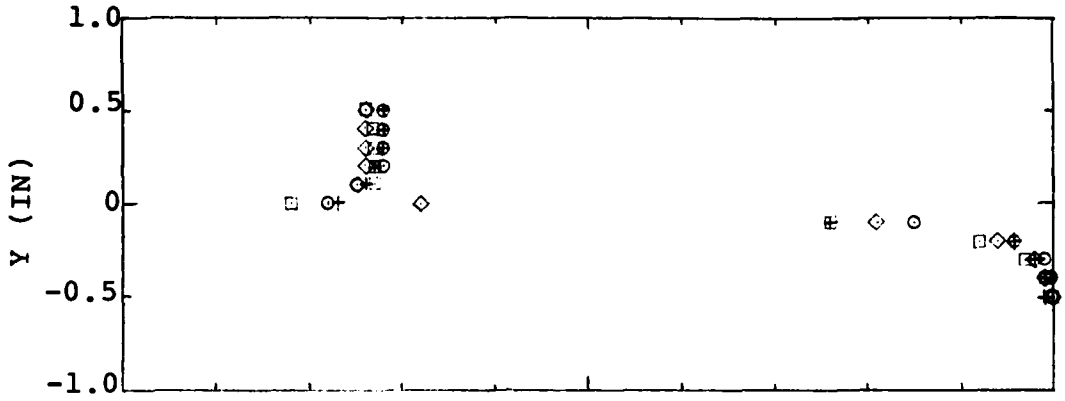

a. Location A

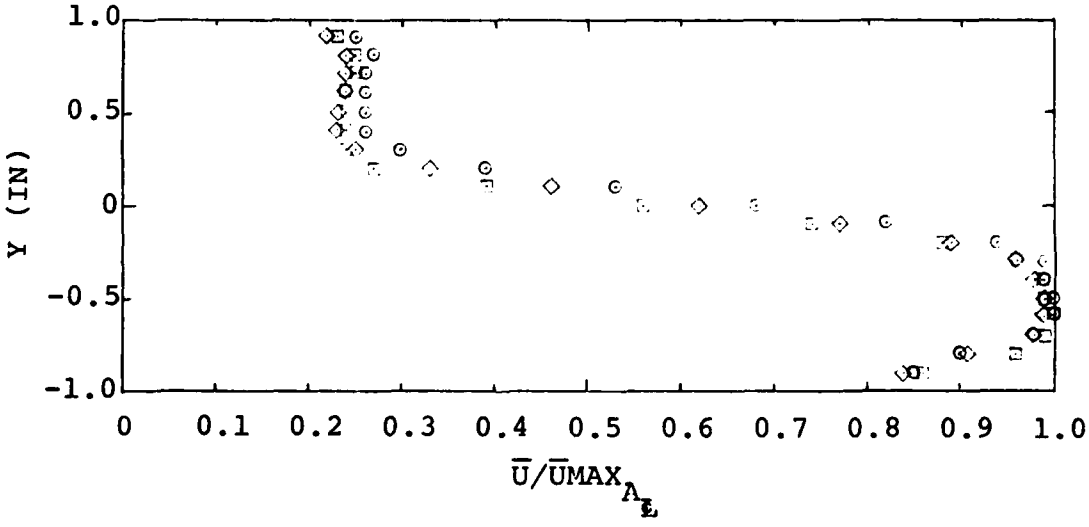

b. Location B

Figure 14. Slot Mean Velocity Profile, Ur=0.3

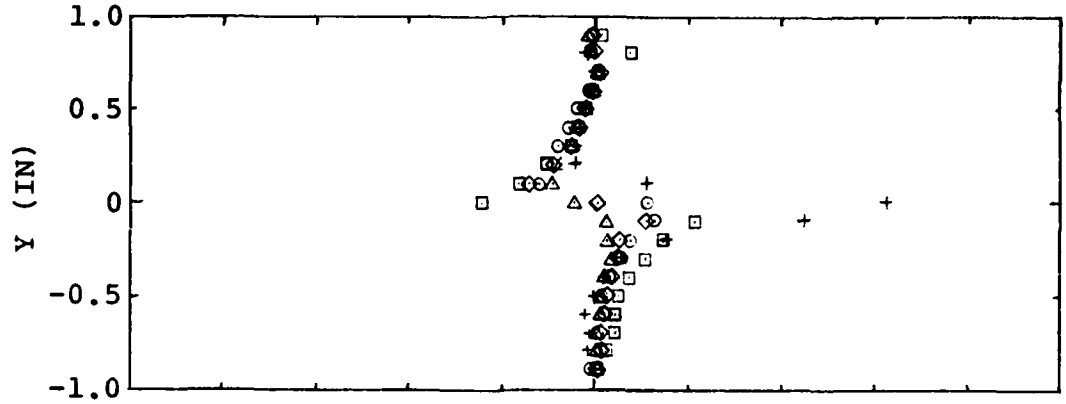

a. Location A

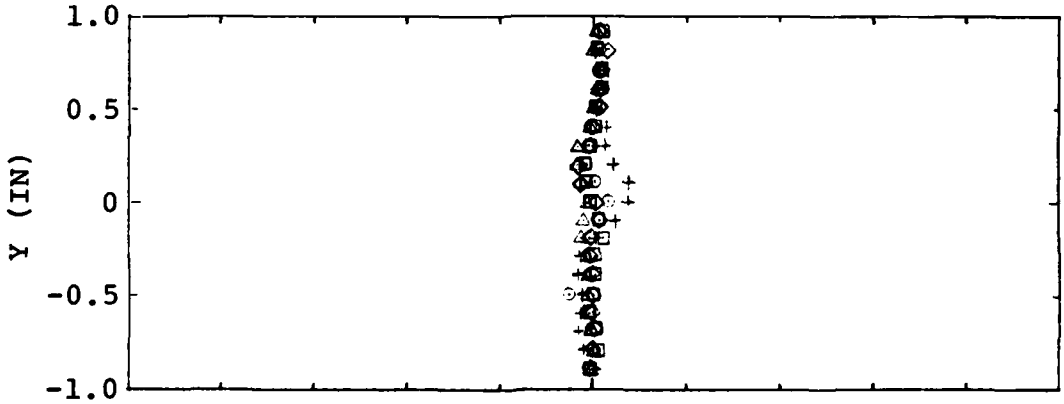

b. Location B

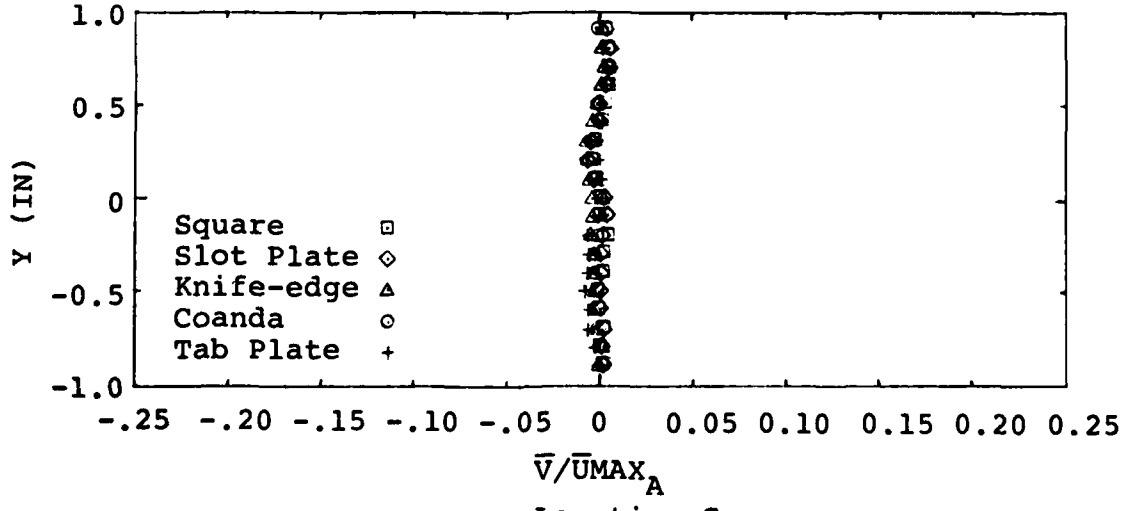

c. Location C

Figure 15. Centerline Mean Velocity Profile, Y-Component, Ur=1.0

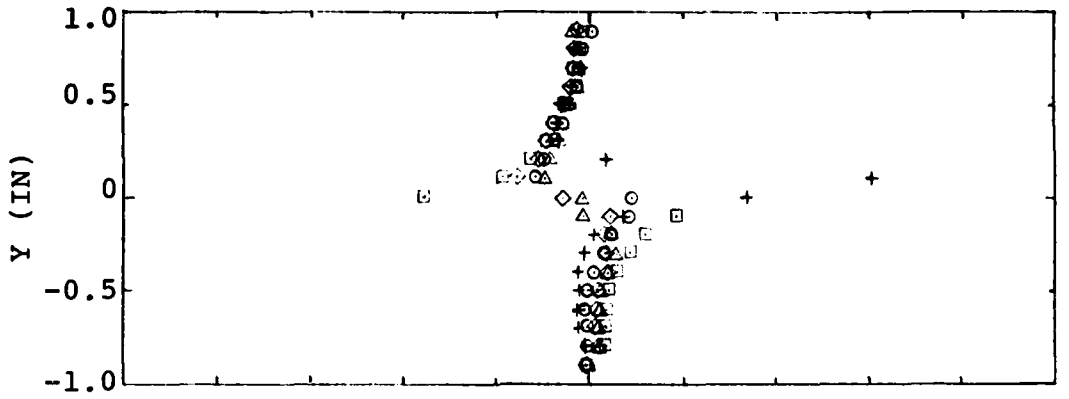

a. Location A

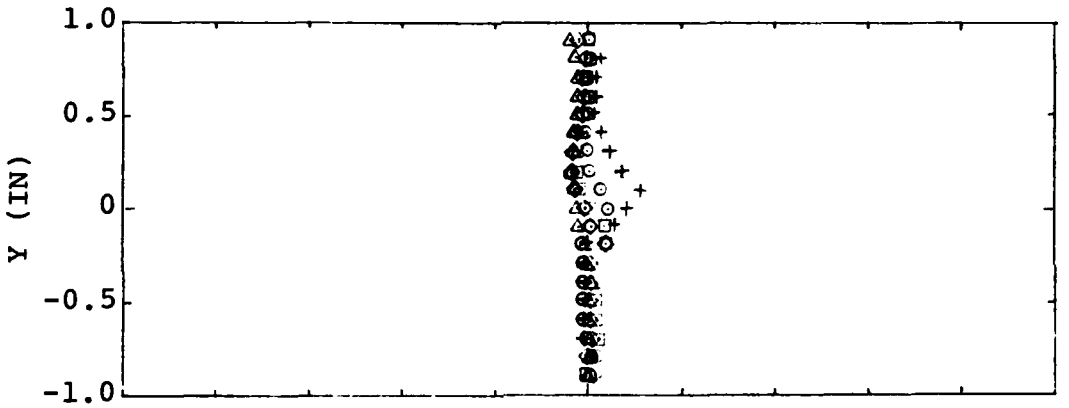

b. Location B

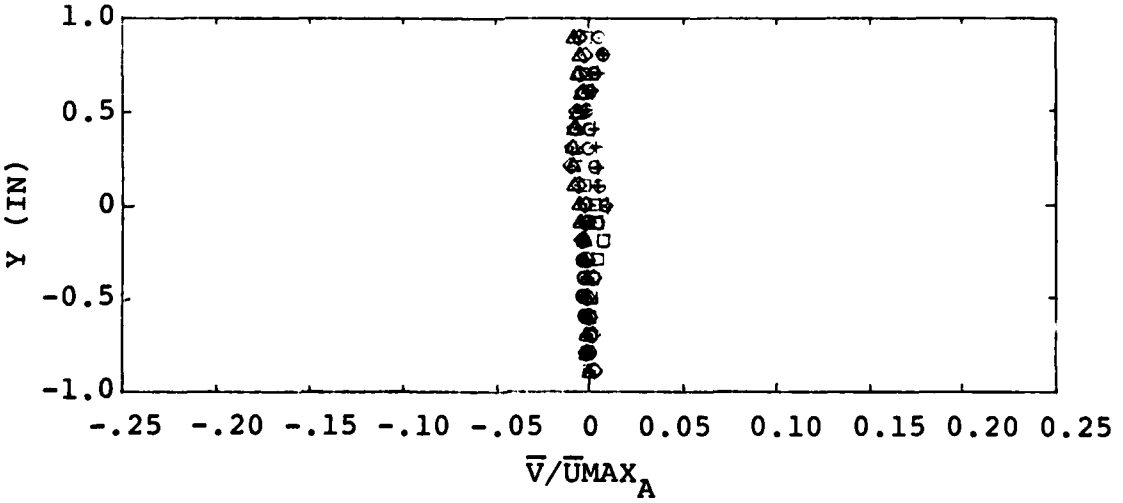

c. Location C

Figure 16. Centerline Mean Velocity Profile, Y-Component, Ur=0.6

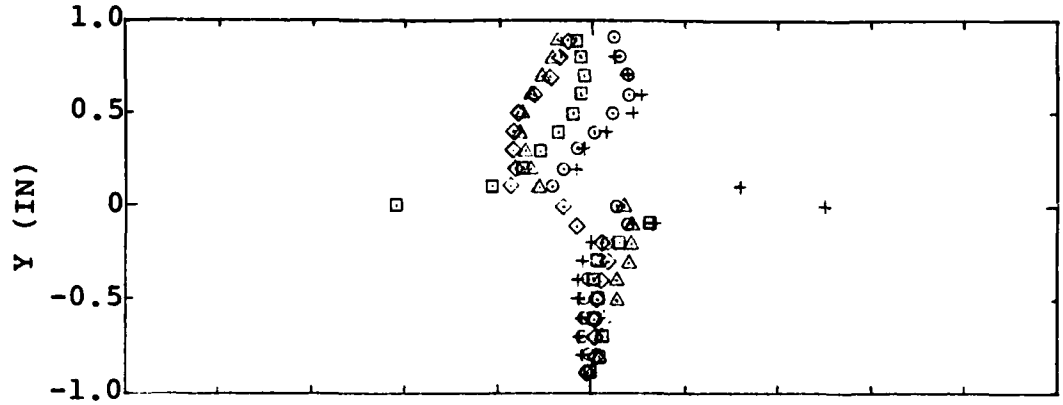

a. Location A

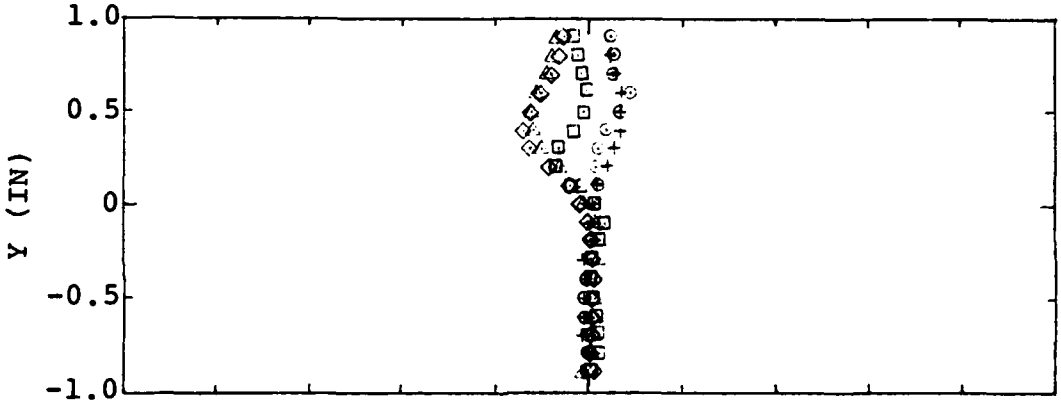

b. Location B

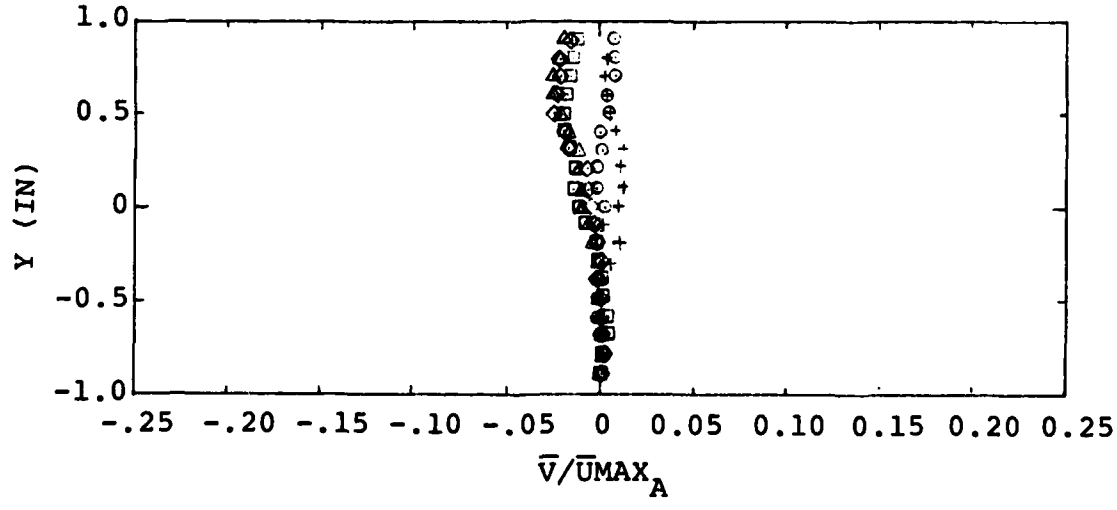

c. Location C

Figure 17. Centerline Mean Velocity Profile, Y-Component, Ur=0.3

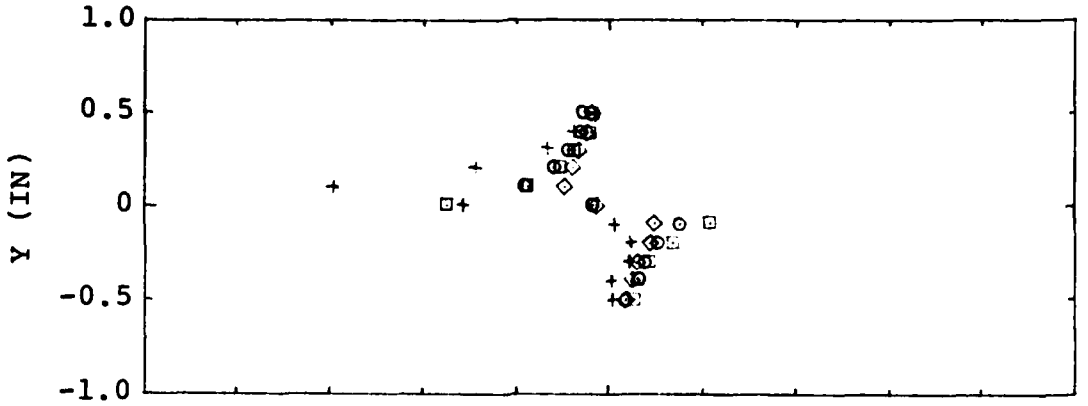

a. Location A

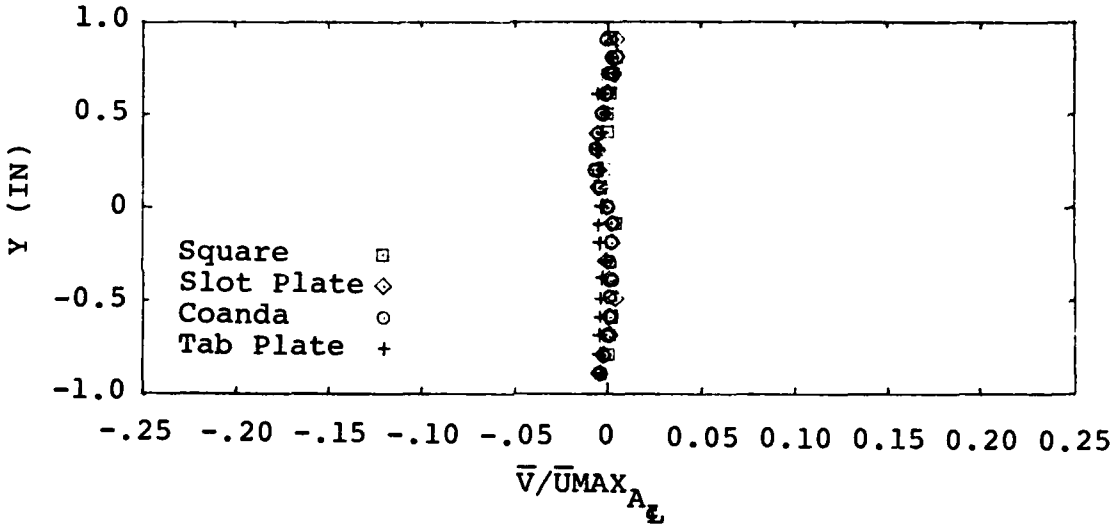

b. Location B

Figure 18. Slot Mean Velocity Profile, Y-Component, Ur=1.0

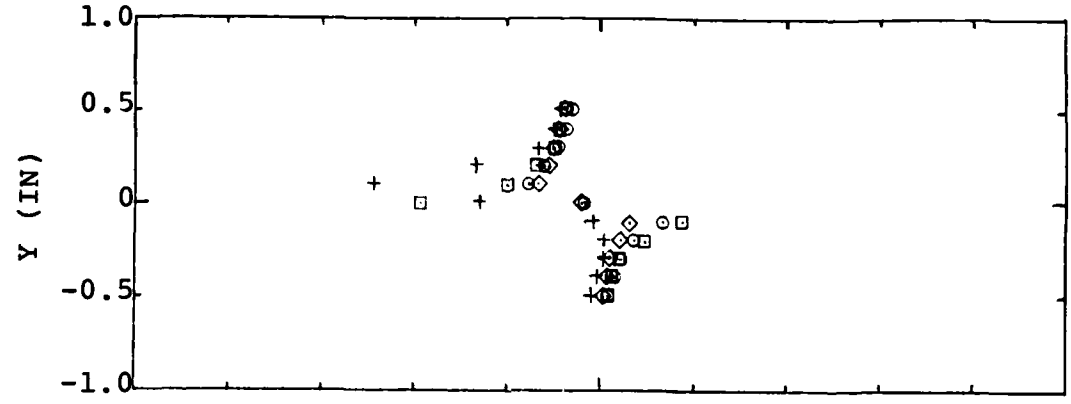

a. Location A

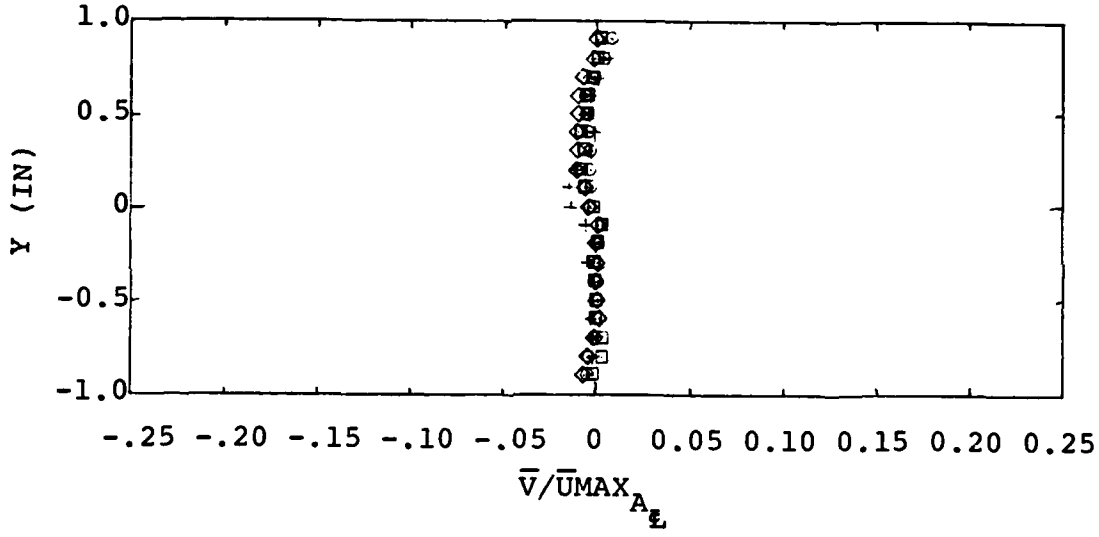

b. Location B

Figure 19. Slot Mean Velocity Profile, Y-Component, Ur=0.6

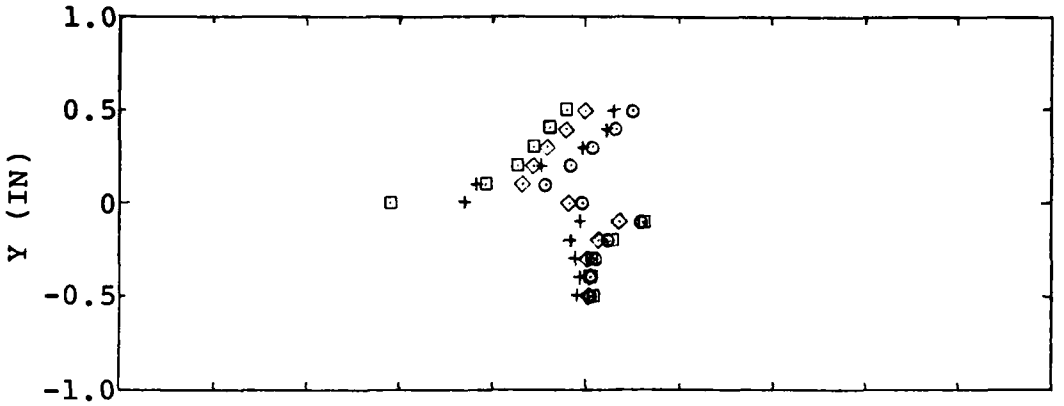

a. Location A

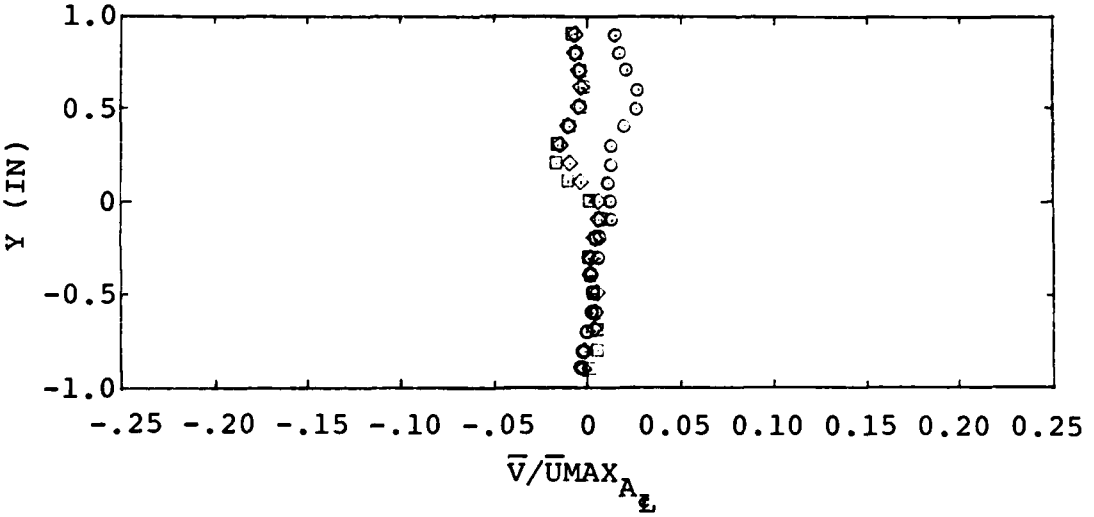

b. Location B

Figure 20. Slot Mean Velocity Profile, Y-Component, Ur=0.3

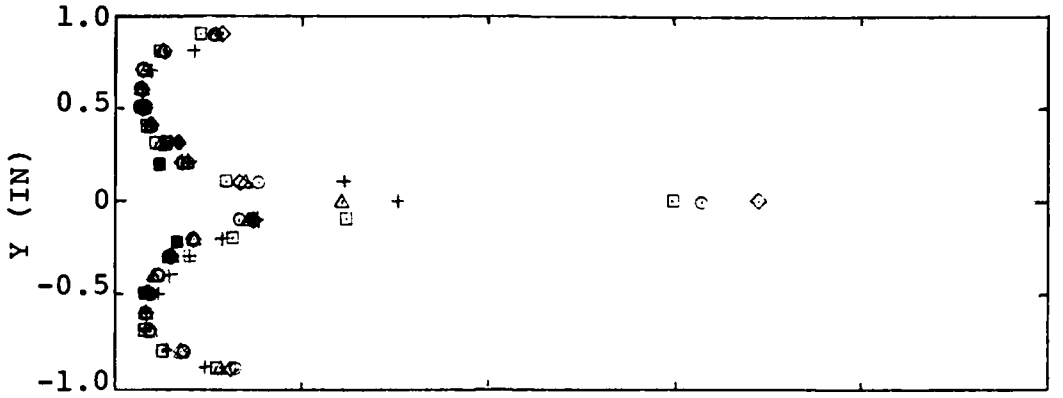

a. Location A

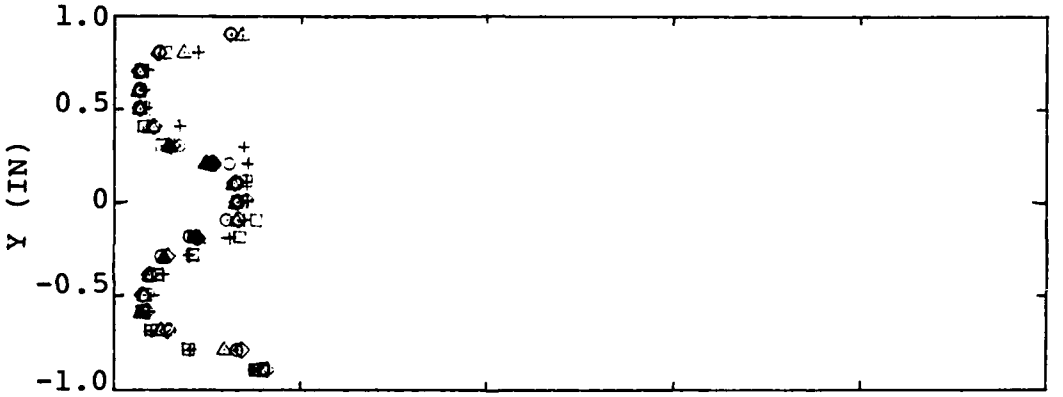

b. Location B

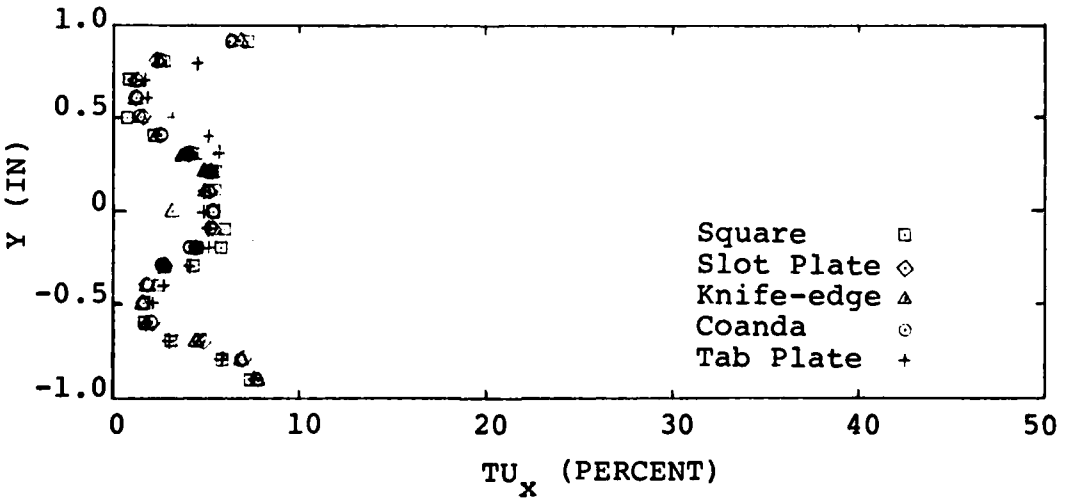

c. Location C

Figure 21. Centerline Turbulence Parameter Profile, X-Component, Ur=1.0

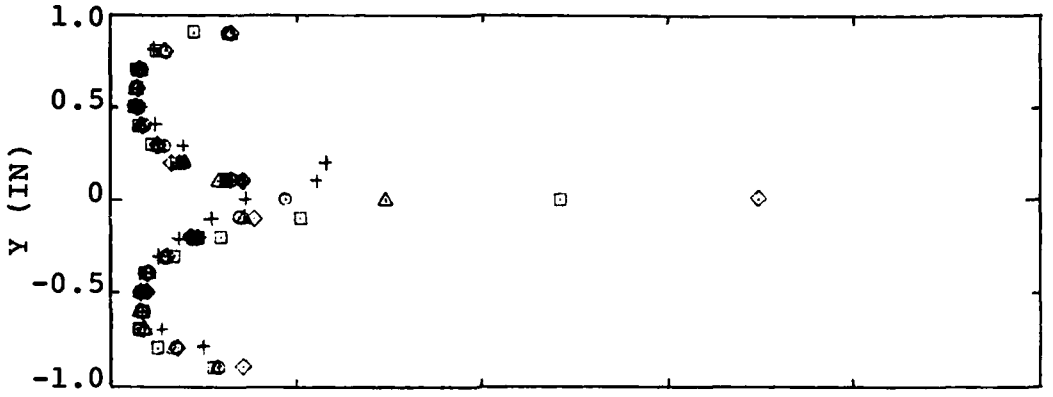

a. Location A

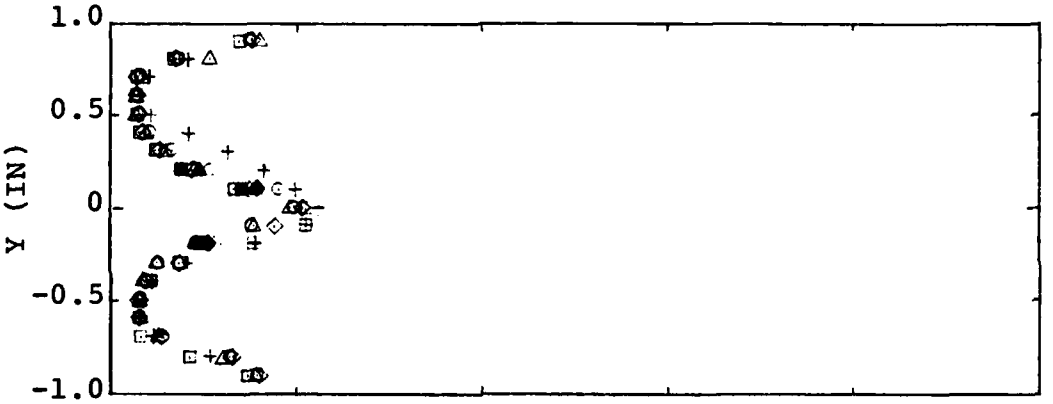

b. Location B

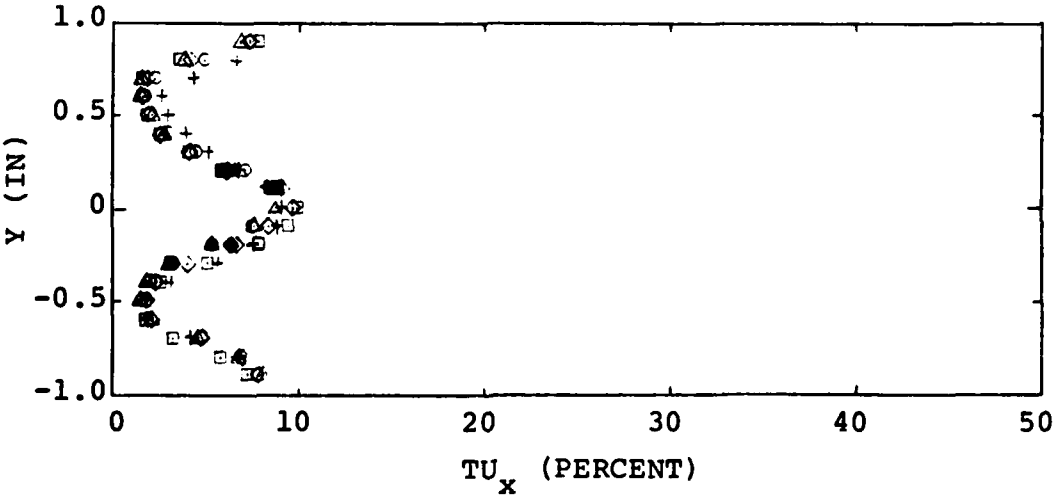

c. Location C

Figure 22. Centerline Turbulence Parameter Profile, X-Component, Ur=0.6

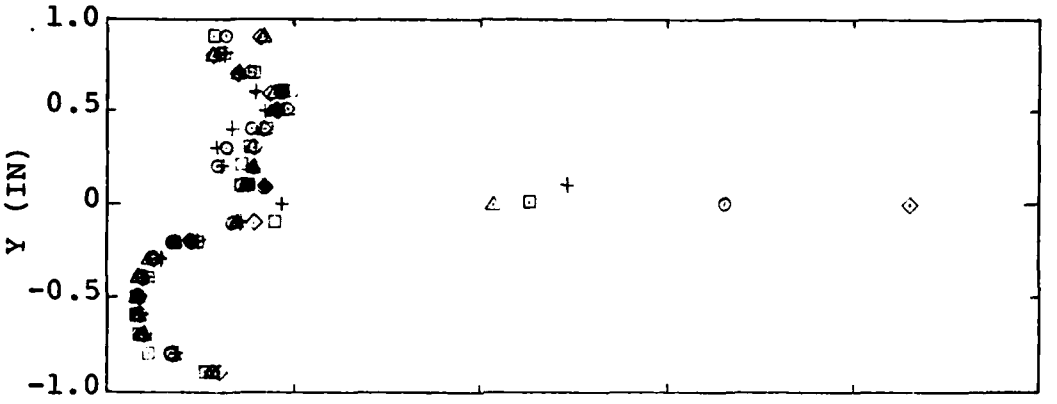

a. Location A

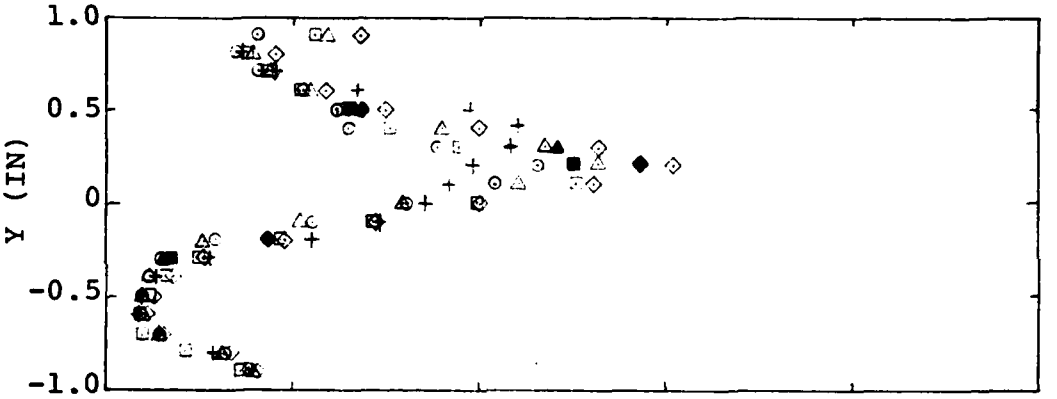

b. Location B

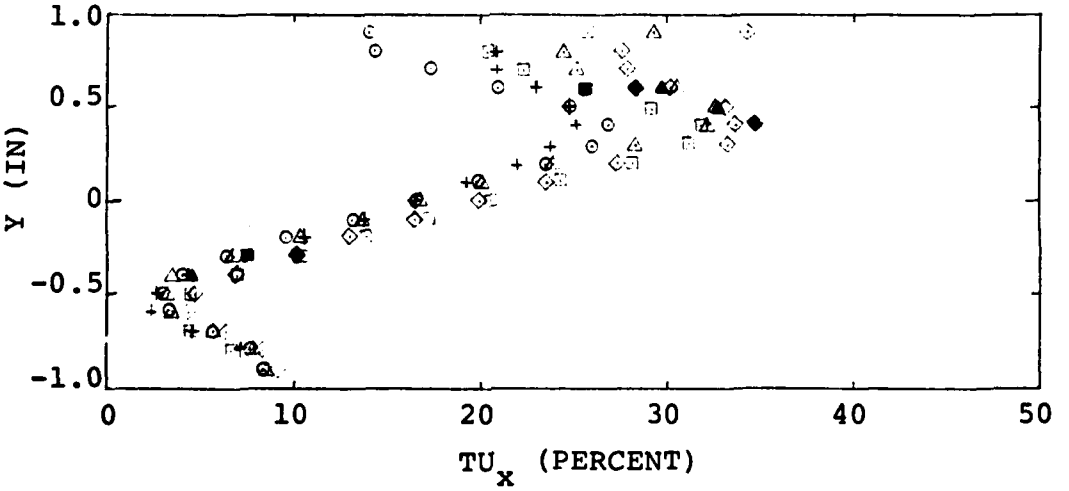

c. Location C

Figure 23. Centerline Turbulence Parameter Profile, X-Component, Ur=0.3

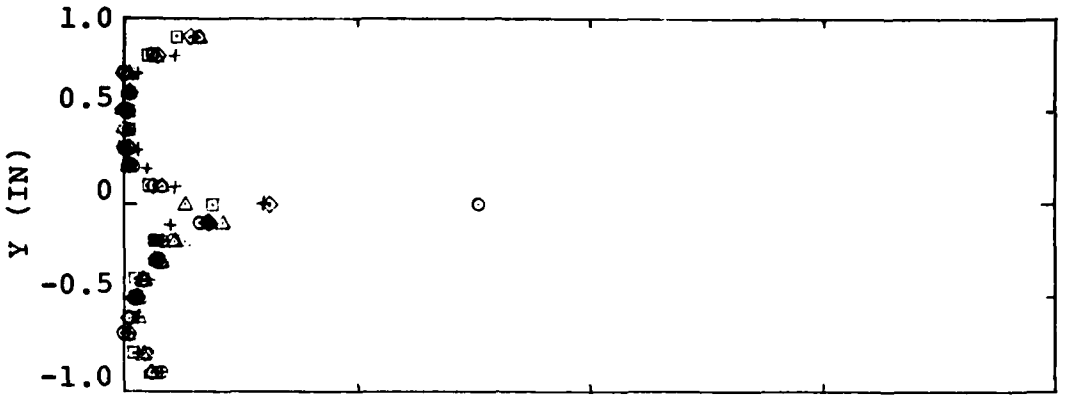

a. Location A

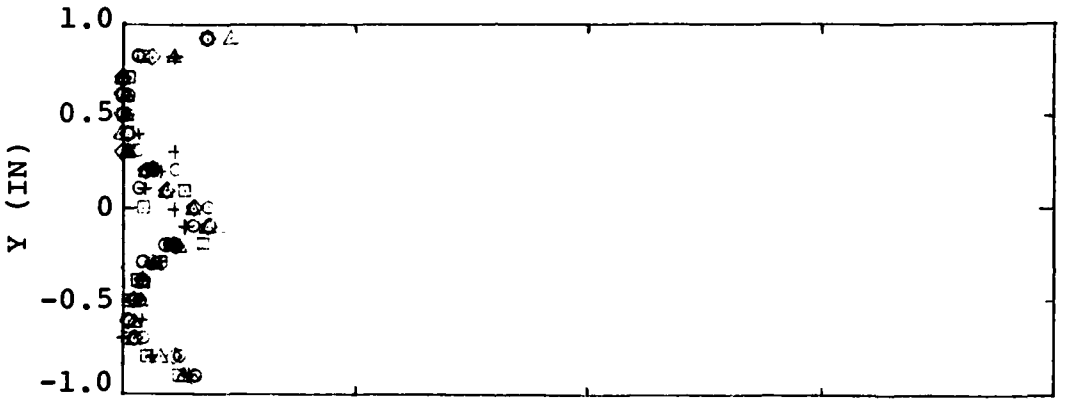

b. Location B

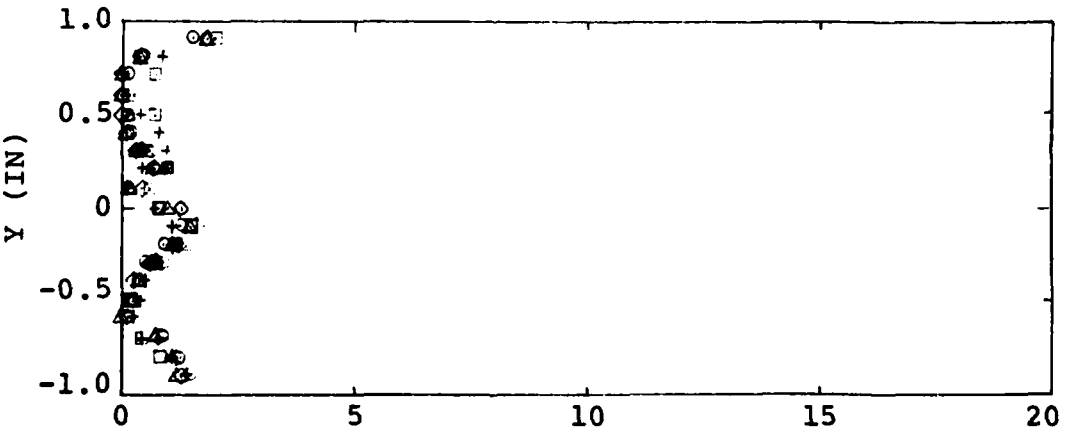

c. Location C

Figure 24. Centerline Turbulence Parameter Profile, Y-Component, Ur=1.0

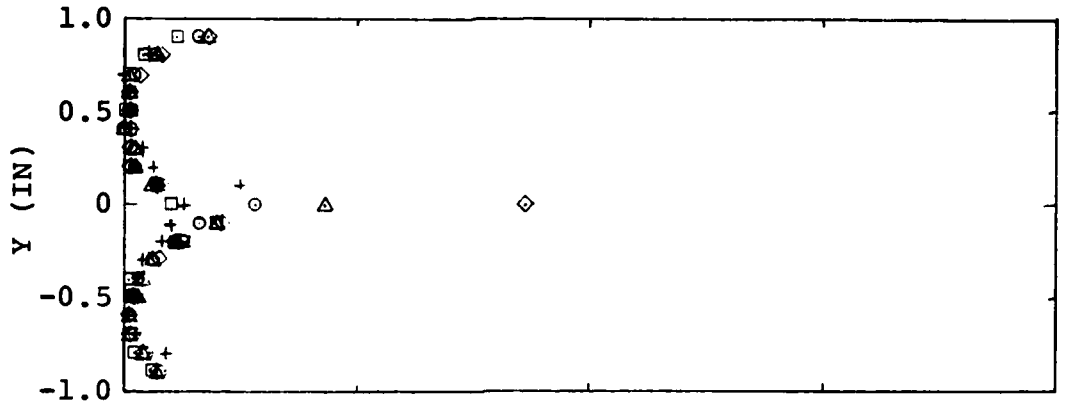

a. Location A

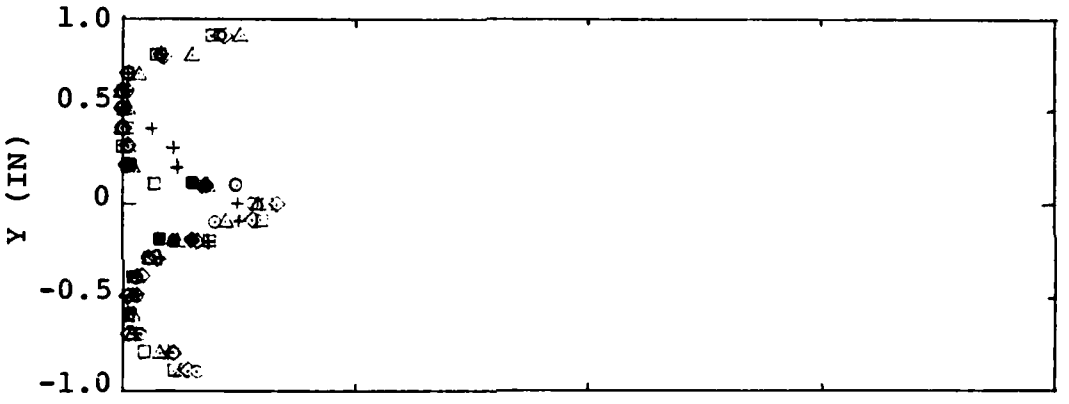

b. Location B

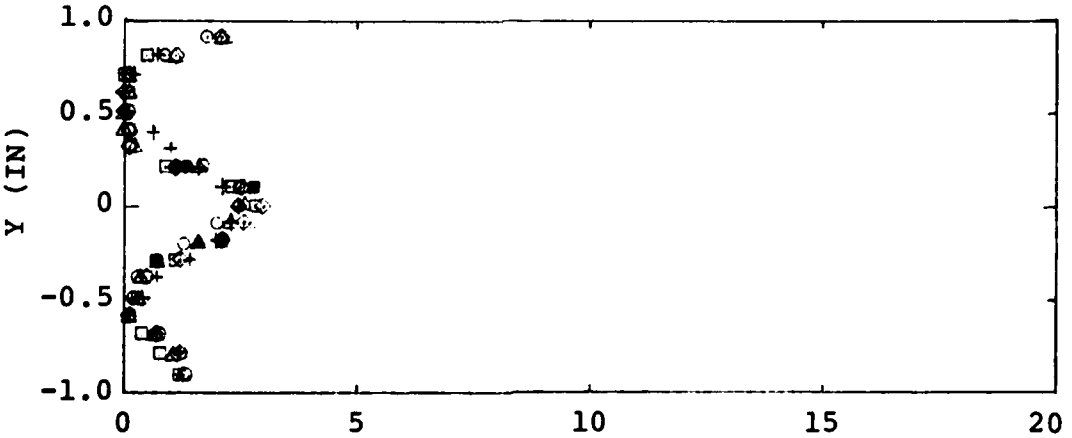

c. Location C

Figure 25. Centerline Turbulence Parameter Profile, Y-Component, Ur=0.6

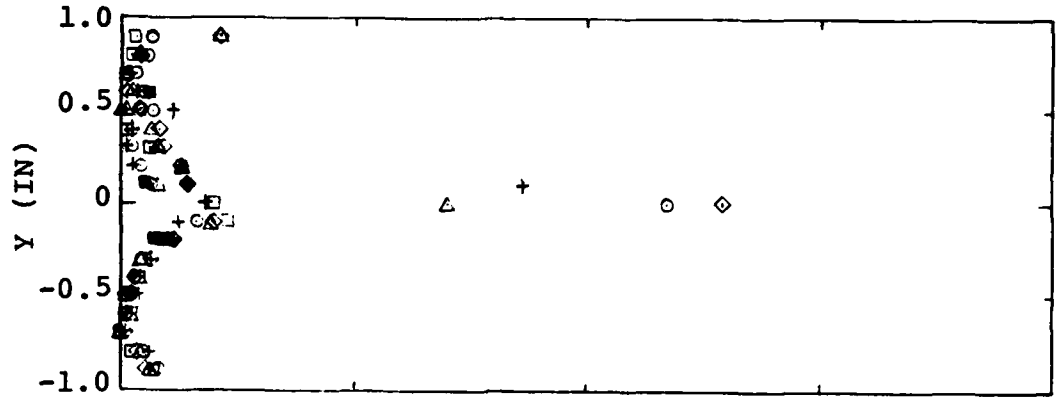

a. Location A

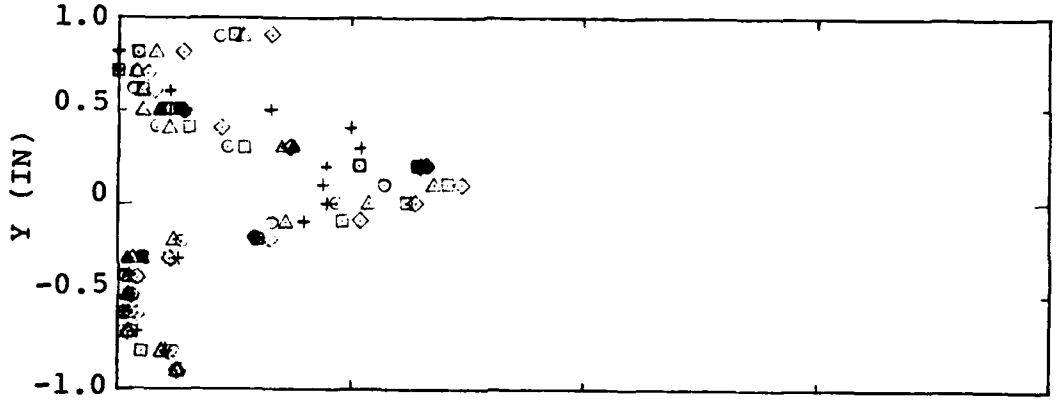

b. Location B

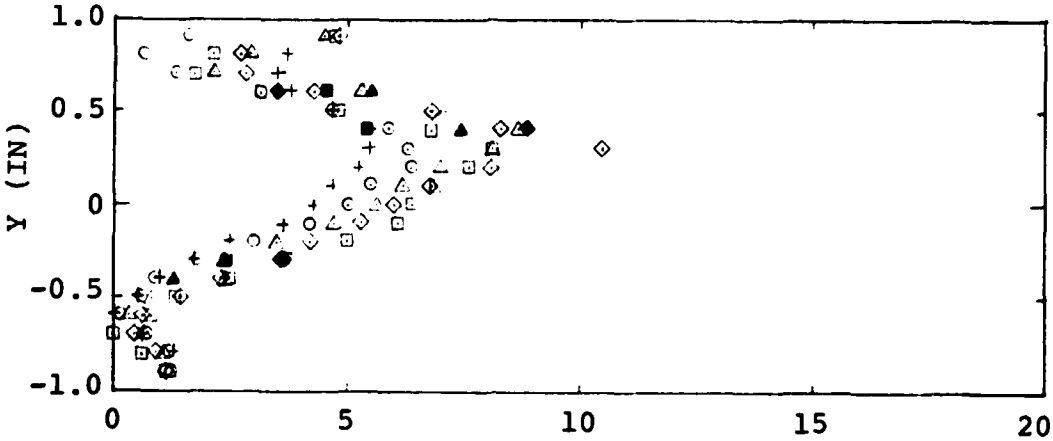

c. Location C

Figure 26. Centerline Turbulence Parameter Profile, Y-Component, Ur=0.3

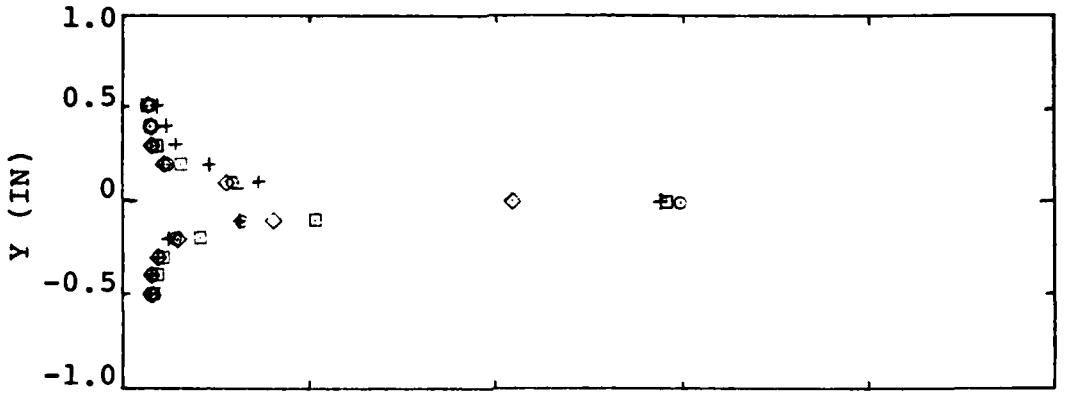

a. Location A

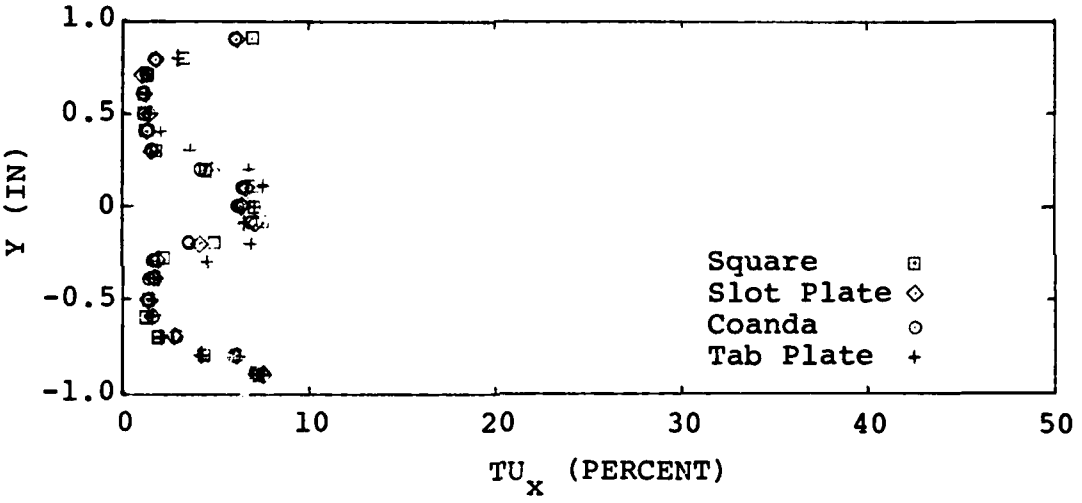

b. Location B

Figure 27. Slot Turbulence Parameter Profile, X-Component, Ur=1.0

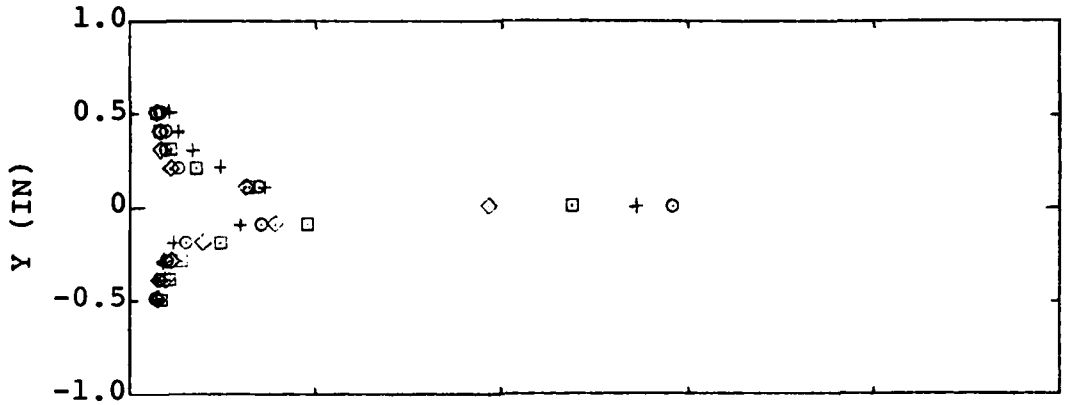

a. Location A

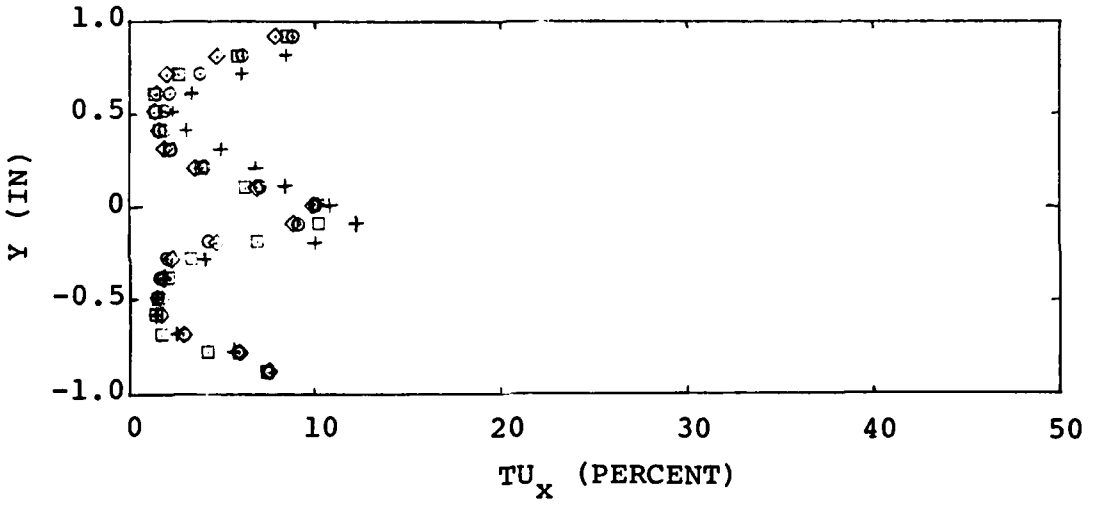

b. Location B

Figure 28. Slot Turbulence Parameter Profile, X-Component, Ur=0.6

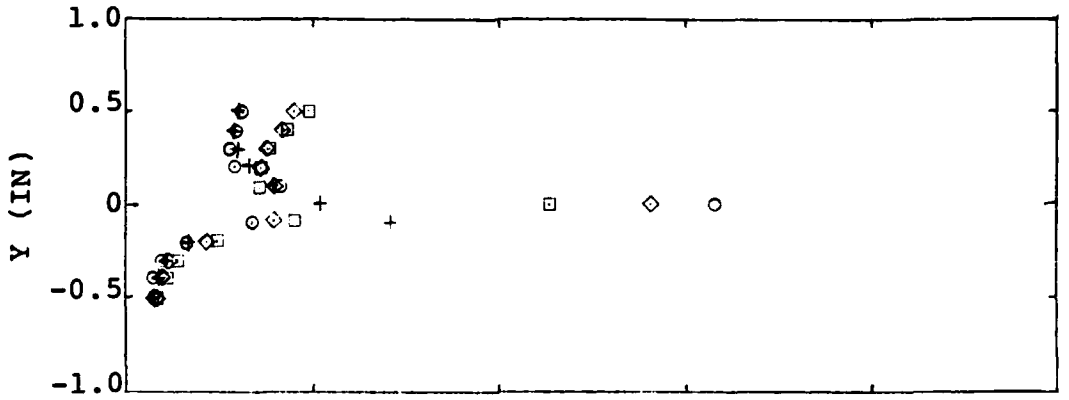

a. Location A

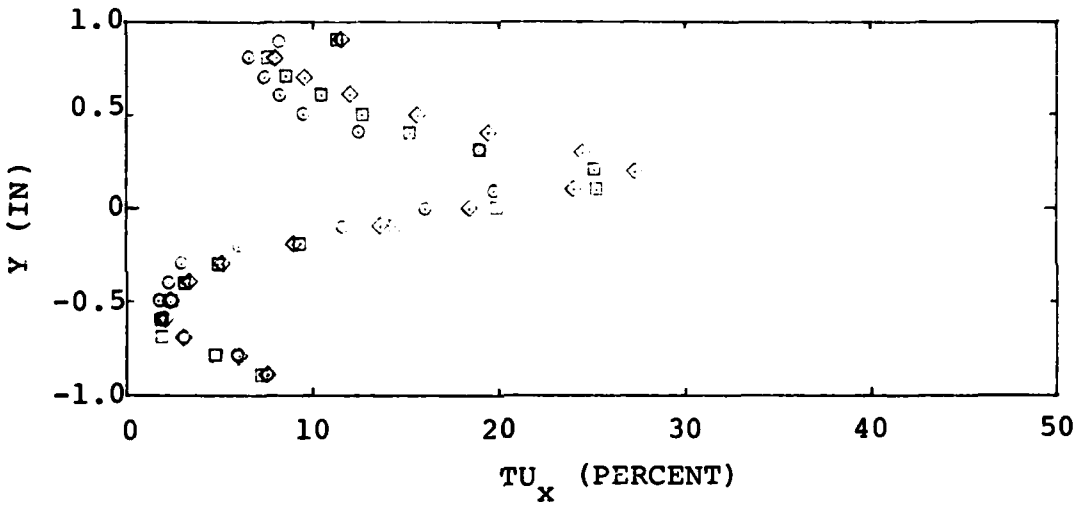

b. Location B

Figure 29. Slot Turbulence Parameter Profile, X-Component, Ur=0.3

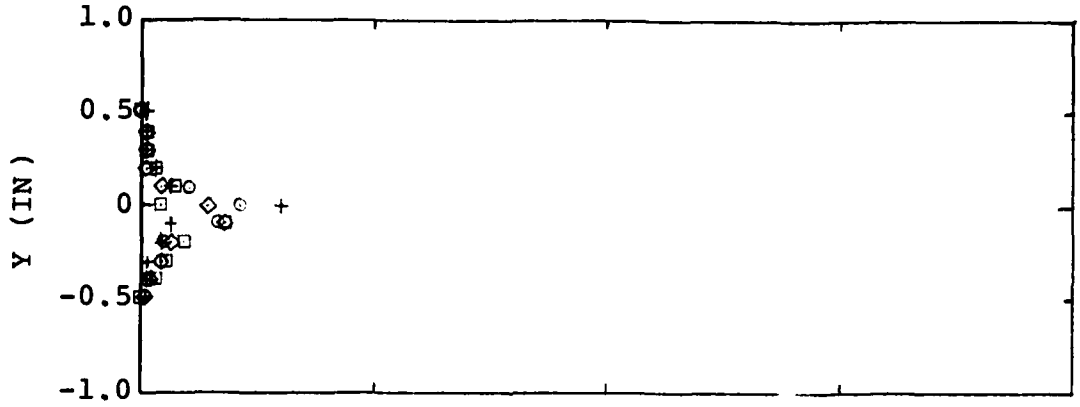

a. Location A

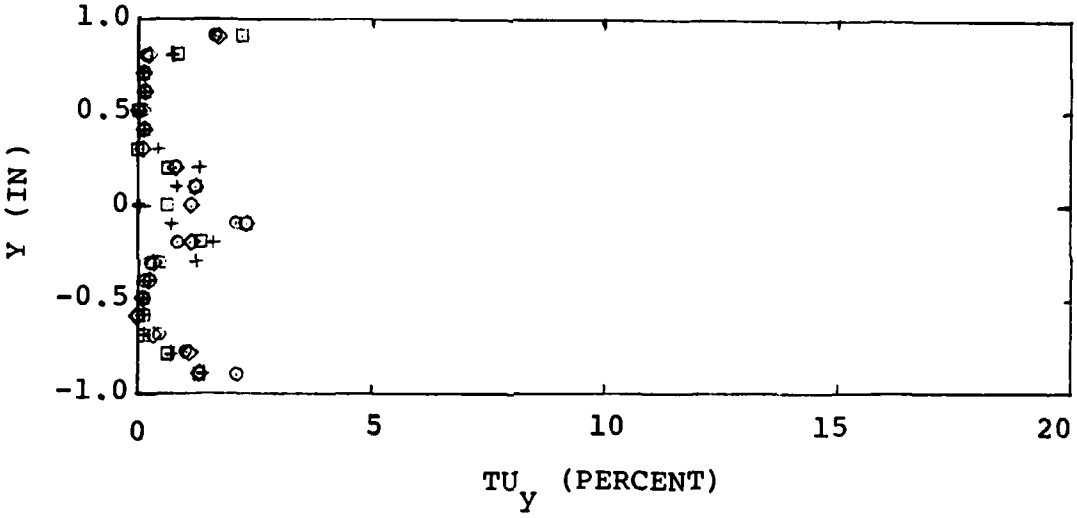

b. Location B

Figure 30. Slot Turbulence Parameter Profile, Y-Component, Ur=1.0

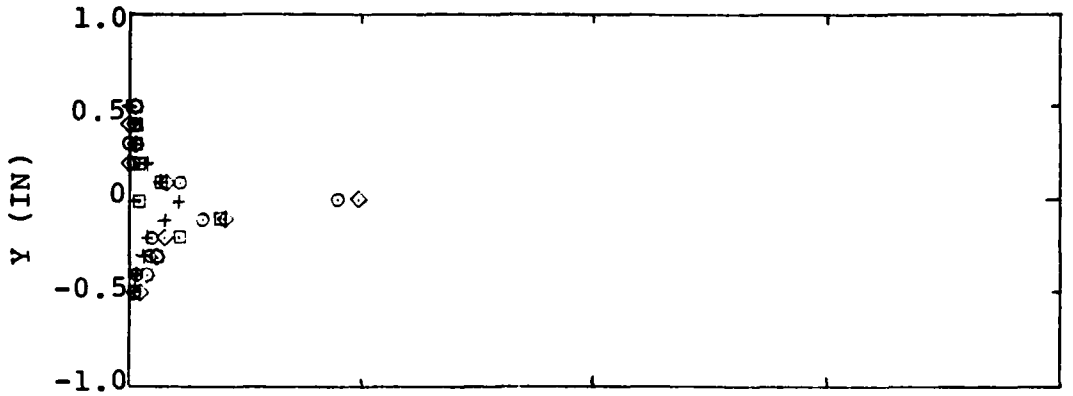

a. Location A

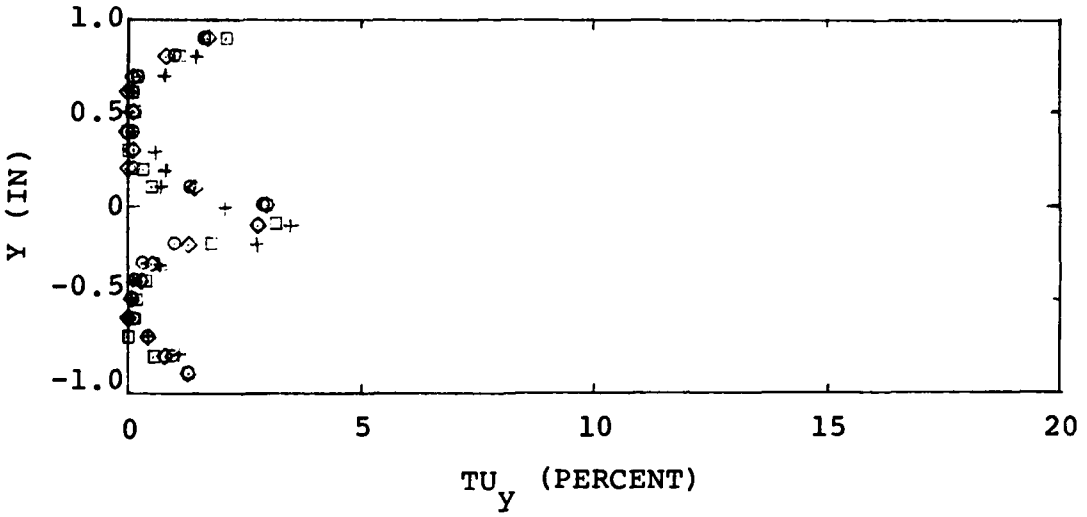

b. Location B

Figure 31. Slot Turbulence Parameter Profile, Y-Component, Ur=0.6

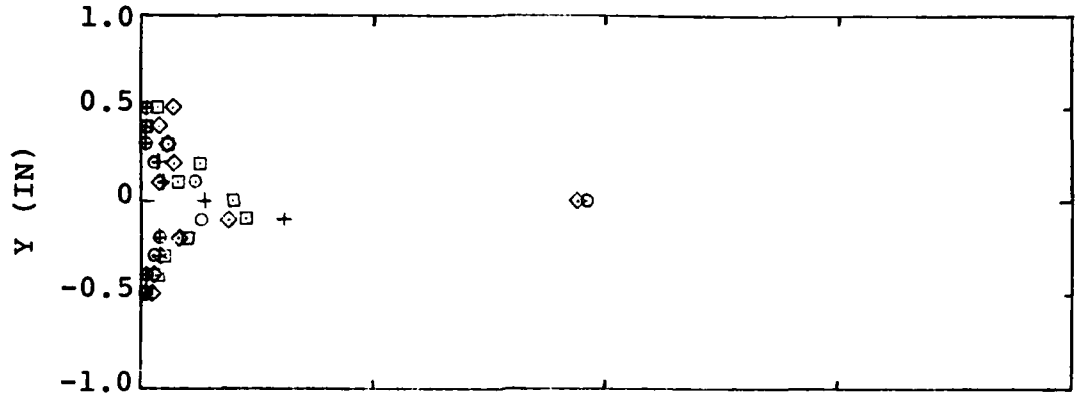

a. Location A

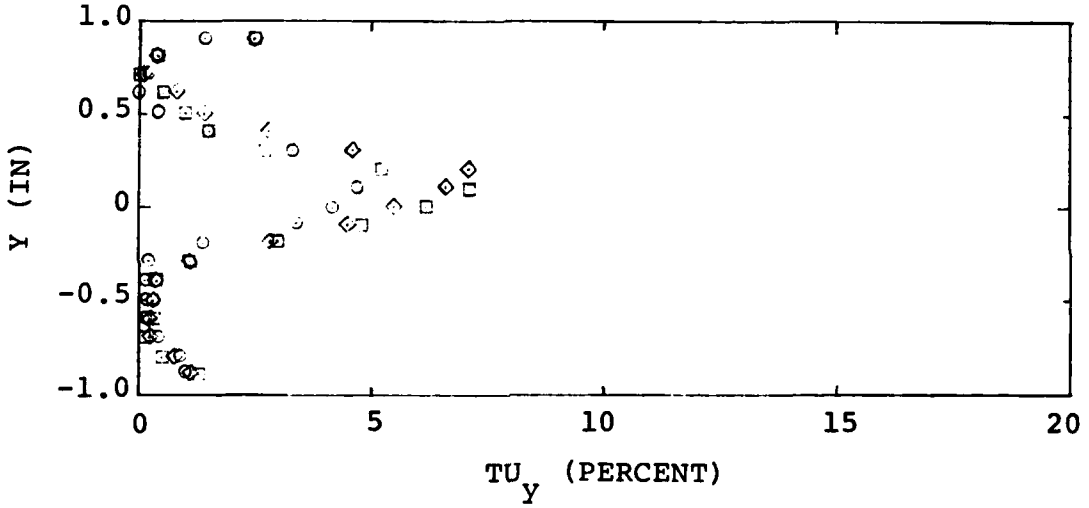

b. Location B

Figure 32. Slot Turbulence Parameter Profile, Y-Component, Ur=0.3

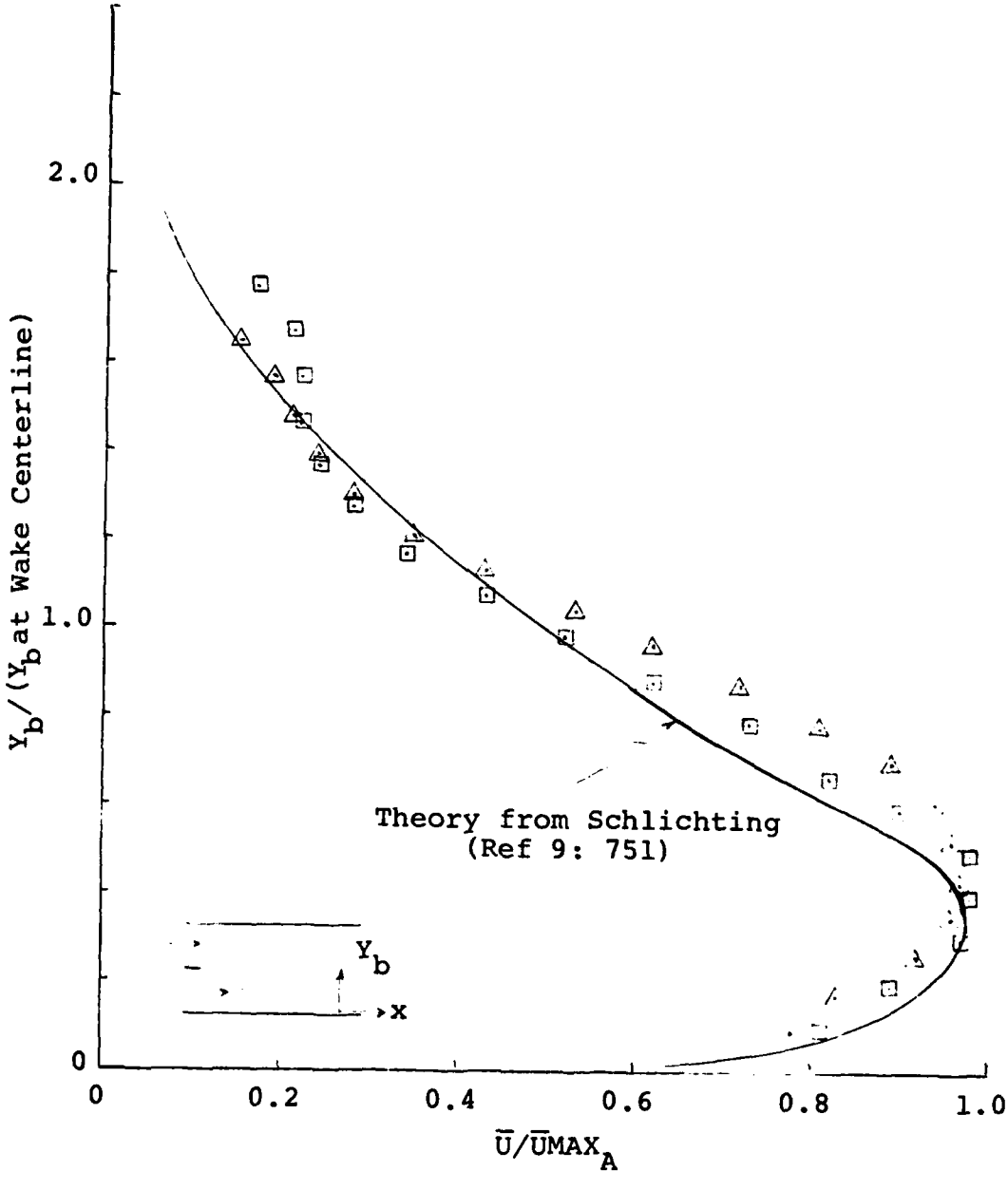

Figure 33. Wall Jet Similarity Profile, Location C

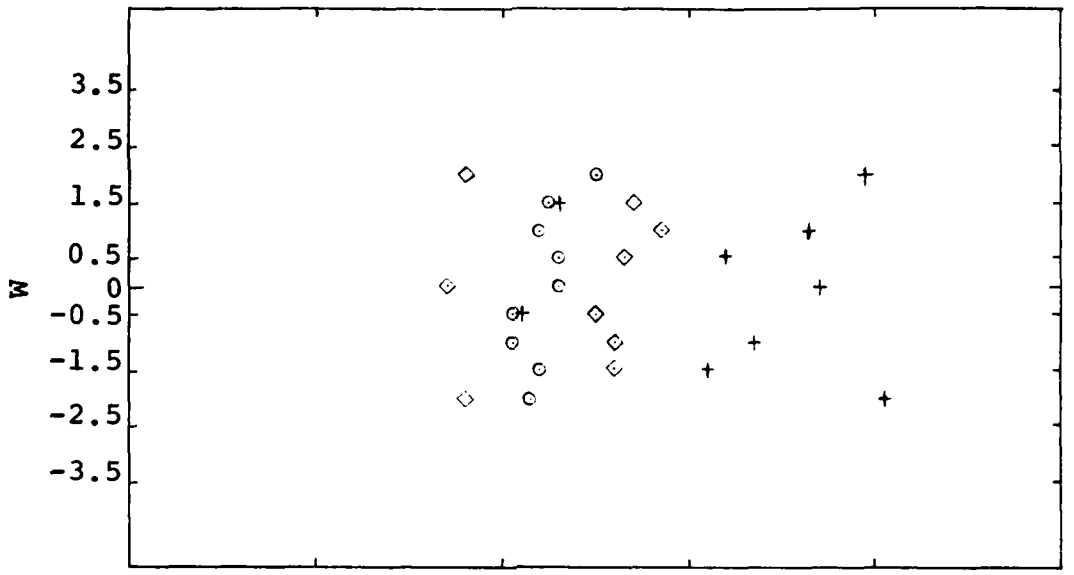

a. Location A

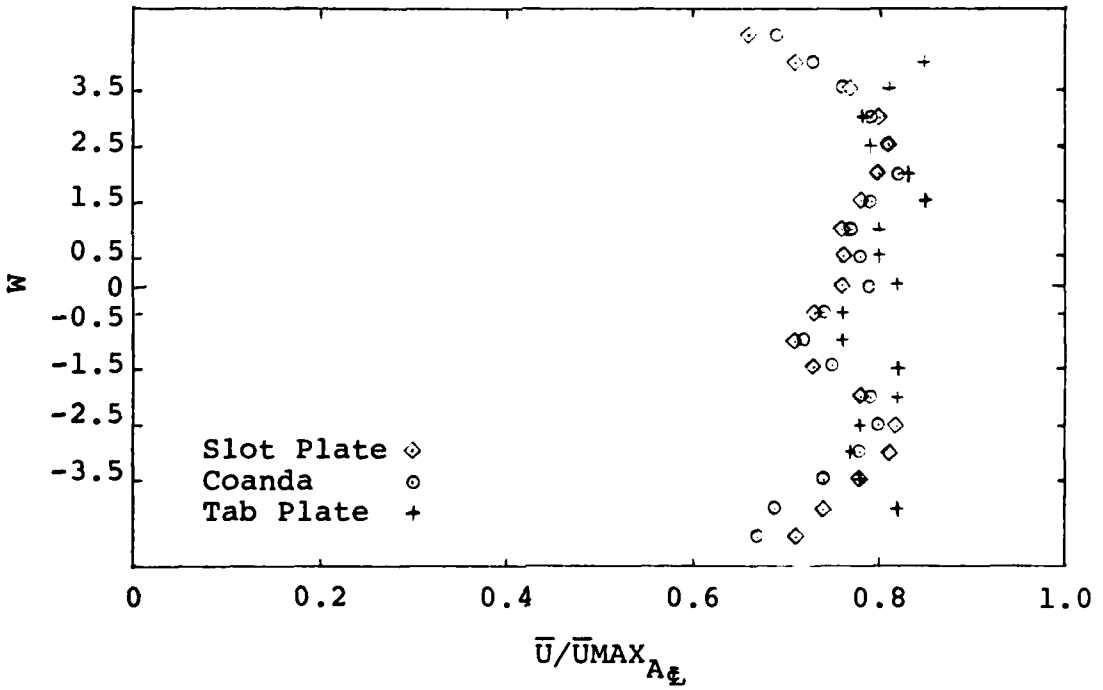

b. Location B

Figure 34. Lateral Mean Velocity Profile, Ur=1.0

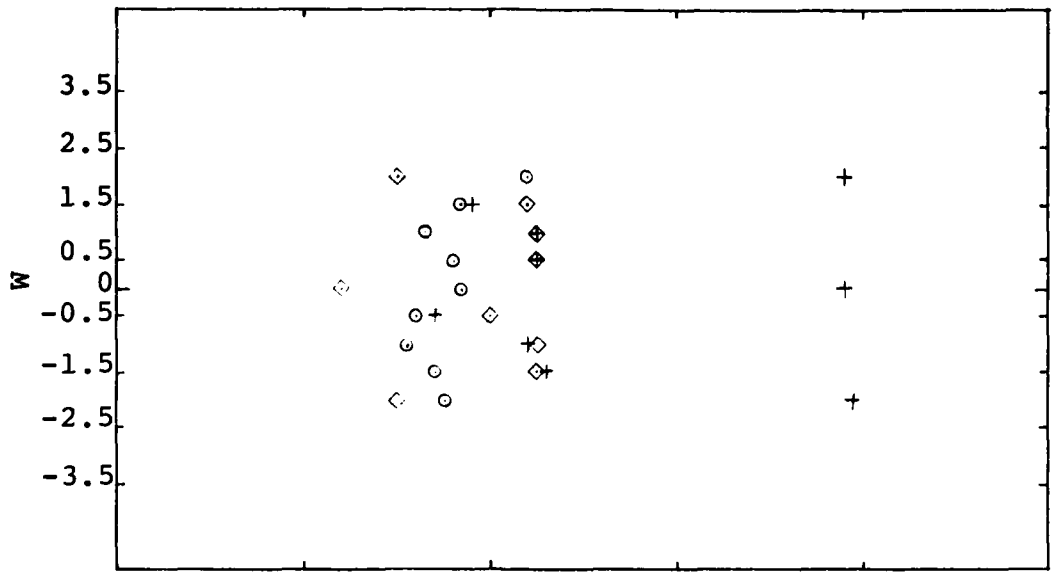

a. Location A

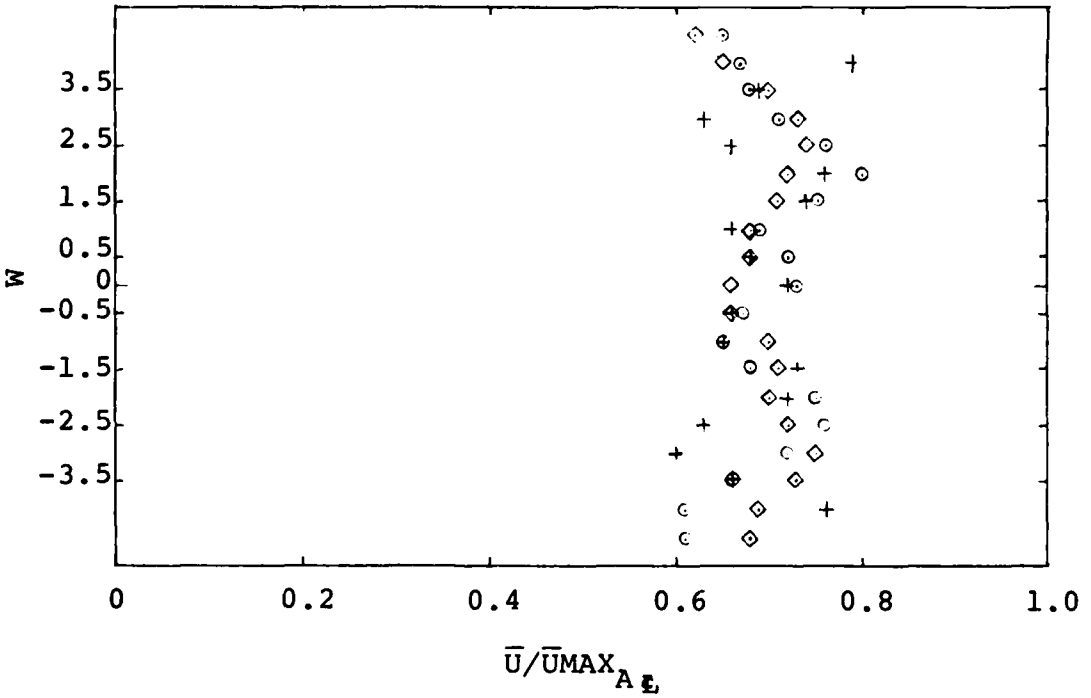

b. Location B

Figure 35. Lateral Mean Velocity Profile, Ur=0.6

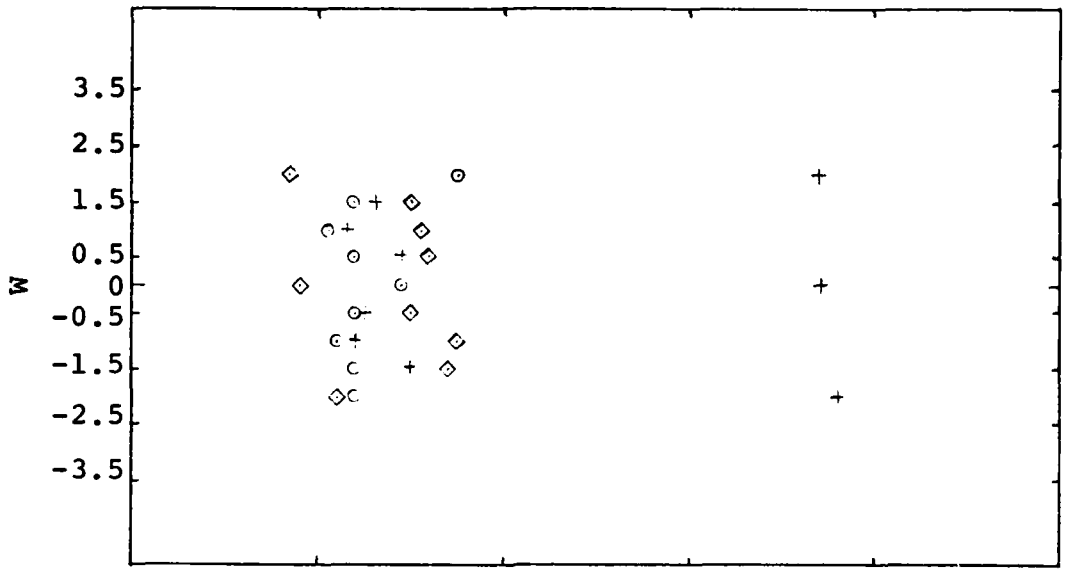

a. Location A

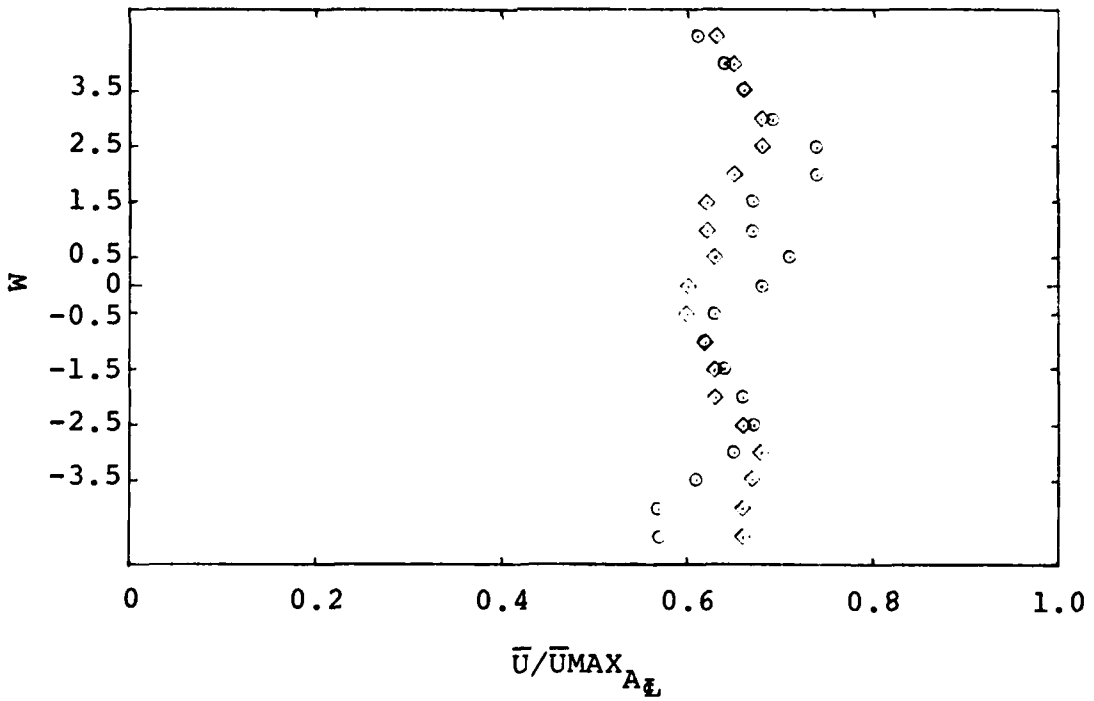

b. Location B

Figure 36. Lateral Mean Velocity Profile, Ur=0.3

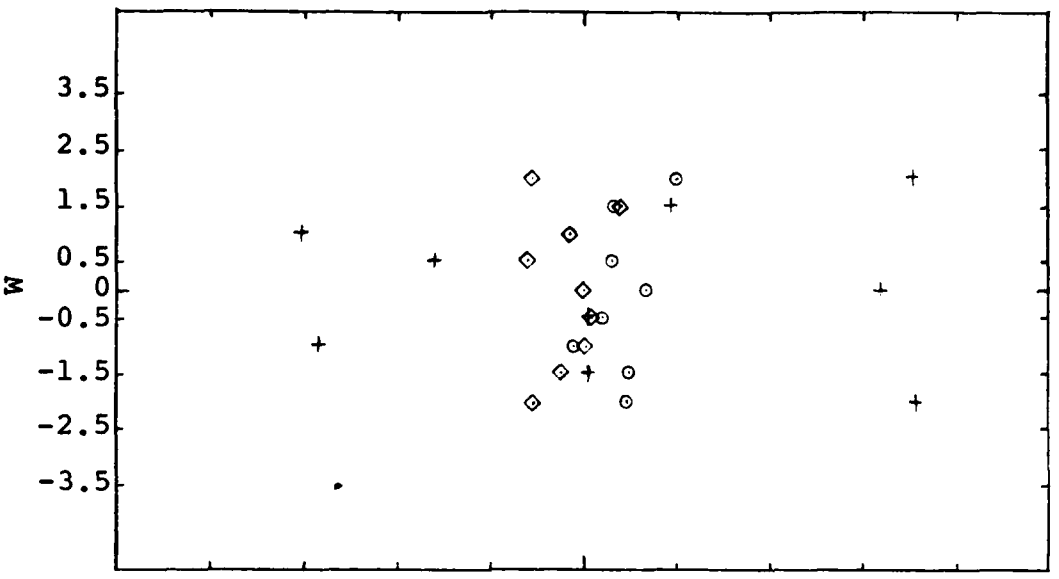

a. Location A

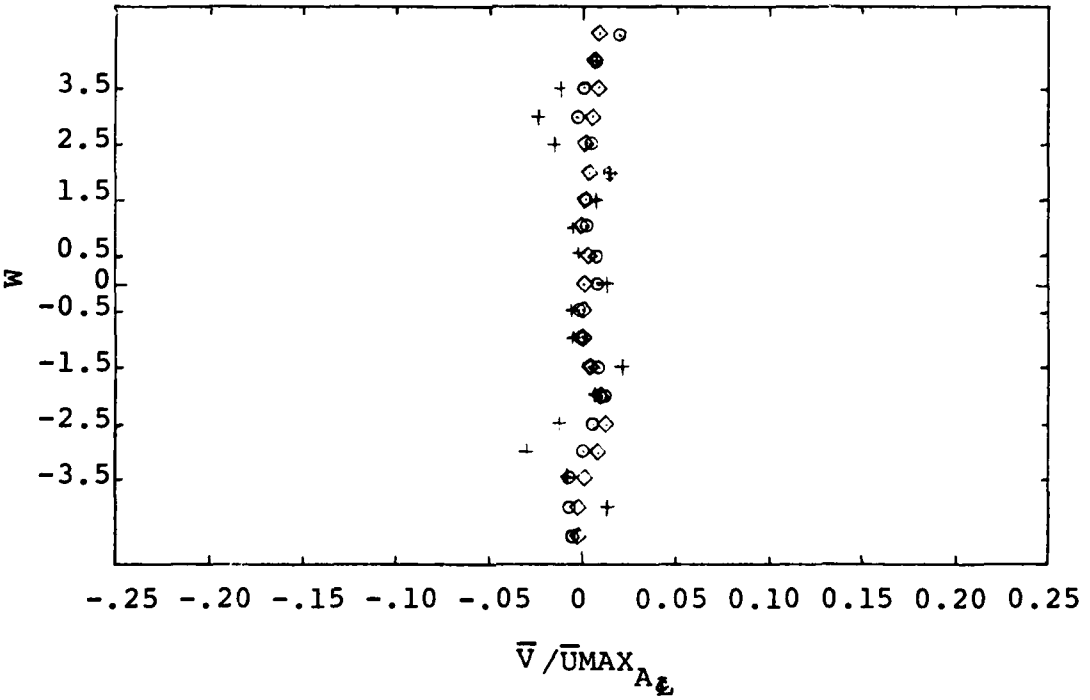

b. Location B

Figure 37. Lateral Mean Velocity Profile, Y-Component, Ur=1.0

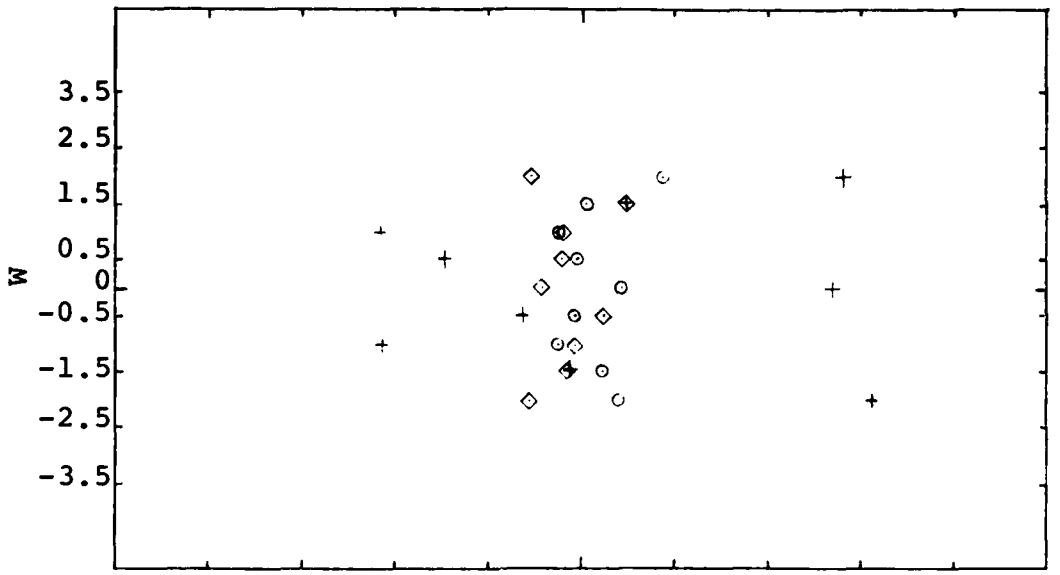

a. Location A

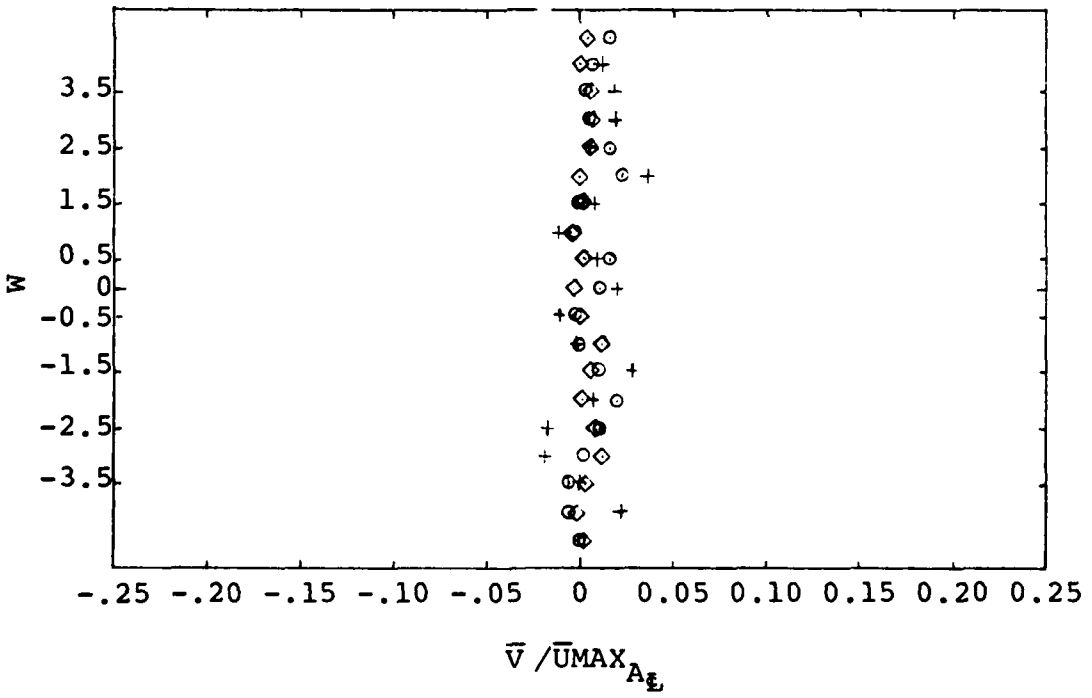

b. Location B

Figure 38. Lateral Mean Velocity Profile, Y-Component, Ur=0.6

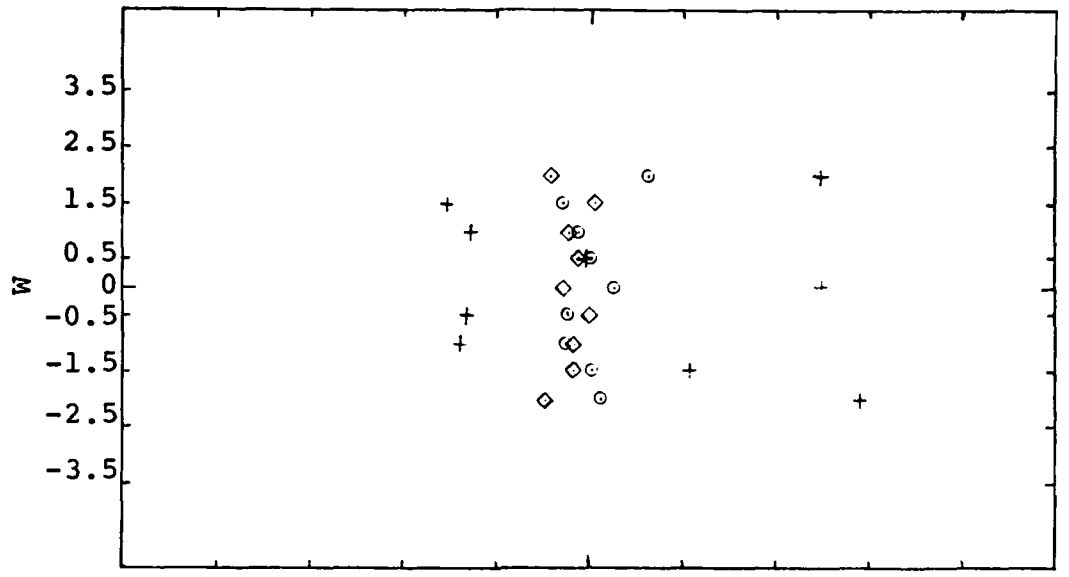

a. Location A

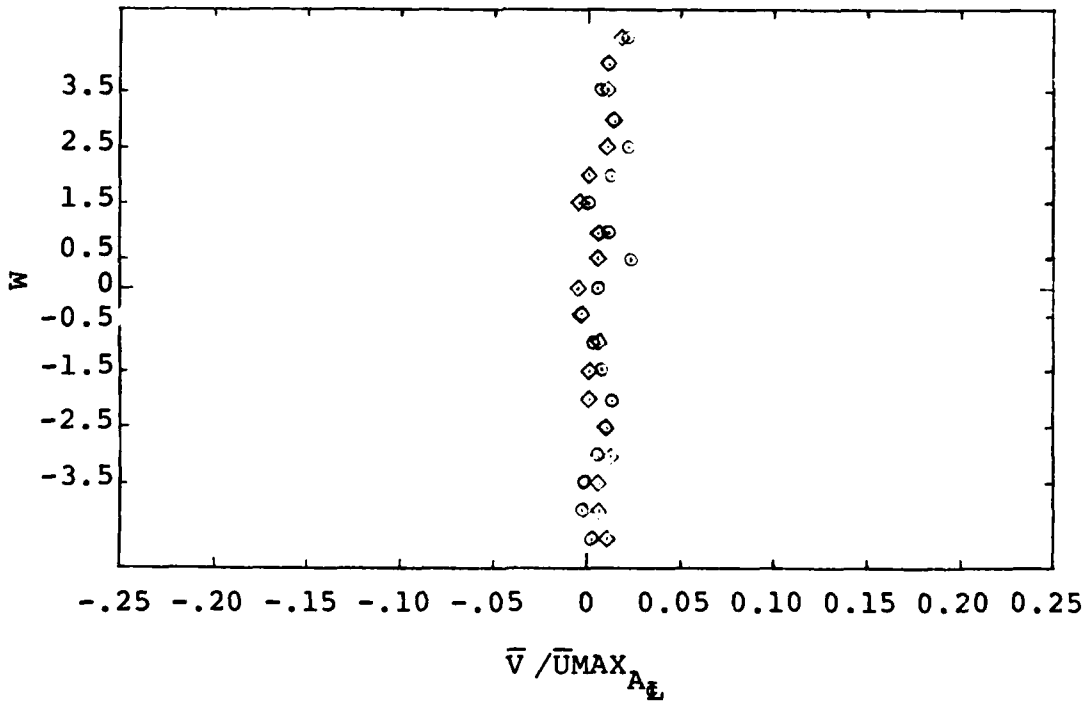

b. Location B

Figure 39. Lateral Mean Velocity Profile, Y-Component, Ur=0.3

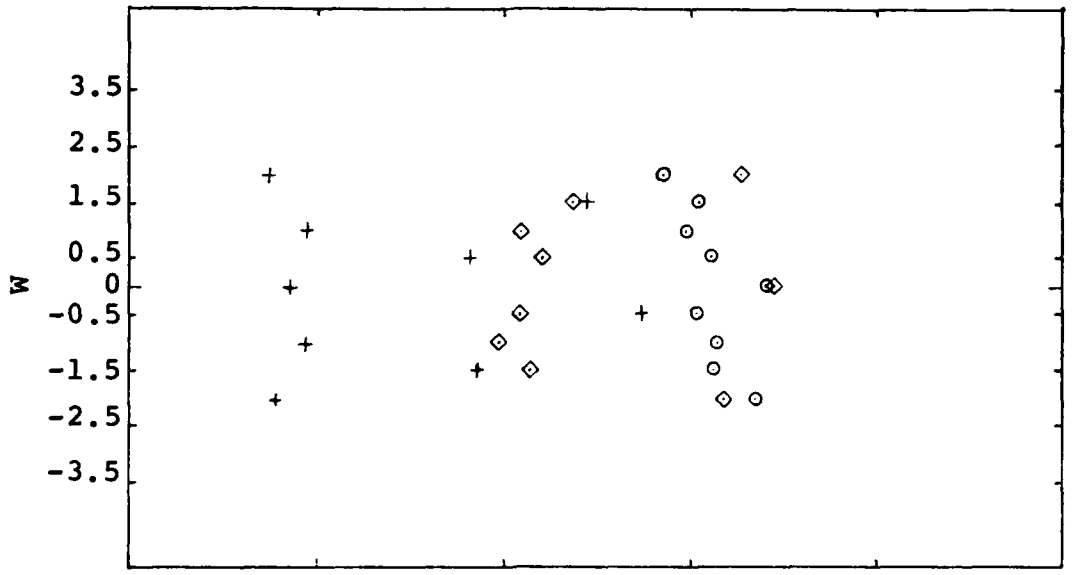

a. Location A

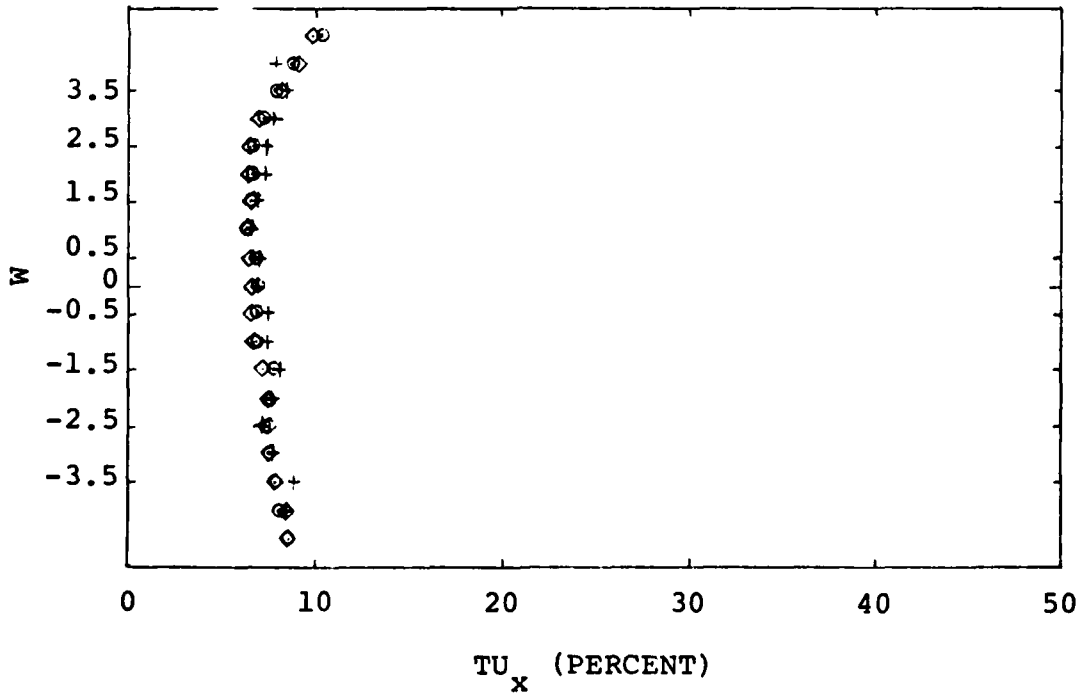

b. Location B

Figure 40. Lateral Turbulence Parameter Profile, X-Component, Ur=1.0

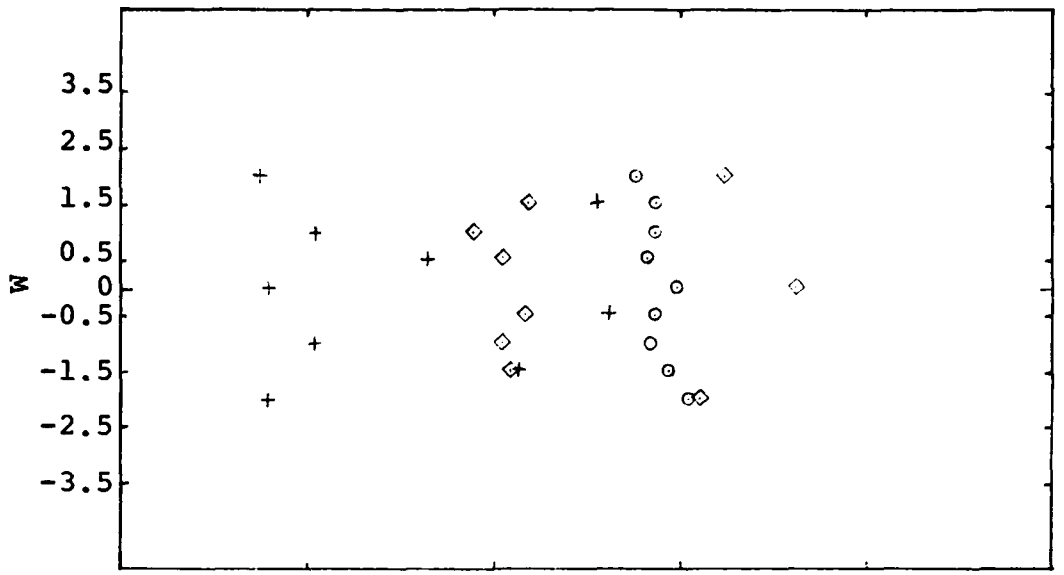

a. Location A

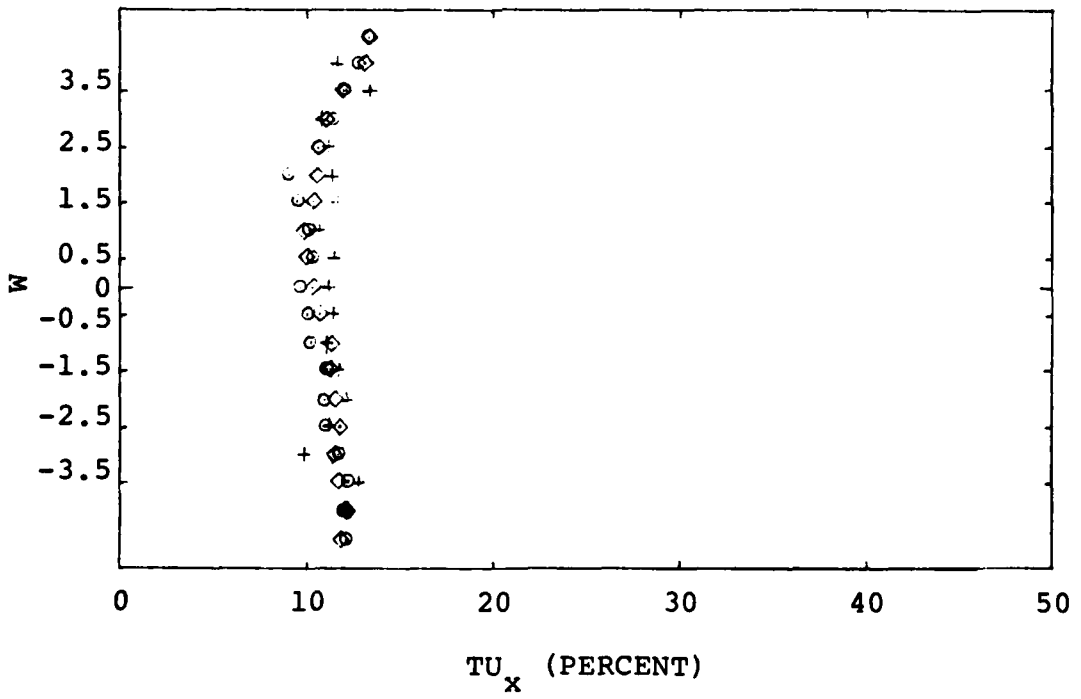

b. Location B

Figure 41. Lateral Turbulence Parameter Profile, X-Component, Ur=0.6

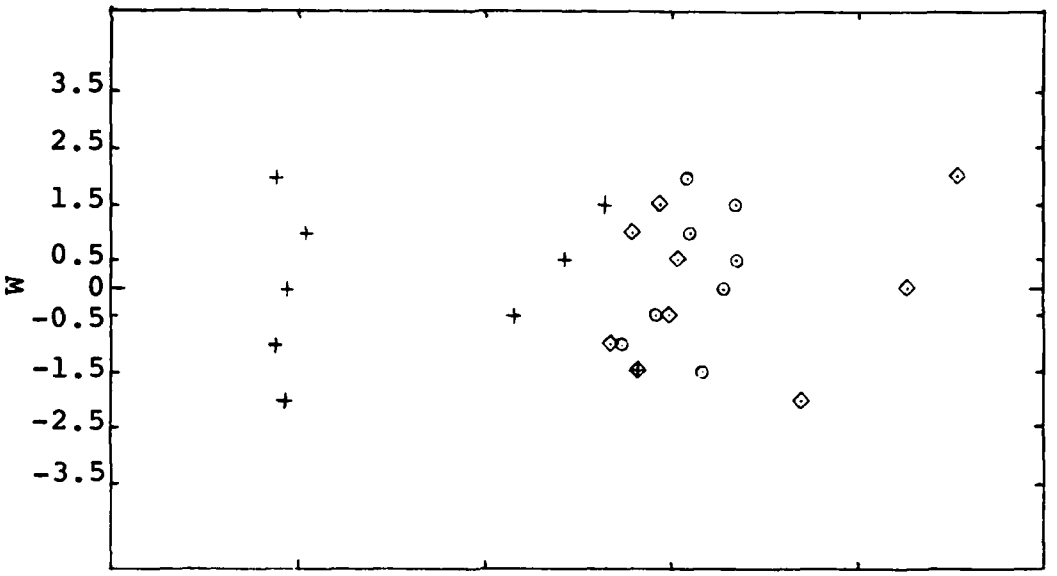

a. Location A

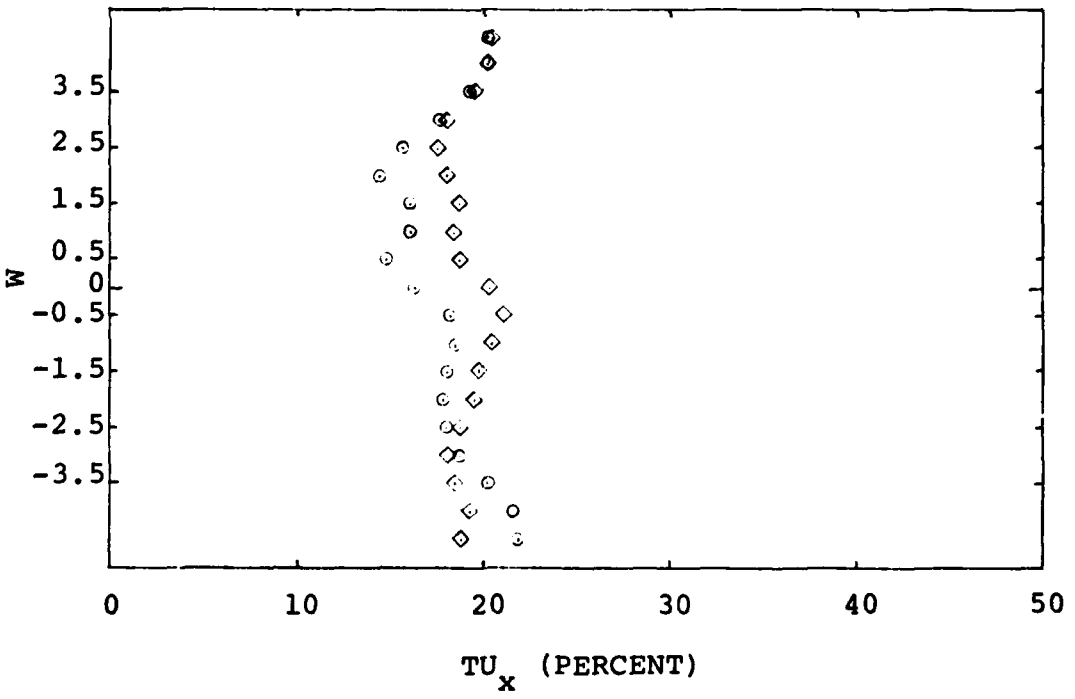

b. Location B

Figure 42. Lateral Turbulence Parameter Profile, X-Component, Ur=0.3

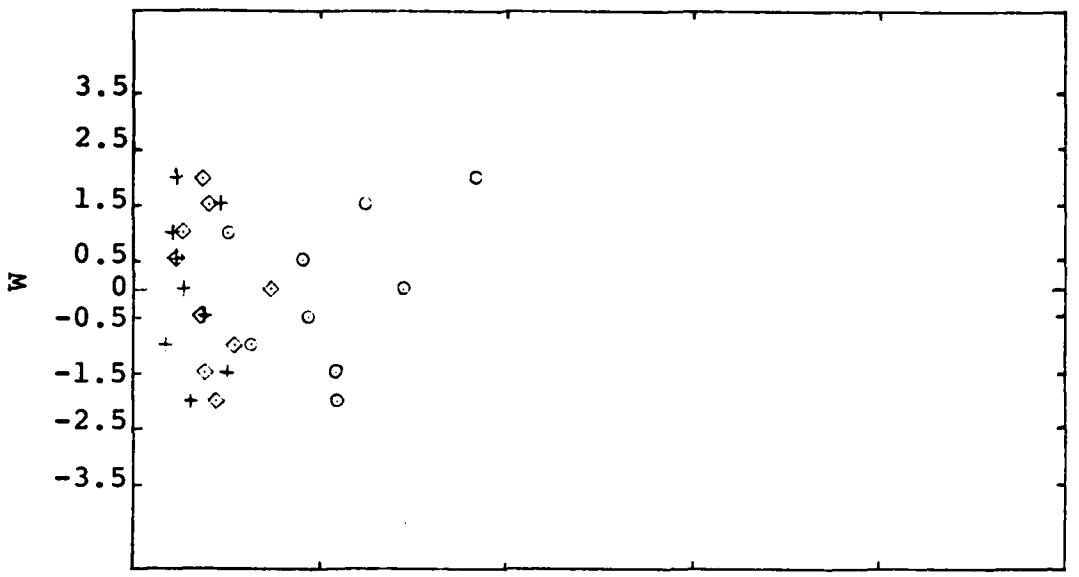

a. Location A

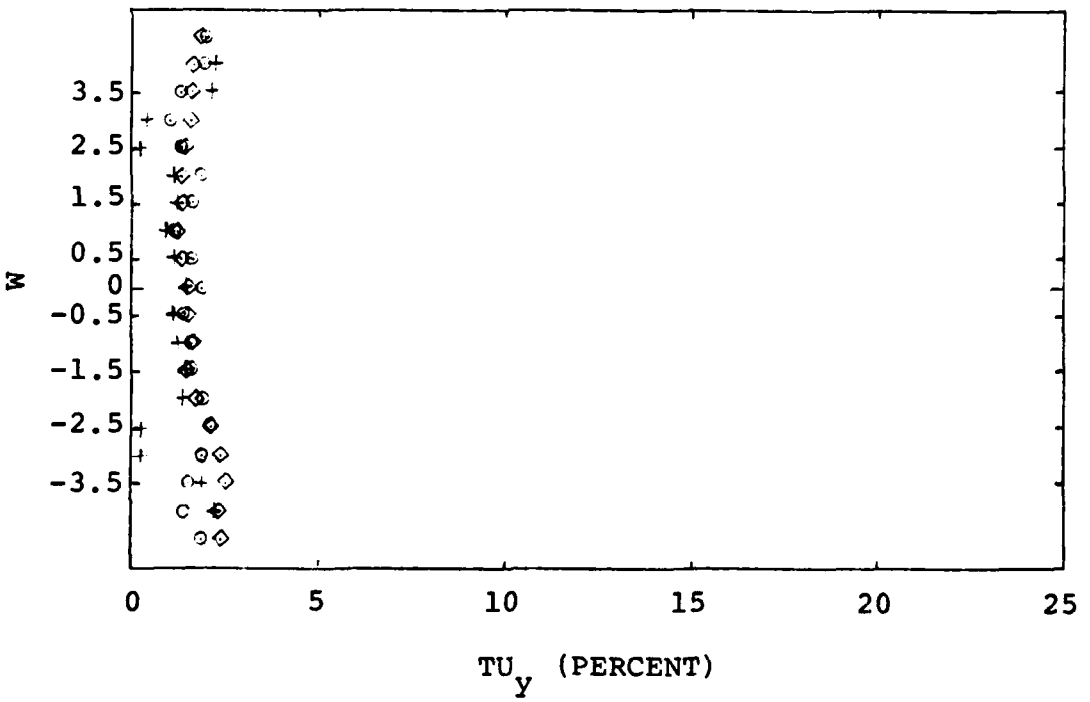

b. Location B

Figure 43. Lateral Turbulence Parameter Profile, Y-Component, Ur=1.0

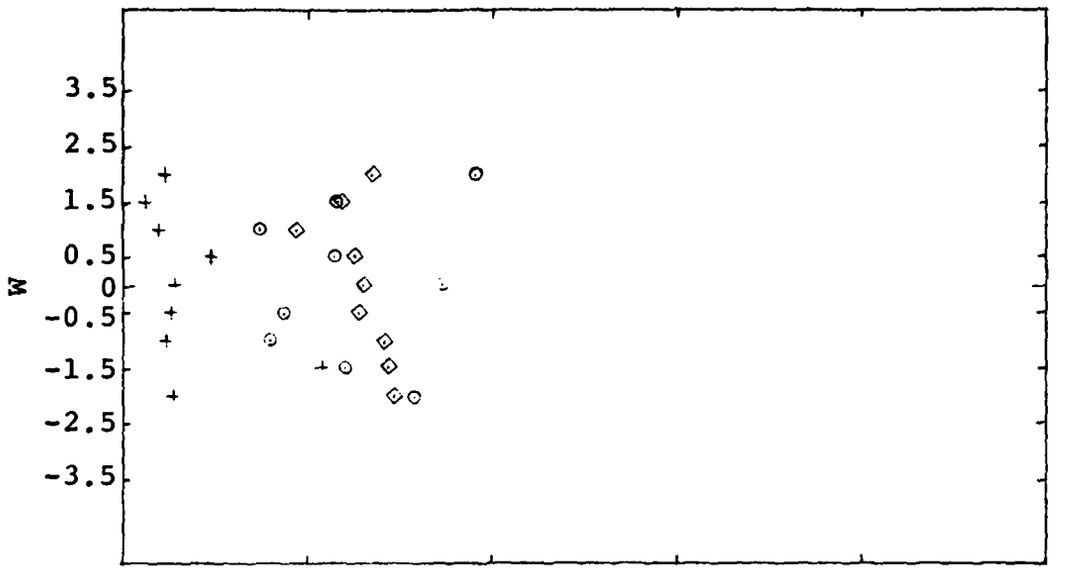

a. Location A

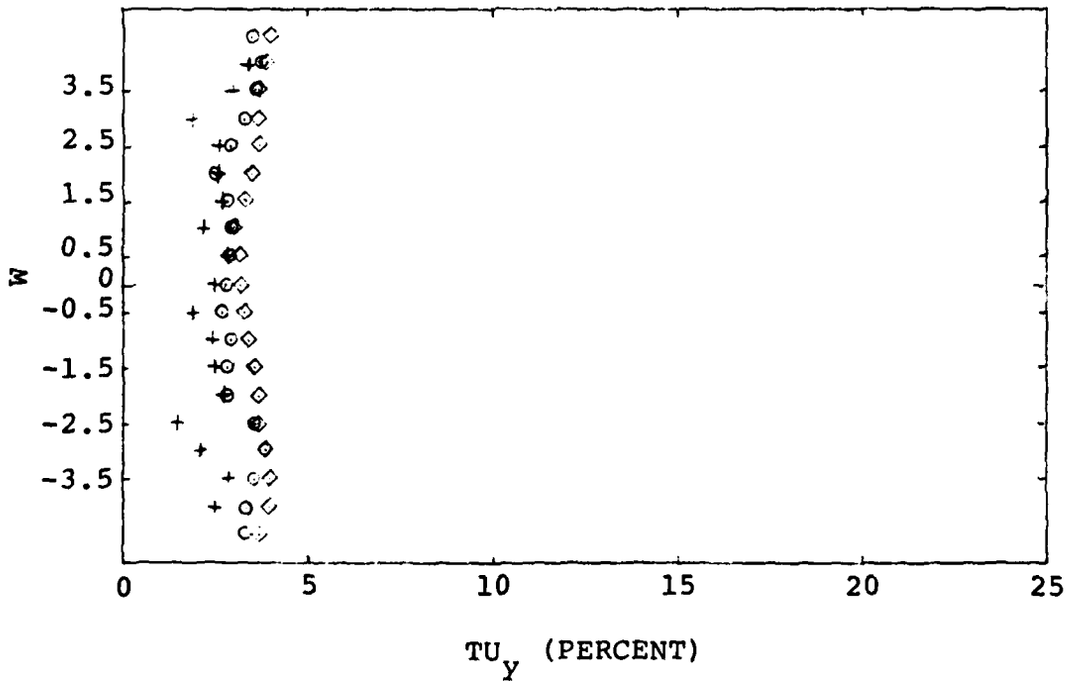

b. Location B

Figure 44. Lateral Turbulence Parameter Profile, Y-Component, Ur=0.6

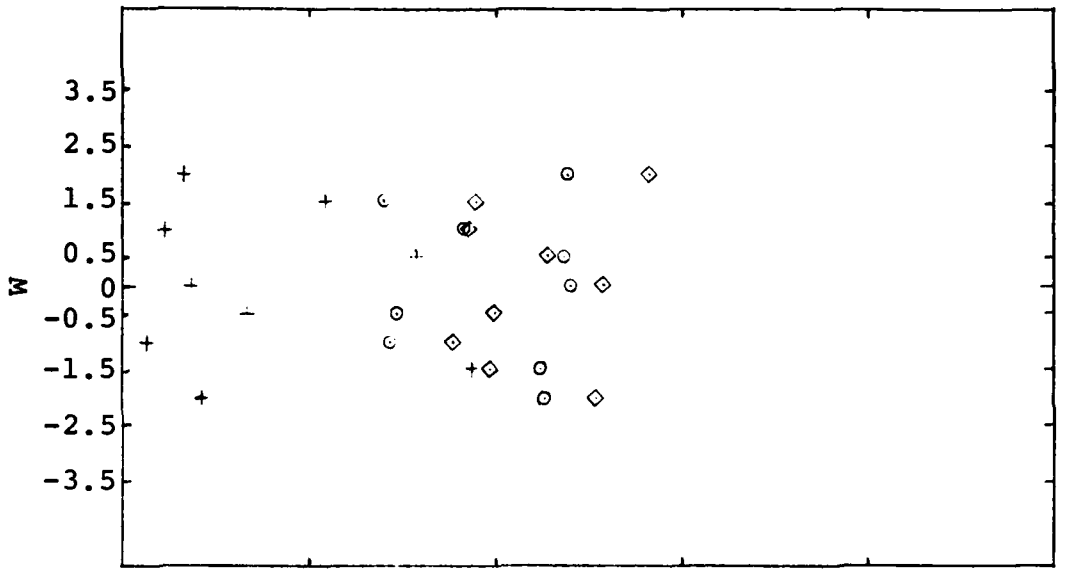

a. Location A

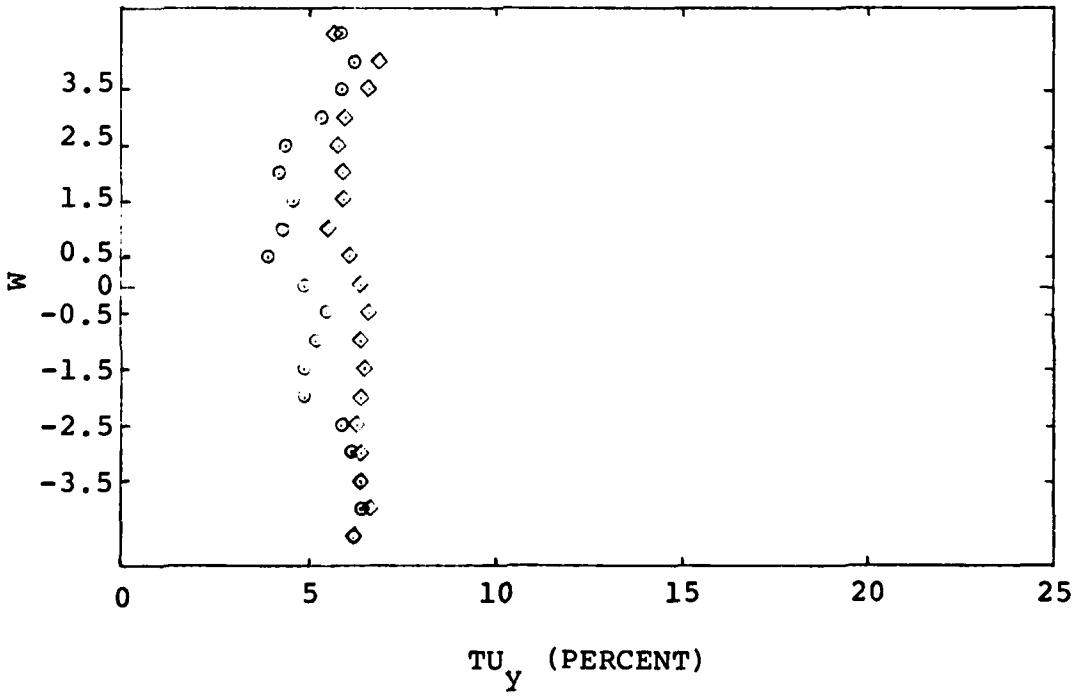

b. Location B

Figure 45. Lateral Turbulence Parameter Profile, Y-Component, Ur=0.3

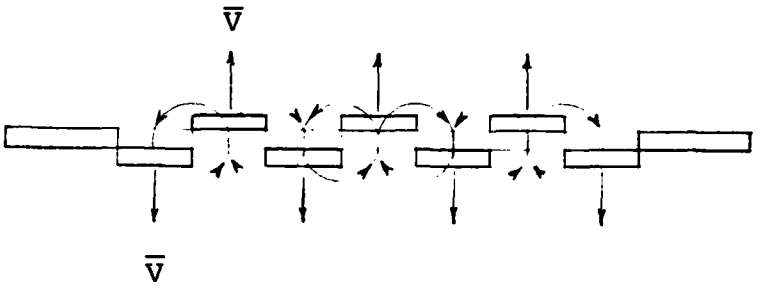

Figure 46. Tab Plate Trailing Edge Flow Pattern

APPENDIX B

Anemometer Calibration Procedure

Appendix B

Anemometer Calibration Procedure

The hot film probe was calibrated by exposing the probe to flow of known velocities and recording the voltage across each of the two sensor elements at each flow velocity.

The procedure required to prepare the anemometer for calibration is given in the TSI Incorporated operators' manual (Ref 7:2-3+). Probe resistance was nulled with the ZERO OHMS and an overheat of 1.5 was used. The STABILITY and TRIM were adjusted for optimum frequency response.

The known flow velocities were provided by flowing air from a stilling chamber through an orifice. A manometer was used to indicate stilling chamber pressure and calibration points were at increments of 2 inches of water from 0 to 22 in. The following equation, derived from the incompressible Bernoulli's equation, was used to determine the flow velocity:

$$\bar{U} = \left[\frac{124\ P_1 T_1}{\frac{P_a}{2.036} + \frac{P_1}{27.681}} \right]^{1/2}$$

where:

$\bar{U}$ = Velocity, ft/sec
P_1 = Chamber pressure, in H_2O
P_a = Ambient pressure, in Hg
T_1 = Chamber temperature, deg R

A calibration curve was created for each element of the probe by plotting 0.707 $\bar{U}$ vs DC voltage V where 0.707 $\bar{U}$ is the velocity component which is normal to the sensor element. The calibration curves are shown in Fig. 4. A Least Squares curve fit of these data for each sensor resulted in the following fourth order equations for the calibration curves with less than 0.5 percent error at each calibration point.

Probe	Calibration	Sensor	Curve
K705	30 Jun	1	$u_1=636.065-395.097V+86.115V^2-8.106V^3+.323V^4$
		2	$u_2=1371.922+914.209V-220.415V^2+22.797V^3-.816V^4$
K705	20 Jul	1	$u_1=1037.407-704.598V+168.047V^2-17.239V^3+.692V^4$
		2	$u_2=1038.887-701.21V+165.913V^2-16.875V^3+.673V^4$
K705	25 Aug	1	$u_1=3411.087-1955.49V+414.065V^2-38.631V^3+1.388V^4$
		2	$u_2=1224.093-722.046V+154.936V^2-14.593V^3+.555V^4$
K691	28 Sept	1	$u_1=3342.208-1997.467V+441.434V^2-42.997V^3+1.611V^4$
		2	$u_2=1698.468-1029.075V+228.306V^2-22.22V^3+.859V^4$

The velocity components u_1 and u_2 are the velocity normal to sensors 1 ard 2 respectively.

AD-A124 738 EFFECT OF DIVIDER PLATE TRAILING EDGE SHAPE ON THE MIXING OF PARALLEL FLOWS(U) AIR FORCE INST OF TECH WRIGHT-PATTERSON AFB OH SCHOOL OF ENGI.. W D VAHLE 2/2

UNCLASSIFIED DEC 82 AFIT/GAE/AA/82D-29 . F/G 20/4 NL

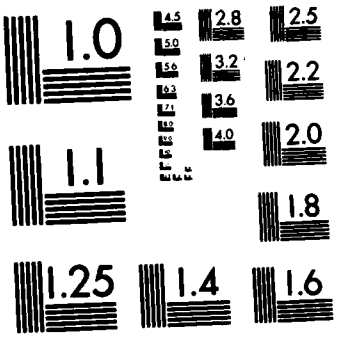

APPENDIX C

Equations for Data Reduction

Appendix C

Equations for Data Reduction

The probe sensor element voltage is a function of the component of velocity which is perpendicular to the sensor. With an x-wire probe, two components of the velocity are obtained and the magnitude and direction of the velocity in the plane of the wires can be determined.

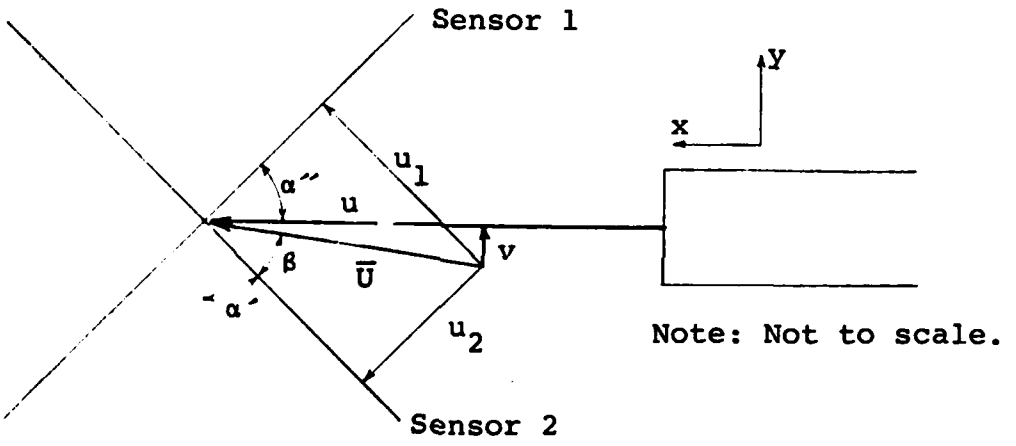

Figure 47. X-Probe Orientation

Figure 47 shows the orientation of an x-wire probe in relation to the divider plate trailing edge and the nomenclature for the following derivation. This orientation allowed calculation of x- and y-velocity components from equations derived by the following method:

Assume: u_1 is velocity perpendicular to sensor 1

u_2 is velocity perpendicular to sensor 2

Sensor 1 is perpendicular to sensor 2

$\alpha \approx \alpha' \approx \alpha'' \approx 45°$

$$u = \bar{U} \cos(\alpha-\beta) = \bar{U}(\cos\alpha\cos\beta + \sin\alpha\sin\beta)$$

$$v = \bar{U} \sin(\alpha-\beta) = \bar{U}(\sin\alpha\cos\beta - \cos\alpha\sin\beta)$$

but: $\alpha \approx 45° \rightarrow \cos\alpha = \sin\alpha = 0.707$

$$u = (0.707)(\bar{U}\cos\beta + \bar{U}\sin\beta)$$

$$v = (0.707)(\bar{U}\cos\beta - \bar{U}\sin\beta)$$

but: $u_1 = \bar{U}\cos\beta$

$u_2 = \bar{U}\sin\beta$

finally:

$$u = 0.707(u_1 + u_2)$$

$$v = 0.707(u_1 - u_2)$$

These equations were used in determining x and y components of the mean velocity as well as the fluctuating velocity.

Vita

William D. Vahle, son of Paul and Grace Vahle, was born on 20 March 1953, in Blair, Nebraska. He graduated from Blair High School in 1971. In the fall of 1971, after qualifying for a four-year Air Force ROTC scholarship, he enrolled in the Mechanical Engineering program at the University of Nebraska. He received a Bachelor of Science Degree and was commissioned as a 2nd Lieutenant in the U. S. Air Force in May 1976. He entered active duty in February 1977 and worked in the Aeronautical Systems Division at Wright-Patterson Air Force Base until entering the Master Degree program at the Air Force Institute of Technology in June 1981.

Permanent address: Route 2
Blair, Nebraska 68008

This thesis was typed by Mrs. Diane Katterheinrich

UNCLASSIFIED

SECURITY CLASSIFICATION OF THIS PAGE *(When Data Entered)*

REPORT DOCUMENTATION PAGE		READ INSTRUCTIONS BEFORE COMPLETING FORM
1. REPORT NUMBER AFIT/GAE/AA/82D-29	2. GOVT ACCESSION NO. AD A124 738	3. RECIPIENT'S CATALOG NUMBER
4. TITLE *(and Subtitle)* EFFECT OF DIVIDER PLATE TRAILING EDGE SHAPE ON THE MIXING OF PARALLEL FLOWS		5. TYPE OF REPORT & PERIOD COVERED MS Thesis 6. PERFORMING ORG. REPORT NUMBER
7. AUTHOR(s) William D. Vahle Captain USAF		8. CONTRACT OR GRANT NUMBER(s)
9. PERFORMING ORGANIZATION NAME AND ADDRESS Air Force Institute of Technology (AFIT-EN) Wright-Patterson AFB, Ohio 45433		10. PROGRAM ELEMENT, PROJECT, TASK AREA & WORK UNIT NUMBERS
11. CONTROLLING OFFICE NAME AND ADDRESS Air Force Institute of Technology (AFIT-EN) Wright-Patterson AFB, Ohio 45433		12. REPORT DATE December 1982 13. NUMBER OF PAGES 100
14. MONITORING AGENCY NAME & ADDRESS*(if different from Controlling Office)*		15. SECURITY CLASS. *(of this report)* UNCLASSIFIED 15a. DECLASSIFICATION/DOWNGRADING SCHEDULE

16. DISTRIBUTION STATEMENT *(of this Report)*

Approved for public release; distribution unlimited.

17. DISTRIBUTION STATEMENT *(of the abstract entered in Block 20, if different from Report)*

18. SUPPLEMENTARY NOTES Approved for public release: IAW AFR 190-17.

LYNN E. WOLAVER
Dean for Research and Professional Development
Air Force Institute of Technology (ATC)
Wright-Patterson AFB OH 45433

19 JAN 1983

19. KEY WORDS *(Continue on reverse side if necessary and identify by block number)*

Wakes
Mixing
Turbulence

20. ABSTRACT *(Continue on reverse side if necessary and identify by block number)*

The objective of this thesis is to investigate the mixing process as characterized by velocity and turbulence data. The effects of divider plate trailing edge modifications upon the mixing of parallel co-flowing air streams is also examined. Five divider plate trailing edge configurations were tested at velocity ratios from 0.3 to 1.0 with a maximum velocity of 300 ft/sec. A two element hot film anemometer was used to determine the flow velocities and turbulence. Wake growth rate determined from velocity and turbu-

DD FORM 1 JAN 73 1473 EDITION OF 1 NOV 65 IS OBSOLETE (continue)

UNCLASSIFIED

SECURITY CLASSIFICATION OF THIS PAGE *(When Data Ente*

20. (continued)

lence profiles was the primary indicator of mixing. The modification which extended beyond the original plate thickness produced the highest wake growth rates and was the best mixer. No reliable correlation between maximum turbulence and mixing ability was determined.